THERMOCATALYTIC DECOMPOSITION OF VULCANIZED RUBBER

A Dissertation

by

FENG QIN

Submitted to the Office of Graduate Studies of
Texas A&M University
in partial fulfillment of the requirements for the degree of

DOCTOR OF PHILOSOPHY

May 2004

Major Subject: Chemical Engineering

THERMOCATALYTIC DECOMPOSITION OF VULCANIZED RUBBER

A Dissertation

by

FENG QIN

Submitted to the Office of Graduate Studies of
Texas A&M University
in partial fulfillment of the requirements for the degree of

DOCTOR OF PHILOSOPHY

Approved as to style and content by:

James C. Holste
(Chair of Committee)

Maria A. Barrufet
(Member)

Charles J. Glover
(Member)

Mark T. Holtzapple
(Member)

Kenneth R. Hall
(Head of Department)

May 2004

Major Subject: Chemical Engineering

ABSTRACT

Thermocatalytic Decomposition of
Vulcanized Rubber. (May 2004)

Feng Qin, B.S., Tsinghua University, Beijing China;
M.S., Tsinghua University, Beijing China
Chair of Advisory Committee: Dr. James C. Holste

Used vulcanized rubber tires have caused serious trouble worldwide. Current disposal and recycling methods all have undesirable side effects, and they generally do not produce maximum benefits.

A thermocatalytic process using aluminum chloride as the main catalyst was demonstrated previously from 1992 to 1995 in our laboratory to convert used rubber tire to branched and ringed hydrocarbons. Products fell in the range of C_4 to C_8. Little to no gaseous products or fuel oil hydrocarbons of lower value were present.

This project extended the previous experiments to accumulate laboratory data, and provide fundamental understanding of the thermocatalytic decomposition reaction of the model compounds including styrene-butadiene copolymers (SBR), butyl, and natural rubber.

The liquid product yields of SBR and natural rubber consistently represented 20 to 30% of the original feedstock by weight. Generally, approximately 1 to 3% of the feedstock was converted to naphtha, while the remainder was liquefied petroleum gas.

The liquid yields for butyl rubber were significantly higher than for SBR and natural rubber, generally ranging from 30 to 40% of the feedstock.

Experiments were conducted to separate the catalyst from the residue by evaporation. Temperatures between 400 °C and 500 °C range are required to drive off significant amounts of catalyst. Decomposition of the catalyst also occurred in the recovery process. Reports in the literature and our observations strongly suggest that the $AlCl_3$ forms an organometallic complex with the decomposing hydrocarbons so that it becomes integrated into the residue.

Catalyst mixtures also were tested. Both $AlCl_3/NaCl$ and $AlCl_3/KCl$ mixtures had very small $AlCl_3$ partial pressures at temperatures as high as 250 °C, unlike pure $AlCl_3$ and $AlCl_3/MgCl_2$ mixtures. With the $AlCl_3/NaCl$ mixtures, decomposition of the rubber was observed at temperatures as low as 150 °C, although the reaction rates were considerably slower at lower temperatures. The amount of naphtha produced by the reaction also increased markedly, as did the yields of aromatics and cyclic paraffin.

Recommendations are made for future research to definitively determine the economic and technical feasibility of the proposed thermocatalytic depolymerization process.

To Xin:

For her sweet love and kind support.

To my parents, grand parents, parents-in-law, brother, and sister:

For their endless love and encouragement.

ACKNOWLEDGEMENTS

I give special thanks to Dr. James C. Holste for serving as Chair of my Advisory Committee and for directing the research and providing support throughout all phases of my work. I also thank Dr. Maria A. Barrufet, Dr. Charles J. Glover, and Dr. Mark T. Holtzapple for serving on my Committee. I thank Mr. Randy Merik for helping in designing, building, and assembling the apparatus. Dr. Dawid Jakobus Duvenhage provided hands-on support and useful hints throughout the study, for which I am very grateful.

I must thank Ms. Lan Liang for being in the same research group and creating an enjoyable work atmosphere. Without her, I could not have finished this project by myself. There are too many fellow students who have provided support and friendship to list.

The Department of Chemical Engineering at Texas A&M provided the best experiment facilities for this research. I truly appreciate the financial support for this project from S-P Reclamation and Cooper Tire.

TABLE OF CONTENTS

CHAPTER Page

CHAPTER Page

LIST OF FIGURES

FIGURE Page

LIST OF TABLES

CHAPTER I

INTRODUCTION

Scrap tires are one of several special wastes that pose difficulties for municipalities. Whole tires are difficult to landfill because they float to the surface a few years later. Stockpiles of scrap tires are found in many communities, resulting in public health, environmental, and aesthetic problems. Outbreaks of encephalitis, a mosquito-carried disease, have been attributed to scrap tire piles in the United States (*1*). Large tire piles also are potential fire hazards. In September, 1999, lightning ignited a pile of 5 million scrap tires near Westley, CA. Costs incurred in fighting and extinguishing the fire, and for subsequent clean-up of site, are estimated at more than $20 million (*2*). In the United States alone, nearly 253 million tires were scrapped in 1997 (*3*), and more than 3 billion tires had accumulated in stockpiles awaiting permanent disposal (*4*). Today, the number of tires in stockpiles is reduced to around 300 million due to the market rise of recycling business (*5, 6*).

The disposal of scrap tires is very difficult due to their properties. The very characteristics that make them desirable as tires, long life and durability, also make disposal almost impossible. The fact that tires are thermal-set polymers means that they cannot be melted easily or separated into their chemical components. Tires also are virtually immune to biological degradation.

Landfilling scrap tires is not considered as a good choice for several reasons. One

---

This dissertation follows the style of the *Environmental Science & Technology*.

reason is that they tend to collect gases and rise to the surface (*7*). More land will be needed to sustain growing populations and our society cannot afford land just for landfilling scrap tires. One of the early disposal methods is burning, which is not environment-friendly (*8*). In 1990, about 25.9 million tires (only 10.7% of total generation) were burned for energy (*7*). Some recycling alternatives use whole tires (like burning for energy), thus requiring no extensive processing, other alternatives require that tires be split or punched to make products (for instance, rubber swings), and still other alternatives involve tires that are finely ground enabling the manufacture of crumb rubber products (typically mulch). Such physical applications of scrap tires also have shortcomings partly because they cannot consume sufficient quantities of the scrap tires to significantly reduce the scrap tire stockpiles. Besides, after their service lifespan, they will definitely have to be disposed of or recycled. Facing these facts, many companies and research and development firms are searching for new, innovative ways to use scrap tires.

CHAPTER II

BACKGROUND

2.1 Information of rubber tires

Modern transportation systems, such as cars, trucks, and airplanes, use rubber tires. Tires are made of vulcanized (*i.e.,* cross-linked polymer chains) rubber and various reinforcing materials. The most commonly used rubber compounds include the co-polymer styrene-butadiene (SBR), natural rubber (NR), and butyl rubber (BR). Natural rubber is known for its high mechanical strength, outstanding resilience, excellent elasticity, abrasion resistance, good low-temperature resistance, and very good dynamic mechanical properties, so it is used extensively in the tire industry (*9, 10*). SBR is by far the world's foremost synthetic rubber and it is easily available world-wide. Practically all automobile tires use SBR, especially in the tread. Butyl rubber also is used in the tire industry because of its low permeability to gases. Butyl rubber can be halogenated, and chlorobutyl and bromobutyl rubbers are available. These rubbers are widely used as tire inner liners due to their properties (*11*).

2.1.1 Natural rubber

Natural rubber (NR) supplies more than one third of the world demand for elastomers and it is the standard by which the performance of synthetic rubbers is evaluated. The original source of natural rubber is from latex, a milky rubber-bearing fluid, obtained by tapping rubber trees (*12*).

Chemically, natural rubber is *cis*-1,4-polyisoprene, a linear, long-chain polymer with repeating units of isoprene C_5H_8 (Figure 2.1). As an unsaturated hydrocarbon, the monomer isoprene can exist in various isomeric forms: *trans*, and *cis*. Natural rubber consists largely of *cis*-1,4-polyisoprene (*13*).

cis *trans*

Figure 2.1 Natural rubber.

Pure crude natural rubber is white or colorless with a density of approximately 915 kg/m^3. At the temperature of liquid air, which is about –195 °C, crude rubber is a hard, transparent solid, and extremely brittle. At 0 °C to 10 °C, natural rubber is brittle and opaque, above 20 °C it is soft, resilient, and translucent, and above 60 °C, it is plastic and sticky (*14*).

Natural rubber is insoluble in water, alcohol, and acetone. It is soluble in gasoline, benzene, chloroform, carbon tetrachloride, carbon disulfide, and turpentine. It is also slightly soluble in ether.

Because of the double bond, natural rubber reacts to form various compounds. For example, natural rubber has little inherent resistance to environmental damage due to the effects of oxygen and ozone in the atmosphere at high temperatures (*15*). To increase the weathering resistance, natural rubber can be modified in many ways to achieve this purpose. Deproteinized rubber (DPNR) is a very useful modified natural rubber. Normal natural rubber has 0.25% to 0.50% nitrogen as protein, while DPNR has only 0.07% (*11*). Oil-extended natural rubber (OENR) is another useful modified natural rubber. About 65 parts of oil, both aromatic and naphthenic, can be incorporated into 100 parts of natural rubber to make OENR. A new modification of natural rubber produced in commercial quantities is epoxidized natural rubber (ENR). The rubber molecule is partially epoxidized with the epoxy groups randomly distributed along the molecular chain (*11*). This modified natural rubber has some unique properties, such as better oil resistance and lower gas permeability than natural rubber.

NR has been used in a large variety of applications such as hoses, conveyor belts, rubber linings, gaskets, seals, rubber rolls, rubberized fabrics, *etc.* Superior fatigue resistance and low heat build-up characteristics make NR a special rubber component used in tires.

2.1.2 Styrene-butadiene rubber

The fact that isoprene is the basis of natural rubber led to the investigation of the polymerization of not only isoprene but also other similar monomers. The possibility of producing a synthetic rubber from a combination of different monomers has also been realized. Styrene-butadiene rubber (SBR) has become the world's foremost synthetic rubber today, and it will probably retain its leading position in the near future. The volume of production is about 60% of the total world production of synthetic rubbers. SBR has been used widely in all automotive tires, especially in the tread.

SBR is a copolymer of styrene, $C_6H_5CH = CH_2$, and butadiene, $CH_2 = CH - CH = CH_2$. The repeating unit in SBR is shown in Figure 2.2.

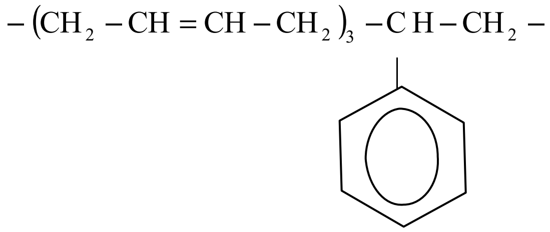

$$-(CH_2 - CH = CH - CH_2)_3 - CH - CH_2 -$$

Figure 2.2 Styrene-butadiene rubber.

The typical production reaction and structure for SBR can be depicted as shown in Figure 2.3 (*16*):

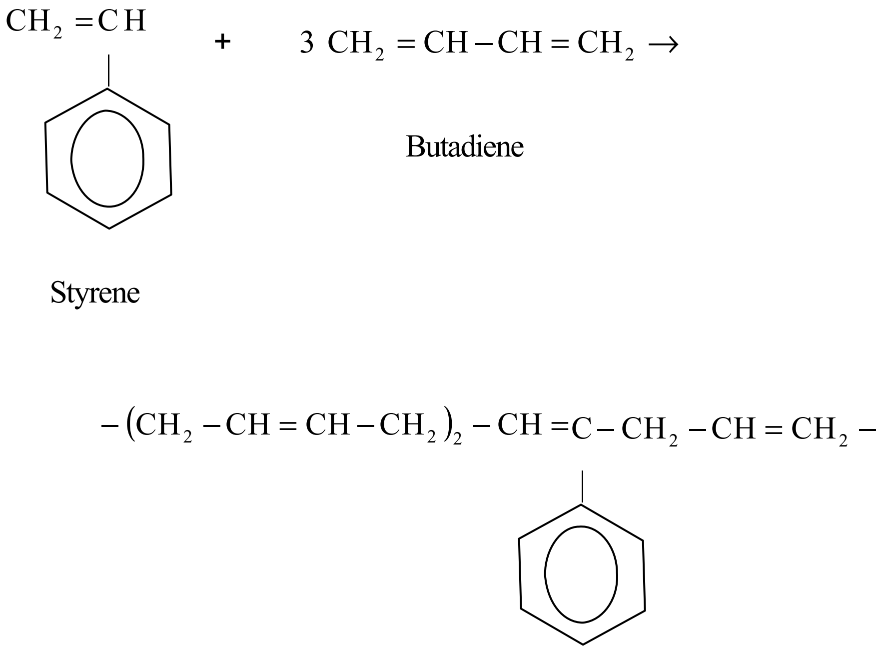

$$CH_2 = CH \quad + \quad 3\ CH_2 = CH - CH = CH_2 \rightarrow$$

$$-(CH_2 - CH = CH - CH_2)_2 - CH = C - CH_2 - CH = CH_2 -$$

75% butadiene + 25% styrene

Figure 2.3 Production and structure of styrene butadiene rubber.

Most SBR is produced by emulsion polymerization at decreased temperature, 5 °C. This type of emulsion SBR is called cold SBR and almost all the emulsion SBR produced in the world at present falls into this category. Emulsion SBR also can be produced at higher temperature (*e.g.,* 55 °C) (*11*). The polymerization temperature affects at least one of the main properties of SBR, *i.e.,* the tensile strength. The tensile strength increases almost linearly as the temperature decreases. Increased tensile strength leads to improved abrasion resistance and flex cracking resistance, which are important properties in tires.

SBR also can be produced by solution polymerization and much interest has been demonstrated recently in the use of the products from this method. Solution SBR offers promise in meeting the demands by automotive manufacturers for tires with low rolling resistance, high wet and dry traction, and excellent wear.

SBR has fewer unsaturated bonds than natural rubber, which suggests that SBR has some properties that natural rubber does not have. Mixture compounds of natural rubber and SBR can be used in a variety of products, the choice may well depend on the properties and relative prices of these two rubbers. Blends of SBR and natural rubber are also widely used in industry today, primarily in the tire industry. It has been reported that blends of SBR and NR exhibit improved oxidative stability compared to either pure component (*17*), and the fatigue and the strain energy vary linearly with the blend composition (*18*).

2.1.3 Butyl rubber

Butyl rubber is a copolymer of isobutylene with small amounts of isoprene as shown in Figure 2.4. The copolymer normally contains about 97-98% by weight polyisobutylene and 2-3% isoprene. During manufacturing, isoprene can be added to the growing chain in three ways: 1,2-, 3,4- or 1,4- addition. Investigations into various methods have established that it is the 1,4- addition that occurs (*11*).

$$-\underbrace{(CH_2-C(CH_3)_2)_n}_{\text{isobutylene}}-\underbrace{CH_2-C(CH_3)=CH-CH_2}_{\text{isoprene}}-$$

Figure 2.4 Butyl rubber.

Butyl rubber has an outstanding property: its low permeability to gases. Before the introduction of the tubeless tire in the 1960s, butyl rubber had almost entirely displaced natural rubber in passenger tire inner tubes. Butyl rubber also has excellent resistance to heat, ozone, and chemical attack. Furthermore, it has a high degree of resistance to water and mineral acids. Butyl rubber will swell in hydrocarbon solvents and oils, but it resists polar liquids, vegetable oils, and synthetic hydraulic fluids. Finally, butyl rubber has good low-temperature flexibility and high rotational flexibility. Butyl rubber is completely soluble in solvents like benzene or hexane.

Butyl rubber polymerization differs from other synthetic rubber polymerizations because the reaction temperature can be very low (–90 to –100 °C). The reaction can be very fast with the introduction of a Friedel-Craft catalyst like $AlCl_3$ (always accompanied by co-catalyst) even at low temperatures (*11*). This fact greatly contributed to the idea of utilizing $AlCl_3$ as the decomposition catalyst for vulcanized rubber.

Butyl rubber still is used in the small market for inner tubes, but extensive additional uses have been found in such items as hoses, pharmaceutical closures, mechanical rubber goods, and wire and cable insulations.

2.1.4 Reinforcing fillers

Tire rubber is a complex mixture of rubber and additives that provide its unique properties. The typical composition for a synthetic rubber tire compound is shown in Table 2.1.

Table 2.1 Rubber Compounding Composition (*19*)

component	weight %
styrene butadiene rubber	62.1
carbon black	31.0
extender oil	1.9
zinc oxide	1.9
stearic acid	1.2
sulfur	1.1
accelerator	0.7
total	99.9

Typical additives to the rubber compound in tires, as indicated in Table 2.1, are

Reinforcing fillers – carbon black is used to strengthen the rubber and aid abrasion resistance. It is a very important part in the tires. More detailed information about carbon black, such as manufacturing methods, properties, functions, grading, *etc.*, are given by Liang (*20*).

Reinforcing fibers – textile or steel fibers provide reinforcing strength or tensile component in tires. By the mid 1990's the use of steel tire cord increased substantially, occupying about 50% of the reinforcing fiber market (*21*).

Extenders – petroleum oils control viscosity, reduce internal friction during processing, and improve low temperature flexibility in the vulcanized product.

Vulcanizing agents – organo-sulfur compounds are used as catalysts for the vulcanization process, and zinc oxide and stearic acid are used to activate the curing (cross-linking) system and to preserve cured properties.

Because tires are composed of such valuable constituents, many researches have been extensively focused on recovering valuable products from waste tires.

2.1.5 Vulcanization of rubber

Rubbers, especially pure natural rubbers, are soft and tacky. The pure rubber polymer chains are nearly perfectly uniform and symmetrical, thus, the molecular attraction between them will reduce flexibility and even lead to crystal formation (*22*). A treatment, called vulcanization, is applied to improve the usability of rubbers. Usually during the vulcanization process, the rubbers are heated in the presence of sulfur. The heating promotes reactions of sulfur with double bonds contained in the polymer, forming cross-links between the polymer chains. The resulted cross-linked products become less plastic and more resistant to swelling by organic liquids and heating. The uniqueness of sulfur as a vulcanizing (or curing) agent stems from the chemistry of S-S bonds. Sulfur systems are still the most commonly used vulcanizing methods by far. Besides sulfur, some new vulcanizing agents are peroxides, phenolic resin, and metallic oxides.

The vulcanizing reactions are very complex and almost all rubber products are vulcanized by one or more of the following six methods (*11*): 1) press curing (including injection and transfer molding), 2) open steam curing, 3) dry heat curing, 4) lead press curing, 5) fluidized-bed curing, and 6) salt bath curing. There are a great number of studies concerned with the mechanism of accelerated sulfur vulcanization (*13, 23-26*). Some of the proposed mechanisms are based on ionic or radical formation. Some structural features that generally are accepted as occurring in sulfur-vulcanized rubber are shown in Figure 2.5 (*27*).

2.2 Literature review of tire recycling

The state of the technology for scrap tire disposal was summarized by Clark *et al.* (*7*) in 1993, and little significant progress has been reported since. The strategies can be divided into three major categories: (1) recycling in whole or by grinding the rubber into small particles for use directly in that form, (2) combustion as fuel or tire-derived fuel (TDF), and (3) decomposition to chemical constituents.

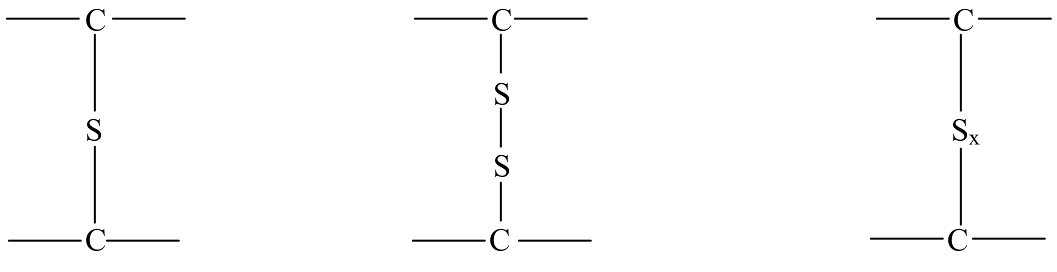

monosulfidic disulfidic polysulfidic

pendant side group intramolecular sulfide

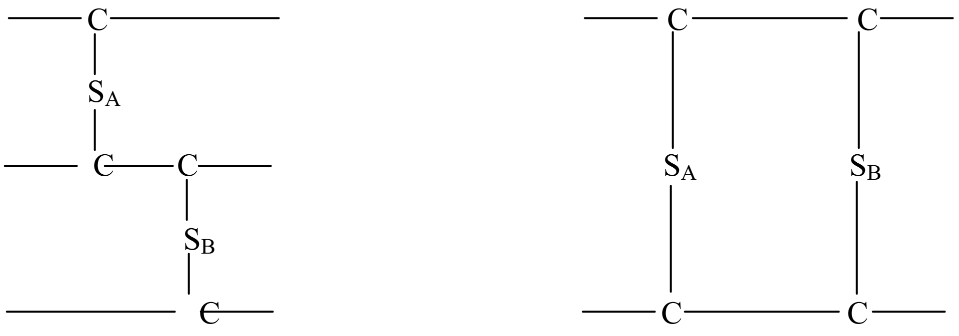

multifunctional vicinal vicinal

Figure 2.5 Structures of sulfur-vulcanized rubber (*27*).

Category (1) is the best developed application to date, but many applications of the crumb rubber (*e.g.*, use as bedding for farm animals, mulch for garden applications) are not attractive because they represent waste of a valuable chemical resource. Furthermore, the crumb product usually is sufficiently fine that it poses a serious fire hazard, both during the grinding process and during the lifetime of the application. On January 23, 2002, a confined space fire involving hundreds of tons of shredded rubber tires occurred at a tire recycling facility owned by EnTire recycling, Inc., Nebraska City, NE (*28*). It took several agencies 11 days to extinguish the fire. The U.S. Environmental Protection Agency (EPA) estimated that the cost of extinguishment and debris cleanup exceeded $1,500,000. However, the damage to the environment, and surrounding area residents' health is inestimable.

The oldest market for scrap tires is burning as a fuel (*29*). Actually, for the period from 1979 to 1992, Tire-derived fuel (TDF) was the only market for scrap tires. Now TDF is being used in a variety of combustion technologies: cement kilns, pulp and paper mill boilers, utility and industrial boilers, and dedicated energy facilities. Several factors greatly affect the future of TDF. First, to be economically viable, the waste rubber as fuel must compete with ordinary fuels, such as natural gas, wood, and coal. Should the cost of energy continue to rise, there likely will be an increased interest in using TDF. Unfortunately the coal price is expected to fall to $22.17 per ton by 2025 (1.0056 ¢ per pound), an annual decline of 0.5%, according to what the Energy Information Administration (EIA) published in its Annual Energy Outlook 2003 (*30*). Another reason why TDF dominated in the late 1970s to early 1990s is that a number of states set up funds and programs to clean up stockpiles of scrap tires and stimulate markets by offering reimbursements to various end users. Recently some states (Wisconsin, Texas, Washington, Oregon, and Idaho) ended their support because most of these states found other ways to keep up with the additional scrap tires being generated (estimated at one disposed tire/(person•year) (*31*)). After the subsidies ended on December 31, 1996, six of the nine plants in Wisconsin using TDF, reportedly decided that it was no longer economical to burn TDF, even though TDF still cost 50 percent less than other fuels. The other three plants that continued burning TDF started buying tires from out-of-state suppliers as they were less expensive and more importantly, these other states and Canada still employed subsidy programs.

Concerning Category (3), most attempts to convert tire rubber into chemicals have involved pyrolysis, the thermal decomposition of rubber at high temperature, or catalysis-assisted pyrolysis. In the last 30 years, many kinds of processes have been designed to pyrolyze tires to valuable components (*32-37*). A variety of reactors, such as, stirred tanks, rotary kilns, fixed beds, fluidized beds, and tray systems are applied in these pyrolysis processes. Several of these processes are claimed to be successful on a pilot or industrial scale (*38*). Basically, three fractions are derived from thermal decomposition of tires: gases, liquid oils, and solid residues. Although the precise product spectrum depends upon the reaction conditions, most pyrolysis processes at the temperature range of 500-900 ºC typically yield (*39*): 10-30% gases, 38-55% oils and 33-38% char by weight. The oils are condensable aromatic hydrocarbon liquids, such as benzene or toluene, and the fuel gases formed are mainly H_2, CO, CO_2, and lighter hydrocarbons, such as CH_4 and C_2H_6. The chars produced by pyrolysis, basically with yields of over 30% in weight, have a high calorific value, but also a relatively high sulfur content. The tough reaction conditions of pyrolysis tend to produce lighter hydrocarbons and low grade carbon black of limited market value (*8*). Some methods for improving the quality of the char have been proposed (*40*), but at the expense of considerable additional process equipment. There are no reports in the literature of successful production of commercial carbon blacks by pyrolysis. This is in part because of the little known fact that process temperatures above 350 °C transform existing carbon black into a form of graphite that does not have the reinforcing properties needed for the majority of carbon black applications (*8*). Therefore, direct thermal pyrolysis does not appear to be a viable method for converting scrap tires to chemicals.

Another approach to the production of chemicals is catalytic degradation of the polymer at lower temperatures (non-pyrolysis conditions). Studies by Larsen *et al.* (*41, 42*) demonstrated that molten salt catalysts with Lewis acid properties, such as zinc chloride, tin chloride, and antimony iodide, can decompose tire rubbers. The decomposition occurs at temperatures between 380 ºC and 500 ºC to yield gases, oil, and a residue. Similarly, Ivanova *et al.* (*43*) investigated the catalytic degradation of butyl rubber using various metal chlorides as catalysts. Both Larson and Ivanova *et al.* showed that the choice of catalyst and operating temperature have significant effects upon the nature of the products. Wingfield *et al.* (*44*) have patented a process for the catalytic treatment of rubber and plastic waste by reaction with Zn and Cu salts (chlorides or carbonates). In another patent (*45*), the authors claim that plastic and rubber wastes also can be degraded in the presence of basic salt catalysts, such as sodium carbonate. Butcher (*46*) has reported on the degradation of polymeric materials over molten mixtures of a basic salt (NaOH or KOH) and a Cu source, mainly metallic Cu and CuO. Processes using solid acid as catalysts have also been patented. According to Chen and Yan (*47*) preprocessed clean plastic and/or rubber wastes are dissolved or dispersed in a petroleum oil, with a high content of polycyclic aromatic compounds at 300 ºC, and catalytically transformed in a Fluid Catalytic Cracking (FCC) reactor at temperature of about 500 ºC.

There is at least one company that claims to have built low-temperature catalytic plants to process 100 tons of scrap tires per day into gaseous and liquid hydrocarbons, steel, and carbon black (*4*). However, there is no referenced technical information describing this process developed by Adherent Technologies, Inc., Albuquerque, NM. To date, researchers are still attempting to build truly commercial plants concerning Category (3).

2.3 Review of thermocatalytic decomposition mechanism

Relatively few publications have been reported on the catalytic decomposition of vulcanized rubber and even fewer have discussed the mechanism involved. A catalytic mechanism for the decomposition of vulcanized rubber using aluminum chloride will be discussed in detail in Chapter V.

2.4 Previous studies at Texas A&M University

It is not a novel idea to employ low-temperature catalytic processes to degrade waste tire rubbers. Previous studies at Texas A&M University emphasized, upon finding a catalyst, a unique set of reactor operating conditions. Almost complete conversion of the tire rubbers is possible by the approaches proposed by Platz (*48-50*). Aluminum chloride was exclusively utilized as a catalyst during the previous studies. Aluminum chloride was selected as the catalyst for the reasons described in the following paragraphs.

Aluminum chloride, $AlCl_3$, is a strong Lewis acid that can accept an electron pair acting as an acid during reaction (*51*). It is a hygroscopic white solid that reacts vigorously with moisture in air at room temperature (*52*). It is an unusual substance in that its triple point pressure 0.229 MPa (33.2 psi) is greater than 1 atmosphere so that it has a sublimation point rather a normal boiling point. The sublimation and triple point temperatures are low, 180.2 ºC and 192.5 ºC, respectively (*53*). Vapor pressure measurements reported by Smits *et al.* (*54*) are shown in Figure 2.6. The elevated vapor pressures of $AlCl_3$ in the range of 180 ºC to 300 ºC introduce significant challenges to the experimental work and to the commercial process.

As an organic synthesis catalyst, $AlCl_3$ is used in a wide variety of manufacturing processes, such as the polymerization of low-molecular-weight hydrocarbons in the manufacture of hydrocarbon resins. The well-known Friedel-Crafts reactions that employ this catalyst are used extensively in the synthesis of agricultural chemicals, pharmaceuticals, detergents, and dyes (*55*). In the manufacture of butyl rubber, which is extensively used for tire rubbers, the monomers isoprene and isobutylene are treated with a catalyst like $AlCl_3$, often with a co-catalyst at the temperature of –90 ºC to –100 ºC. Even at such low temperatures, the reaction is very fast (*11*). Because depolymerization is the reverse of polymerization, it is reasonable to expect that the same catalyst will work on both reactions. Moreover, $AlCl_3$ is abundant and its price is reasonably low. Based upon the above information, aluminum chloride appears to be a suitable catalyst for depolymerizing tire rubbers and therefore has been the preferred and confirmed choice since the beginning of the project.

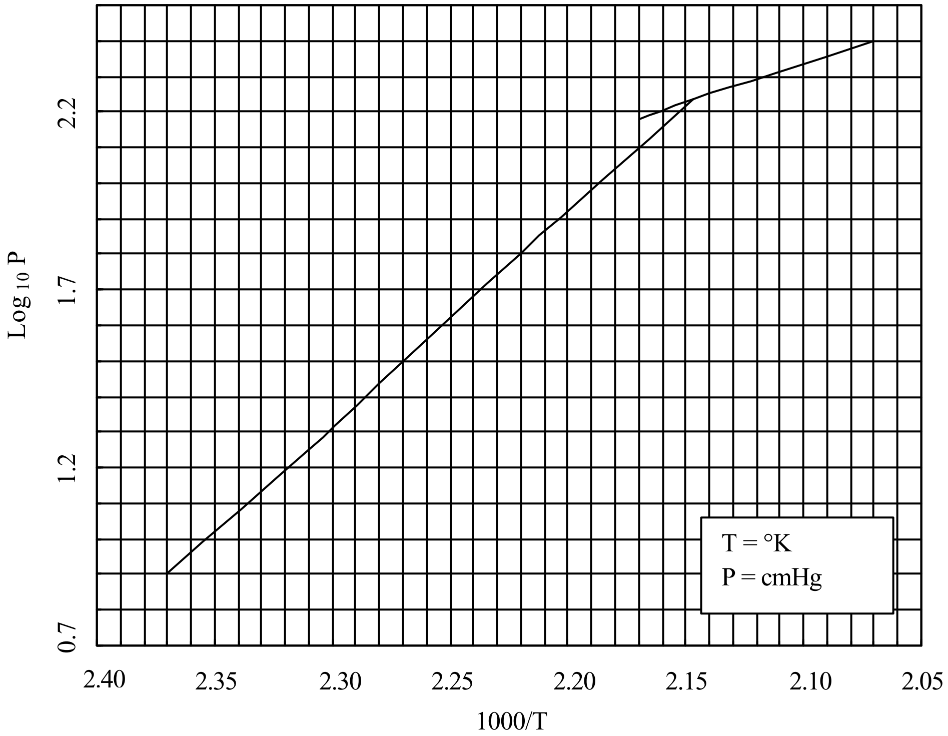

Figure 2.6 Vapor pressure of aluminum chloride (*54*).

During the summer of 1992, studies on the depolymerization of tire rubber were begun at Texas A&M University. Three initial depolymerization experiments with a 1:2 mole ratio mixture of $AlCl_3$ and $MgCl_2$ as the catalyst in a 300-cm^3 glass reactor at atmospheric pressure indicated promising results. The temperature was controlled at 300 ºC to 320 ºC, which is among the lowest reported working temperatures for tire rubber recovering processes. At that time, the catalyst concentration was 1 unit catalyst per 1 unit rubber by weight.

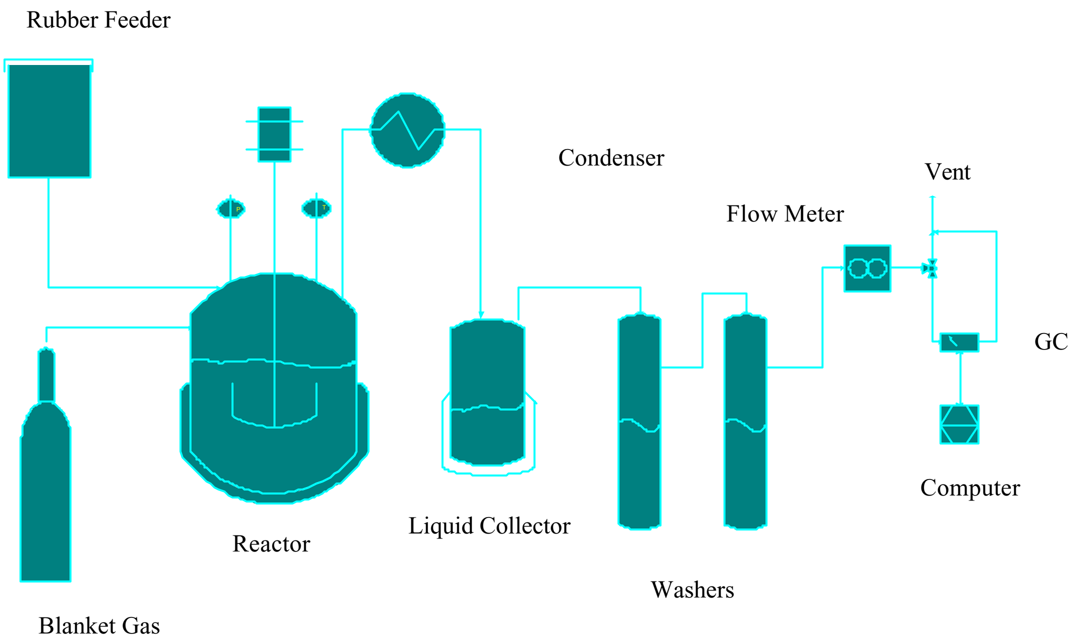

Figure 2.7 Schematic diagram of previous experiment.

Another 25 depolymerization runs were conducted during August, 1993. A more complex experimental system was implemented, and the size was scaled up from 70 to 80 grams of mixture of rubber and catalyst to almost 1 kg. A carbon steel reactor with a volume of 10 L and rated for operation at 6.5 MPa (1,000 psia) was used for most of these experiments. A rubber feeder was attached to the reactor top plate as shown in Figure 2.7 (*56*). A reflux condenser was placed directly on the top of the reactor to improve the product quality and keep the catalyst from exiting the reactor to the downstream units. The reflux condenser was followed by one liquid knockout trap. A set of gas sampling tubes was used to collect products for analysis by off-line gas chromatography. Both pure and mixed salt catalysts with lower concentration were studied. Reaction temperatures as low as 220 ºC were employed successfully.

These experiments demonstrated that essentially no light gases (CH_4, C_2H_6, CO, or CO_2) were produced. The fluid products at room temperature generally fell in C_4 to C_8 range, with very few, if any, heavier hydrocarbons or heavy oil products present. The product composition from one experiment is shown in Table 2.2. The hydrocarbon composition varied with reactor operating conditions, but always was predominantly branched and ring hydrocarbon molecules. These products are attractive because they have greater market value than the fuel gases and fuel oils that are recovered from pyrolysis processes (*8*).

Table 2.2. Representative Hydrocarbon Product Distribution (wt%) (*8*)

carbon number	*n*- paraffins	*iso*-paraffins	olefins	naphthenes	aromatics
1,2	0.00	0.00	0.00	0.00	0.00
3	0.82	0.00	0.00	0.00	0.00
4	4.24	23.58	1.20	0.00	0.00
5	0.95	23.40	1.42	0.22	0.00
6	0.21	30.35	0.66	2.06	0.40
7	0.06	4.46	0.41	1.24	0.24
8	0.05	2.15	0.11	0.87	0.04
9	0.07	0.10	0.00	0.12	0.20
10	0.00	0.00	0.09	0.00	0.18
11+	0.00	0.00	0.00	0.00	0.00

CHAPTER III

SPECIFIC OBJECTIVES

Previous experiments and analyses mainly focused on material balances, tire rubber characterization, depolymerization, and black solid residue workup. The specific objectives of this research are to address the key issues related to commercial viability of recycling tire rubber through conversion to chemical feedstocks. These issues lead to the following specific objectives for this research:

1. To determine the effect of reactor operating conditions such as temperature, and choice of blanket gas upon the nature of the solid reactor residue and the fluid hydrocarbon products using pure anhydrous aluminum chloride and its mixtures with certain salts as catalyst.
2. To evaluate the extent of depolymerization of natural, styrene butadiene, and butyl rubber achieved using a Lewis acid catalyst as described above.
3. To create a general understanding of the depolymerization decomposition mechanism.
4. To evaluate processes for recovering and recycling of the catalysts. This issue is also dealt with by Liang (*20*).

This research expands our understanding of the reaction mechanics for the thermocatalytic decomposition of rubber tires using aluminum chloride and its mixtures as catalysts. The results of this work represent progress toward developing an economically viable thermocatalytic process that converts scrap tires to chemical feedstocks.

CHAPTER IV

EXPERIMENTAL

4.1 General apparatus and setup

The existing 10 L reactor from previous experiments (see Figure 2.5) was reconditioned for use in this research. The tire rubber feeding system, temperature measurement and control system, and pressure measurement and control system were redesigned. The new system used a simple setup for capturing all gaseous and liquid hydrocarbon products. The catalyst and the reaction residue were kept in the reactor upon completion of experiment for further analysis. The evaluation and characterization of the solid residue are described elsewhere (*20*). The experimental variables were the catalyst composition, the reflux condenser temperature, the reactor temperature, and the composition of the blanket gas. The system pressure was maintained constant throughout the runs unless indicated otherwise.

4.1.1 Reactor system

After recondition and redesign, the carbon steel 10 L reactor was used in this research. Although the reactor was rated for operation at 6.5 MPa (1,000 psia), the highest working pressure was set at 0.7 MPa (100 psig) by a relief valve. On the top of the reactor, various openings were adapted for different applications (Figure 4.1). They are

1. Rubber feeder opening
2. Catalyst-loading opening

3. Hot condenser opening
4. Relief valve opening
5. Two openings for temperature measurement and blanket gas feeding
6. Two spare openings that are plugged when not used
7. The center opening is for a stirrer shaft. The shaft is driven by a motor and sealed by a commercial packing gland assembly supplied by Parr. The packing gland was cooled by circulating a refrigerated mixture of ethylene glycol and water through it (Figure 4.2).

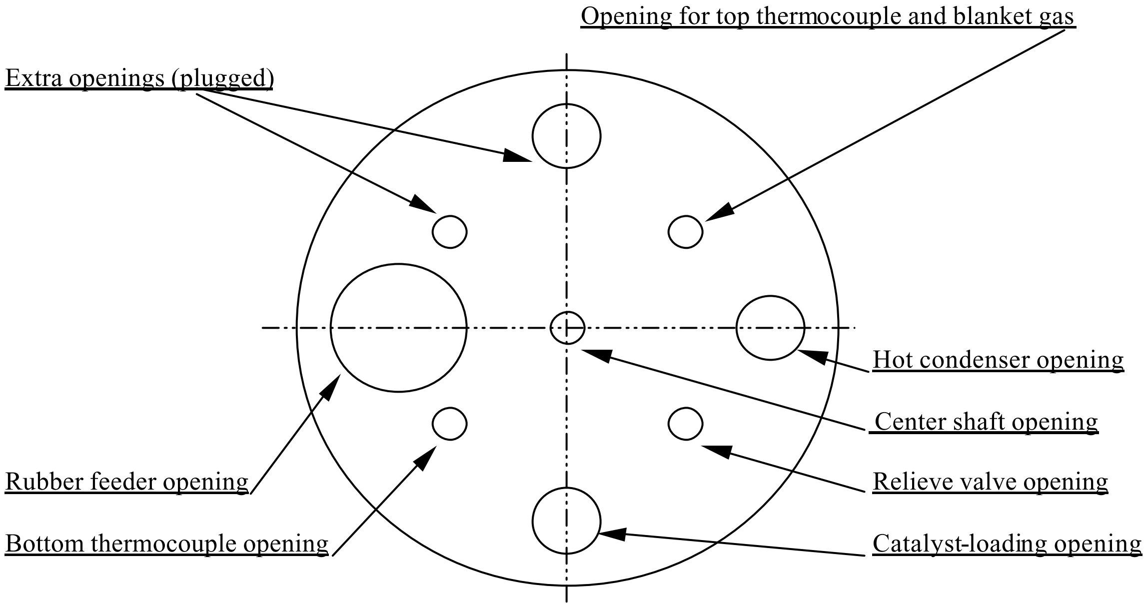

Figure 4.1 Top view of the reactor top plate.

The reactor was heated by four individual heating bands. The outside of the reactor vessel was covered with insulating material. The four heating bands were divided into two heating zones, a top heating bundle and bottom heating bundle (Figure 4.2). Various thermocouples were used to monitor and control the system temperatures.

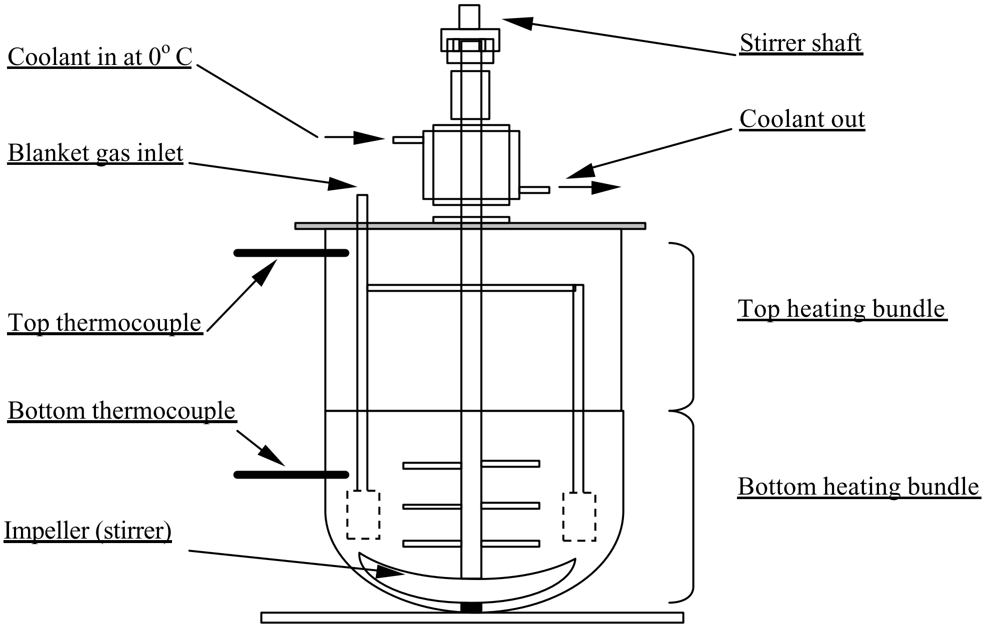

Figure 4.2 Side view of reactor system.

4.1.2 Feeding system

The feed hopper, which had a volume of 7 L, was constructed of clear acrylic plastic to allow observation of the feeding of rubber samples. Visual observation was necessary because bridging of the rubber particles in the feed hopper caused significant difficulties during feeding operations in the previous experiments. The feed hopper was at the same pressure as the reaction vessel during an experiment. The two-auger system shown in

Figure 4.3 provided a reliable and consistent feed of the rubber samples. The vertical auger was needed to minimize and compensate for deposition of solid catalyst in the feeder from the overhead vapors in the reactor. The manual horizontal auger was used to propel the rubber samples from the feeder hopper to the reactor. The use of the manual stirrer was very important to break the bridging inside the hopper and ensured a complete feeding of rubber samples.

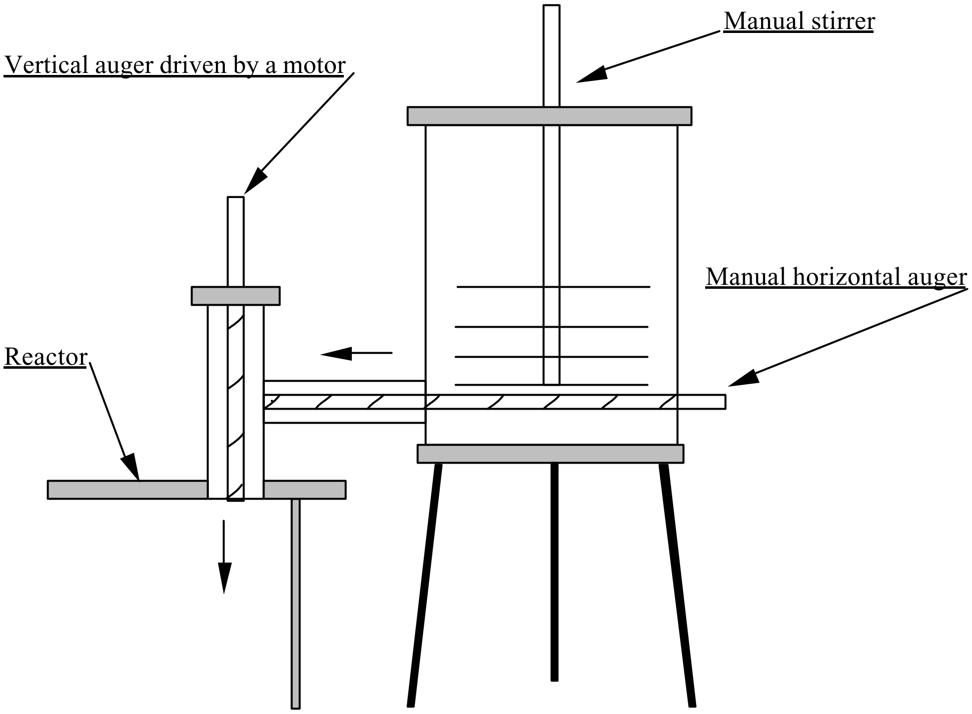

Figure 4.3 Rubber feeding system.

4.1.3 Condenser system

Various condensers designs were tested during the start-up experiment. Eventually, two customized tube-in-tube stainless steel condensers were arranged as shown in Figure 4.4. The reflux condenser was connected directly to the top plate of the reactor and maintained at temperature (70 °C to 100 °C) by circulating mineral oil through the outer tube. The liquid condenser was positioned down-stream of the main condenser, above the liquid product collector, and cooled (usually to 0 °C) by circulating a liquid mixture of ethylene glycol and water through the outer tube.

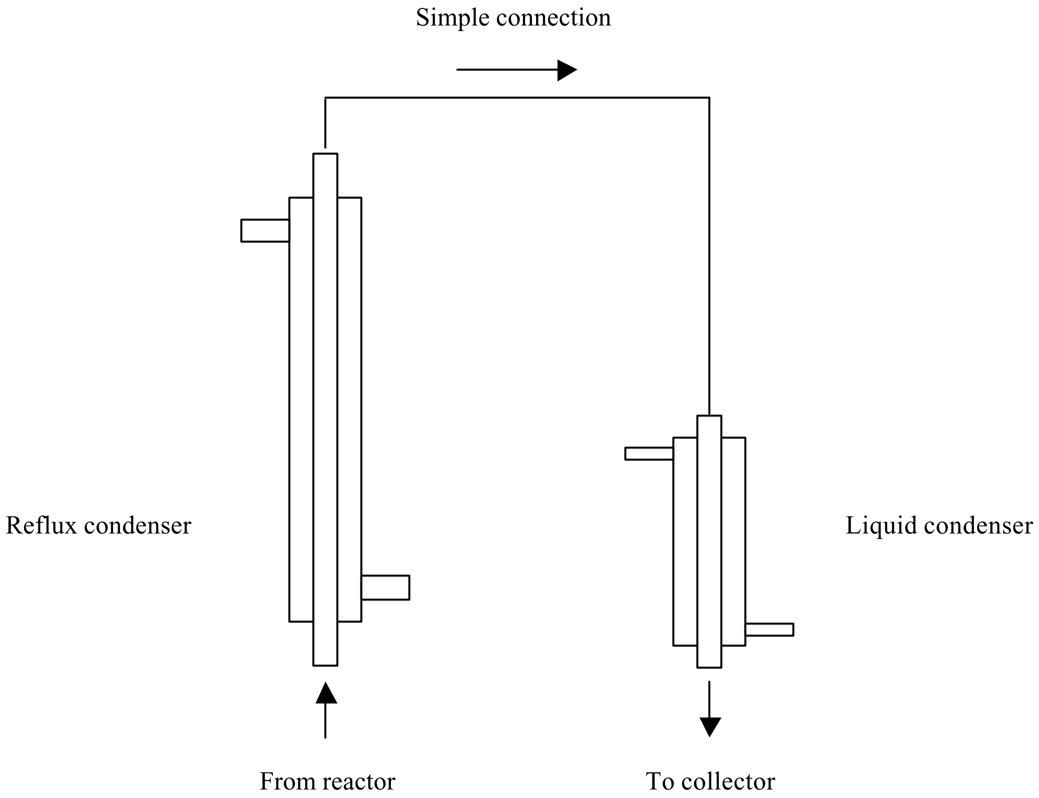

Figure 4.4 Arrangement of reflux and liquid condensers.

4.1.4 The manual plunger and scraper system

The manual plunger and scraper device (Figure 4.5) was placed in the reflux condenser. Due to the heavy plugging of aluminum chloride in the reflux condenser, we had to push this device through the reflux condenser and rotate it at least once per minute to remove catalyst condensing on the lower wall of the condenser. This small device made the research possible with pure $AlCl_3$.

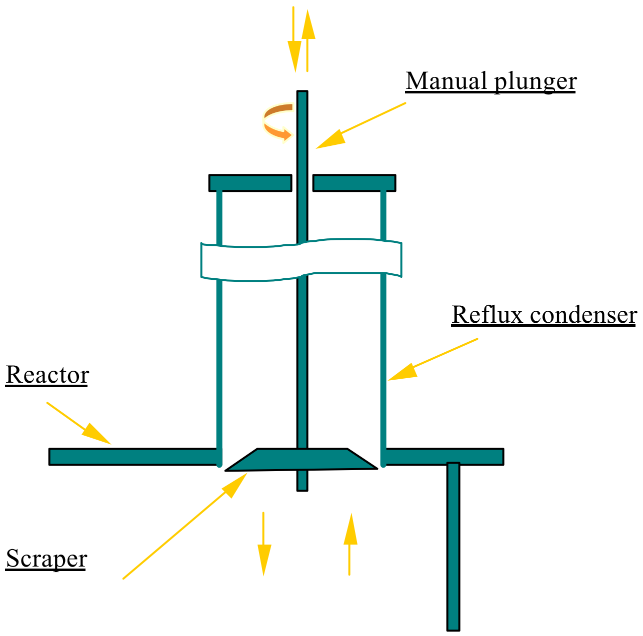

Figure 4.5 The manual plunger and scraper system.

4.1.5 Liquid collector

For safety reasons, the glass liquid collector used in the previous experiments was replaced with a 1 L stainless steel container. This liquid collector was pressure tested up to 0.7 MPa (100 psig), which is the allowed working pressure of the reactor. Although the collector often was operated at ambient temperature, it could be cooled by circulating a mixture of ethylene glycol and water through cooling coils clamped to the exterior. The collector assembly was covered with insulating material.

4.1.6 Acid gas scrubbing system

After leaving the liquid product collector, the vapor products were expanded to atmospheric pressure and passed through two traps, as shown in Figure 4.6. The sodium hydroxide trap (25% aqueous solution by weight) removed acid compounds, principally hydrogen chloride, from the gas stream and the cadmium acetate trap (25% aqueous solution by weight) removed sulfur compounds, principally hydrogen sulfide. The scrubbed vapor was collected as a whole over water, vented to atmosphere, or passed through a sample valve to a gas chromatograph for online analysis.

4.1.7 Heating and cooling system

Various heating and cooling systems were utilized to control the temperature of reaction system during the experiment.

a. Heating bands were used to control the reactor temperature.
b. A circulating bath was used to control the temperature of the mineral oil circulated through the reflux condenser.
c. Low temperature liquid circulating bath was used to maintain the temperature of the ethylene glycol + water mixture circulated through the liquid condenser, liquid collector coils, and the packing gland cooling jacket.

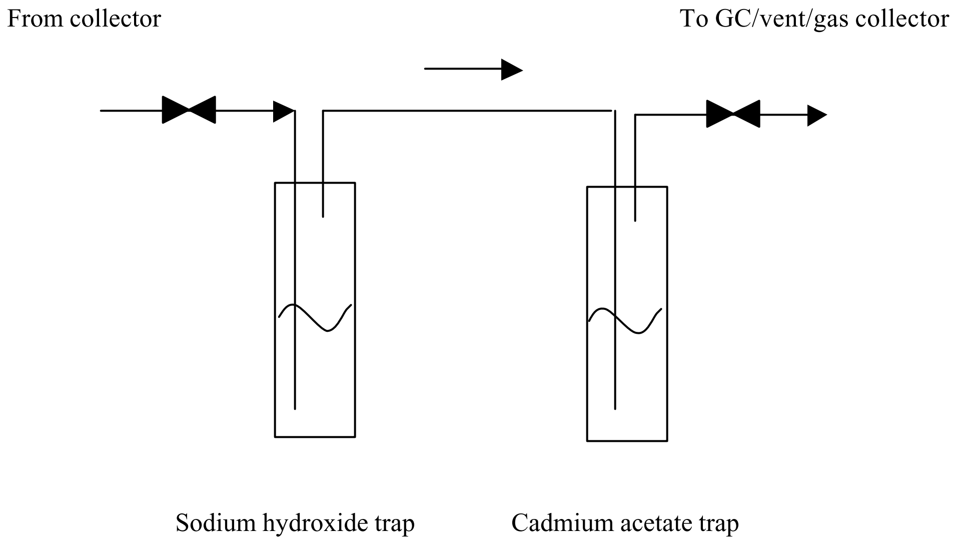

Figure 4.6 Acid gas scrubbing system.

4.1.8 Temperature monitoring and control system

The temperatures inside the reactor were monitored and controlled at two points, top and bottom by using thermocouples. The reactor temperature was controlled by using two band heaters located on the side walls of the reactor and a set of thermal couples outside of the reactor connected with a feedback control loop.

The following temperatures were measured and displayed continuously on the control panel: 1) reactor vessel: at two points inside the vessel, one near the top and the other near the bottom, and two points on the outside for controlling the band heaters (controllers); 2) reflux condenser: this was inferred by measuring the temperature of the circulating oil; 3) liquid condenser: this was measured by using a thermocouple located inside the condenser; 4) liquid collector, and 5) ambient temperature. All readings were recorded manually at 5-minute intervals during an experimental run.

4.1.9 Pressure monitoring and control system

A relief valve (burst disk with a pressure rating of 0.7 MPa (100 psi)) was mounted on the reactor top plate to prevent excessive pressures within the reactor. The outlet of the relief valve was connected directly into an exhaust fan intake manifold. Initially, a solenoid-controlled safety cut-off valve was located between the reflux and liquid condensers, however it was removed later because solid catalyst condensing in the small orifice obstructed the flow and prevented proper operation of the valve. The reactor pressure was controlled by adjusting the down stream flow-rate using the pressure control valve located immediately after the liquid collector.

The following pressures were measured by either pressure transducers or mechanical pressure indicators, and displayed continuously on the control panel: 1) blanket gas supply line; 2) reactor pressure: this inferred by measuring the pressure between the reflux and liquid condensers; 3) directly downstream of the pressure control valve; and 4) at the inlet to the gas flow meter. All readings are recorded manually at 5-minute intervals. The control panel also was equipped with an “Emergency” button that could shut off all electricity to the apparatus when activated.

4.1.10 Analysis

1. Liquid product analysis

After completing the experiment, the liquid product was removed from the room-temperature collector, weighed, and kept for further analysis. Liquid product samples were analyzed quantitatively by gas chromatography, or qualitatively by mass spectrometry. The mass spectrometry analysis was performed by Dr. Shane Tichy of the Department of Chemistry, Texas A&M University.

Six samples were submitted to Core Lab – Petroleum Services, Houston, Texas, for detailed characterization of the liquid fractions generated during the depolymerization experiments.

2. Liquefied petroleum gas (LPG) product analysis

The LPG product (typically C_3 to C_6) was analyzed during the experiment using a gas chromatograph. The gas chromatograph was set up so that the LPG could be sampled online during the experiment. Before each experiment, the gas chromatograph was calibrated using a standard gas containing CH_4, C_2H_6, C_3H_8, i-C_4H_{10}, n-C_4H_{10}, i-C_5H_{12}, and n-C_5H_{12}.

4.1.11 Carbon black and catalyst recovery system

Carbon black and catalyst recovery directly impacts the economic viability of the thermocatalytic decomposition process for vulcanized rubber. The experimental equipment and procedures for catalyst recovery are described by Liang (*20*).

4.2 Experimental materials

4.2.1 Rubber samples

Several model compounds were prepared for this work. Three compounds, each containing a single rubber and a single grade of carbon black, were designed to understand the effect of the process upon individual rubbers and carbon blacks that are significant ingredients in tires. Three model composites were designed to represent all ingredients present in black sidewall tires, white sidewall tires, and tires containing silica as a reinforcing agent. The model compounds and composites were prepared by the Cooper Tire Company, a Division of Cooper Tire & Rubber Co.

1. Model rubber compounds

The three vulcanized model rubber compounds were: a styrene butadiene rubber containing N234 grade carbon black (SBR/N234), a butyl rubber sample containing

N550 grade carbon black (BR/N550), and a natural rubber sample containing N121 grade carbon black (NR/N121). The model rubber compounds also contained zinc oxide, sulfur, and other chemical constituents in minor quantities.

2. Model tire composites

The model tire composites were silica rubber (Silica), white side wall rubber (WSW), and black side wall rubber (BSW). All rubber samples were supplied as particles approximately 5 – 10 mm in diameter.

4.2.2 Catalyst

The salts used as catalysts in this work were $AlCl_3$, and mixtures of $AlCl_3$ with $MgCl_2$, NaCl or KCl.

$AlCl_3$ is unstable in air and decomposes on contact with water vapor to form hydrochloric gas and aluminum oxide by reaction 1 (*57*):

$$AlCl_3\text{ (solid)} + 3\ H_2O\text{ (gas)} \rightarrow 6\ HCl\text{ (gas)} + Al_2O_3\text{ (solid)} \qquad (1)$$

The atmosphere contains sufficient water vapor to induce this reaction. Consequently, the catalyst must be handled in a controlled-atmosphere glove box containing a dry inert gas, while using rubber gloves and appropriate respiratory protection. Exposure to liquid phase water results in a violent, exothermic reaction. The reaction proceeds according to reaction 2, producing a hydrochloric acid solution that also contains aluminum ion complexes (*58*):

$$2\ AlCl_3 + 10\ H_2O \rightarrow [Al_2H_{18}O_{10}]^{+4} + 2\ H^+ + 6\ Cl^- \qquad (2)$$

Therefore, the aqueous solutions resulting from this reaction become quite acidic in nature. $AlCl_3$ catalyst poses additional challenges during the experiments, because its vapor pressure exceeds atmospheric pressure at the reaction temperatures. The elevated partial pressure of the catalyst causes considerable transport of catalyst vapor throughout the apparatus during the experimental walk.

Anhydrous $AlCl_3$ (Grade 0025) was purchased from Gulbrandsen Chemicals, La Porte, Texas. The catalyst was supplied in a 5-gallon bucket with a PVC liner. Anhydrous $MgCl_2$ (H_2O content < 5%) was purchased from VWR Scientific Products (catalog number is 20,833-7). It was manufactured by Aldrich Chemical Company, Inc., and shipped in a brown glass container containing 1 kg. The NaCl was purchased from the local grocery store.

Anhydrous $MgCl_2$ is deliquescent and tends to adsorb moisture on long time exposure to a wet atmosphere. It also needs to be handled in a controlled-atmosphere glove box containing a dry inert gas, while using rubber gloves and appropriate respiratory protection. The NaCl is considered stable at short time contact with the open surroundings and does not need specific handling procedures.

4.3 Experimental procedure

In all cases, a known amount of rubber was loaded into the feed hopper during equipment assembly. The mass of rubber was typically around 1 kg, mainly depending on the amount of residue material needed for further analysis and characterization. During the startup, the circulation baths were brought to operational conditions while the reactor was pressure tested at a pressure higher than the expected operating pressure using an inner gas, such as nitrogen or argon. In most cases the reflux condenser was controlled at 100 ^{o}C, the liquid condenser at 0 ^{o}C, and the liquid collector at ambient temperature, 25 ^{o}C. After reducing the reactor pressure to atmospheric pressure, catalyst was loaded into the reactor through a port in the top plate, while providing an inert flow of argon or nitrogen to maintain a water-free environment (see Figure 4.7). The stirrer was operated continuously at approximately 50 rpm. Then the catalyst feed port was closed and the system pressurized to approximately 0.4 MPa (45 psig) for a final pressure test. The pressure test criterion was that the rate of decrease in internal pressure was less than 2 kPa (0.4 psi) over 15 min. The depolymerization runs were performed at a lower pressure, typically 275 kPa to 310 kPa (25 psig to 30 psig). Then the reactor was increased to the desired reaction temperature, typically 220 ^{o}C, while carefully noting any changes to the system pressure and bed temperature profile. All experimental

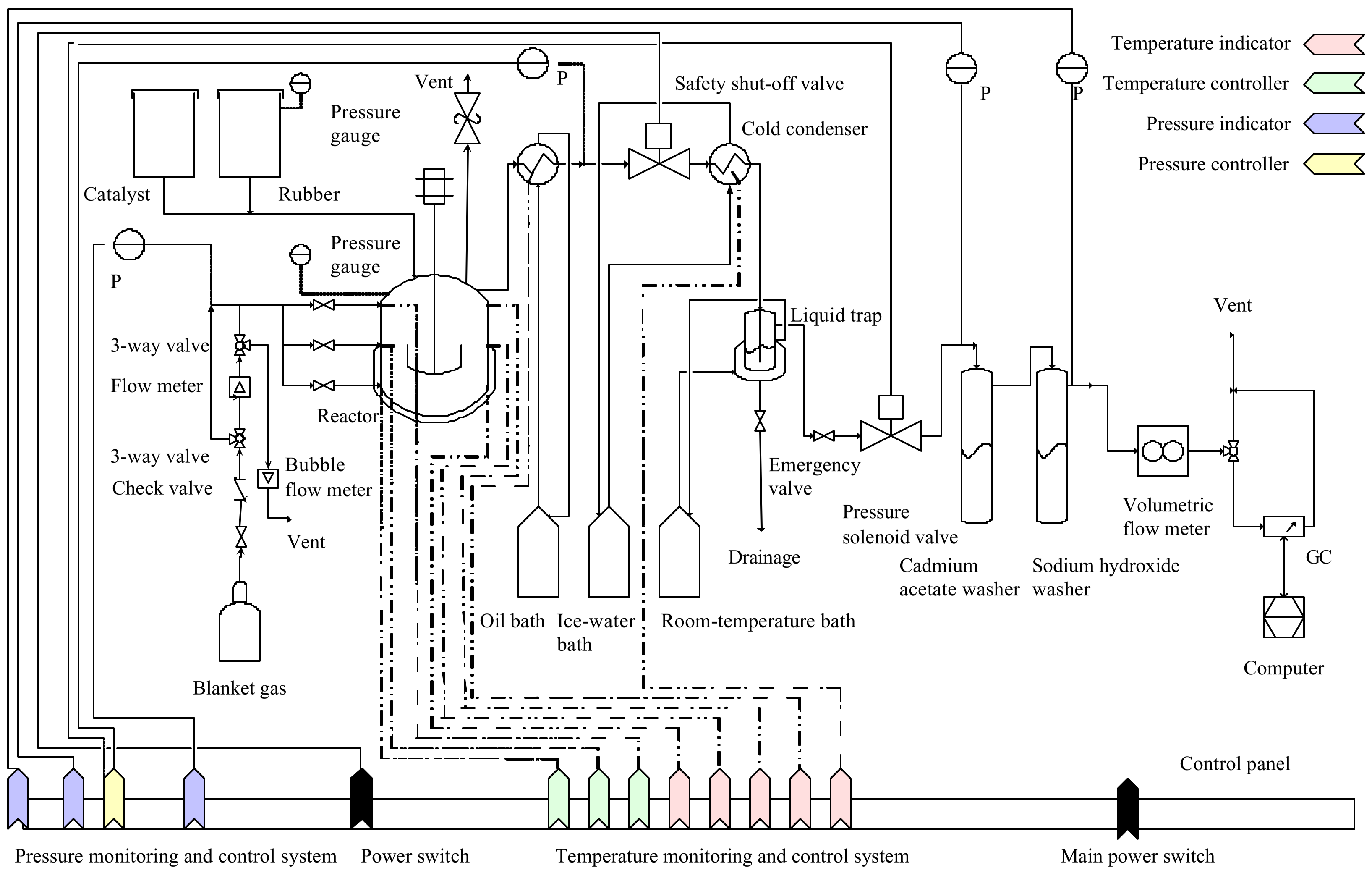

Figure 4.7 Process flow diagram.

variables, such as temperatures, pressures, and flow rates, were recorded at 5-min intervals. Upon reaching the desired reaction conditions, the rubber was added by operating the horizontal rubber feeder auger manually, again noting any changes in temperature and pressure. After adding all of the rubber feedstock, the reactor conditions were maintained at reaction temperature and pressure for at least 2 more hours to ensure complete decomposition of the rubber. During one run (Run III-07), this period was extended to 6 hours, except that there was no decomposition more than 2 hours after the last rubber fed. Once the reaction was completed, the reactor heaters and the circulating baths were shut down. In most cases, the stirrer was kept running until the reactor temperature dropped to approximately 50 ^{o}C.

The procedures for catalyst recovery, carbon black recovery, and residue workup are given by Liang (*20*).

CHAPTER V

RESULTS AND DISCUSSION

The study (Phase III) began in June 2001 with the intention of verifying the performance of the proposed process with aluminum chloride, evaluating the economic potential of the process, and obtaining sufficient information to allow design of a pilot- or commercial-scale unit. The study was performed in two stages. The first stage used model rubber compounds containing a single rubber and a single grade of carbon black. The second stage used model tire rubber composites representing black side wall tires, white side wall tires, and silica-reinforced tires (see also Sections 4.2.1). Some experiments were performed to evaluate the effect of co-catalyst system in reducing catalyst costs for the process. Six naphtha samples from the current study were submitted to a commercial laboratory (Core Lab – Petroleum Services, Houston, Texas) for detailed analysis of the composition of the naphtha fraction generated during the depolymerization runs. The information from this and previous work was used to develop a possible mechanism for the thermocatalytic depolymerization of vulcanized rubber using aluminum chloride as a pure or co-catalyst. The experimental results and the resulting hypothesis are discussed in the following sections.

5.1 Model rubber compounds

Approximately 30 runs were completed on model rubber compounds between December 27, 2001 and May 31, 2002. Fifteen runs (III-00A to III-00N and III-0S1) were performed during equipment set-up and verification. These runs will not be discussed in detail, but the information gained from these runs was used in the interpretation of the runs performed for the Phase III program (III-1, III-1A, III-1B, III-1C, III-1D, III-2, III-2A, III-2B, III-3, III-3A, III-4, III-5, III-6, III-7). In this notation, the numerals 1, 2, 3, *etc.* denote different experimental conditions and the suffixes A, B, C, *etc.* denote replications of a particular set of experimental conditions.

5.1.1 Process related issues

1. Catalyst plugging problem

The Phase III start-up experiments, after modification of the Phase II equipment, revealed some unexpected operational difficulties. The following changes were made to eliminate glassware from the reaction system: the glass rubber feeder was replaced by a brass and acrylic assembly, glass condensers were replaced by stainless steel units, and more heating power was supplied to the reactor vessel. Those changes provided more efficient condensation of catalyst as a solid from the vapor phase, resulting in repeated plugging of the downstream equipment. Similar problems initially were encountered in the rubber feeder section. The upstream problems were eliminated by providing adequate torque to drive the vertical feeder auger. The blockages observed in the downstream equipment were more difficult to prevent. All the solenoid valves introduced to provide emergency shut-off capability had to be removed. They contained small orifices that plugged with catalyst during the run, even though the condensers removed most of the catalyst from the vapor stream.

Many of the earliest Phase III start-up experiments were terminated prematurely due to blockage by condensed catalyst. The catalyst condensation effect was cumulative, so the probability of blockage increased as time elapsed during an experiment. Several runs were terminated after only 5 to 60 min on-line because of blockages. To avoid plugging, high rubber feed rates were employed to complete the experiments as quickly as possible. However, high rubber feeding rates also had a disadvantage. Early in the run, while the catalyst vapor pressure was still high, the vapor products carried the catalyst into the condensers. Runs typically lasted for approximately 1 h before the bottom section of the reflux condenser would plug completely, requiring termination of the run. In an effort to inhibit catalyst vaporization, the reactor vessel was filled with argon and heated while maintaining an internal pressure of approximately 140 kPa (20 psig). However, once the feeding of the rubber began, the pressure was allowed to rise to approximately 180 kPa (26 psig) under the assumption that the vapor expelled from the reactor initially was predominantly argon. It now is clear that, once the catalyst was heated past its melting point, most of the argon already had been expelled from the reactor and the vapor phase was composed mostly of catalyst.

In the later runs, plugging of the reflux condenser was avoided by manually pushing a combination plunger and scraper device through the reflux condenser at least once per minute to remove catalyst condensing on the lower wall of the condenser. After approximately 200 to 300 grams of rubber was fed, catalyst condensation became less problematic, so that during most runs, the plunger operation was stopped after the rubber was fed. It was observed that the tendency of the catalyst to leave the reactor vessel decreased as the accumulated amount of rubber fed increased. In addition, for the current equipment, the severity of the plugging problem increases with the amount of catalyst initially loaded into the reaction vessel. These observations are consistent with the results of previous experimental programs.

The improvements made to the reactor heater in this project contributed to the severity of the plugging. In previous work, the 2 L reactor clearly had several cold spots, especially at the top plate. Such cold spots also were present to some extent in a 10 L reactor. When significant cold spots are present, catalyst condenses on the cold surfaces, thereby lowering the partial pressure of catalyst in the vapor phase and minimizing the condenser blockages. Also, the glass condensers used previously were less efficient, so that more catalyst could pass through the condenser, and, because glass is less porous than steel, the condensed catalyst did not adhere as strongly to the glass surfaces.

2. Heating profiles in reactor

The heater bands around the reactor were driven with PID controllers and SCR power packs. Experiments with no catalyst and rubber in the reactor vessel revealed that the bottom and top of the reactor could be heated and maintained within 20 ^{o}C of each other with no difficulty. The empty reactor also could be heated easily to a temperature of 300 ^{o}C. The heating profile for the empty vessel is shown in Figure 5.1. However, when the vessel initially was loaded with catalyst and the rubber added later, the heating profile changed significantly. Figure 5.2 shows the heating profiles for a loaded reactor.

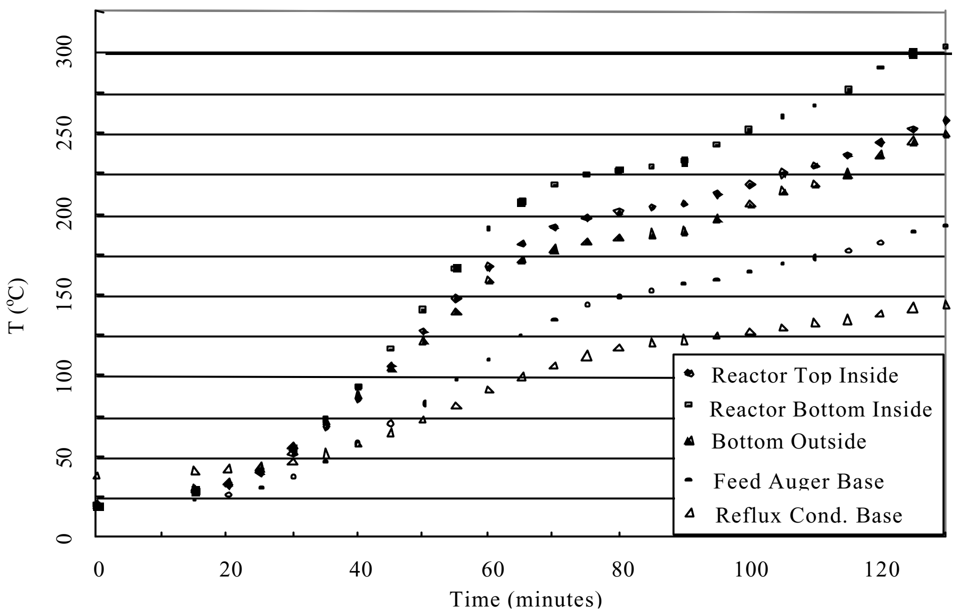

Figure 5.1 Temperature profile as a function of time for empty reactor vessel.

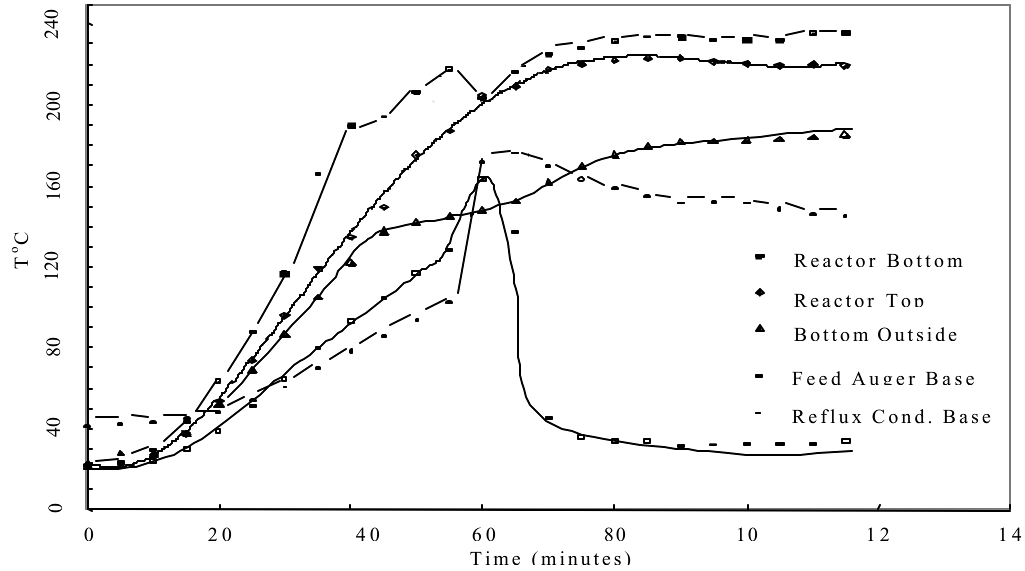

Figure 5.2 Temperature profile as a function of time for the reactor vessel charged with catalyst.

It is clear from the reactor bed profile that the heating pattern deviates from its linear heating pattern upon reaching a temperature of 180 °C to 185 °C where catalyst vaporization and melting become significant. (The triple point temperature and pressure of $AlCl_3$ are approximately 192.5 °C and 230 kPa (34 psia) respectively). The temperature profiles tend to flatten until the reactor contents reach an approximate temperature of 194 °C to 195 °C. Above 195 °C, the temperature increase is again linear, but at a much slower rate, to at least 210 °C. Above 210 °C, the heating profiles differed significantly from run to run, in some cases easily reaching 220 °C, but in most cases laboring to get to 215 °C. Although the thermocouple around the feed auger base failed in the middle of testing, its temperature profile showed the same trend as that around condenser base before the termination of this experiment.

The phase diagram of the catalyst, including the temperature dependence of the sublimation and vapor pressure curves, provides insight for interpreting the heating profiles and other observations of reactor operation. Figure 2.6 shows the sublimation and vapor pressure curves for $AlCl_3$. Clearly, the catalyst becomes more difficult to contain as the reactor temperature increases. For an isothermal reactor (no cold spots), the vapor pressure would be approximately 70 kPa (10 psia) at 175 °C, rising exponentially to 410 kPa (60 psia) at ~225 °C (the temperature at which most of the experiments were performed). Elevated vapor pressures clearly contribute to the difficulties caused by catalyst transport in the current apparatus, especially at 250 °C (aborted Run III-05). The operating pressures maintained in the reactor during experiments corresponded to $AlCl_3$ vapor pressures between 210 °C and 215 °C. The catalyst vapor pressure is a significant design consideration for the reactor configuration, especially for operation at temperatures above 225 °C.

The observation in this work strongly suggest that the runs performed successfully in the previous 2 L reactor at 300 ^{o}C were possible only because cold surface areas sufficient to suppress the catalyst vapor pressure existed in the reactor unit. The reduced size and scale of the runs at that time, and the reactor geometry, also contributed to their successful completion. It also is likely that heat transfer effects associated with refluxing within the reactor, *i.e.*, liquid catalyst condensing on the top of the reactor and then falling to the bottom, contributed significantly to the slow increases in reactor temperature when the upper surfaces exceeded 195 °C. The current experimental equipment probably better represents the behavior and dynamics of the catalyst in a larger scale reactor.

The reactor loaded with catalyst exhibits the heating profiles shown in Figure 5.2 when heated from room temperature to the reaction temperature. Upon the first addition of rubber, the temperature typically, although not always, dropped sharply, with the magnitude of the drop consistent with the thermal effect of the amount of rubber fed. At the same time, the reflux condenser and feeder assembly temperatures rose sharply, probably as the result of an exothermic reaction between the catalyst and the hydrocarbon products initially present in the vapor phase.

3. Recovery of catalyst

Because of the high vapor pressure of the catalyst, the conceptual design of the process assumed that the catalyst could be separated from the nonvolatile reaction products by evaporation. However, the experiment showed the catalyst does not evaporate from the residue as expected. A complete discussion of the observations and implications for catalyst recovery is given by Liang (*20*).

5.1.2 Experimental result analysis

We completed depolymerization studies on three different kinds of rubber compounds: synthetic (SBR), natural, and butyl rubber, each containing a different grade of carbon black. All of these samples are model compounds prepared by Cooper Tire. The compositions of the samples are given in Table 5.1, both in terms of parts per hundred parts of rubber and as an overall weight fraction. The experimental results are summarized in Table 5.2. The runs were performed at a nominal reactor temperature of 225 ^{o}C and a reflux condenser temperature of 70 ^{o}C, except for one run (III-04) with the reactor at 250 °C and another (III-06) with the reflux condenser at 100 °C. We did not observe any indication of unreacted rubber remaining in the reactor after these experiments.

1. Terminology

In this section, we define the terminology to be used in the discussion of the results through the following discussions to avoid ambiguity and misinterpretation. There are two classes of products formed by the depolymerization reaction: *volatile hydrocarbons* (VHC) and *nonvolatile hydrocarbons* (NVHC). The volatile hydrocarbons are mostly saturated compounds with vapor pressures sufficiently high that they leave the reactor as a vapor upon formation. The nonvolatile hydrocarbons with sufficiently low vapor pressures remain in the reactor, probably trapped on the surface of the carbon black particles present in the feedstock rubber. The rubber samples also contain carbon black and zinc oxide, which are not expected to participate in the reaction. These will be referred to as *nonreactables* (NR) in the discussion.

Table 5.1 Compositions of Model Rubber Samples

Cooper sample designation	402		403		404	
shorthand sample designation	SBR		natural		butyl	
ingredients	PHR [a]	wt. %	PHR	wt. %	PHR	wt. %
natural rubber	0.0	0.0	0.0	0.0	100.0	57.7
SBR rubber, cold emulsion, 23.5% styrene	137.5	54.7	0.0	0.0	0.0	0.0
isobutylene isoprene rubber	0.0	0.0	100.0	55.9	0.0	0.0
N234 carbon black [b]	90.0	35.8	0.0	0.0	0.0	0.0
N650 carbon clack [b]	0.0	0.0	60.0	33.5	0.0	0.0
N121 carbon black [b]	0.0	0.0	0.0	0.0	52.0	30.0
zinc oxide [b]	3.0	1.2	5.0	2.8	5.0	2.9
stearic acid	2.0	0.8	2.0	1.1	2.0	1.2
dimethylbutyl p-phenylene diamine	3.0	1.2	0.0	0.0	3.0	1.7
wax	1.5	0.6	0.0	0.0	1.5	0.9
diaryl-p-phenylendiamine	0.5	0.2	0.0	0.0	0.5	0.3
aromatic petroleum oil	10.0	4.0	0.0	0.0	6.0	3.5
napthenic petroleum oil	0.0	0.0	10.0	5.6	0.0	0.0
elemental sulfur	1.8	0.7	0.5	0.3	2.0	1.2
tert, butyl benzthiazole sulfenamide (TBBS)	1.8	0.7	0.0	0.0	1.2	0.7
2,2 benzothiazyl disulfide	0.0	0.0	1.5	0.8	0.0	0.0
tetramethyl thiuram disulfide (TMTD)	0.2	0.1	0.0	0.0	0.0	0.0
total	251.3	100.0	179.0	100.0	173.2	100.0
total assumed nonreactable	93.0	37.0	65.0	36.3	57.0	32.9

[a] sample compositions in parts per hundred parts of rubber
[b] defined as nonreactables

Table 5.2 Experimental Measurements

run number		III-01D	III-02B	III-03	III-03A	III-04	III-06	III-07
run date(mm/dd/yy)		05/15/02	04/29/02	05/01/02	05/22/02	05/03/02	05/17/02	05/24/02
feedstock	(rubber)	SBR	natural	butyl	butyl	SBR	SBR	SBR
carbon black type		N234	N121	N650	N650	N234	N234	N234
carbon black content	(wt %)	35.8	30.0	33.5	33.5	35.8	35.8	35.8
feed gas		argon	argon	argon	argon	argon	argon	argon
nominal reactor temperature	(°C)	225	225	225	225	250	225	225
reflux condenser temperature	(°C)	70	70	70	70	70	100	70
pressure	(psig)	25	25	25	25	25	25	25
time on line after last feed	(h)	2	2	2	2	2	2	6
rubber in	(g)	682.0	675.0	609.0	609.0	664.0	691.0	621.0
catalyst in	(g)	837.8	851.3	839.8	827.1	850.5	848.3	842.6
ratio (catalyst : rubber)		1.23	1.26	1.38	1.36	1.23	1.23	1.23
rubber feed rate	(g/min)	13.6	9.0	24.36	30.5	11.1	15.4	12.4
residue in reactor	(g)	1345.4	1289	1194.6	1165.5	1297.0	1338.9	1279.8
evaporated catalyst	(g)	28.4	66.0	44.7	39.6	69.0	65.2	39.4
washed & dried residue	(g)	322.9	426.8	268.2	315.9	399.4	537.4	480.2
naphtha product (mass)	(g)	9.0	12.0	16.7	13.9	12.6	9.3	3.8
LPG products (mass)	(g)	149.3	142.1	203.9	236.0	134.4	171.3	225.1
flow rate (gas volume)	(L)	87.73	82.5	105.89	119.5	82.18	98.89	126.47
naphtha density	(g/cm^3)	---	---	---	0.79	0.74	0.72	---
LPG-average molecular weight	(g/mol)	54.279	56.083	58.187	58.016	52.741	53.302	54.118
LPG composition								
C_1	(vol %)	0.34	0.00	0.00	0.00	0.00	0.00	0.27
C_2	(vol %)	0.00	0.15	0.00	0.00	0.42	0.14	0.20
C_3	(vol %)	35.44	19.64	13.90	6.59	46.77	43.06	40.55

Table 5.2 (continued)

run number		III-01D	III-02B	III-03	III-03A	III-04	III-06	III-07
i-C_4	(vol %)	44.75	57.55	67.15	86.82	31.84	34.02	44.75
n-C_4	(vol %)	11.01	17.44	5.68	1.10	11.80	14.36	11.01
i-C_5	(vol %)	6.57	4.30	11.39	5.19	6.53	5.91	6.57
n-C_5	(vol %)	1.31	0.75	0.43	0.00	1.09	1.29	1.31
un-C_5 [a]	(vol %)	0.00	0.00	0.06	0.00	0.29	0.14	0.00
i-C_6	(vol %)	0.59	0.17	1.06	0.26	0.71	0.52	0.59
n-C_6	(vol %)	0.00	0.00	0.30	0.00	0.26	0.17	0.00
un-C_6 [a]	(vol %)	0.00	0.00	0.00	0.00	0.00	0.17	0.00
i-C_7	(vol %)	0.00	0.00	0.02	0.03	0.29	0.21	0.00
n-C_7	(vol %)	0.00	0.00	0.00	0.00	0.00	0.00	0.00
un-C_7 [a]	(vol %)	0.00	0.00	0.00	0.00	0.00	0.00	0.00
C_8^+	(vol %)	0.00	0.00	0.00	0.00	0.00	0.00	0.00
total	(vol %)	100.00	100.00	100.00	100.00	100.00	100.00	100.00

[a] The prefix *un*- denotes unidentified isomers of C_n

The volatile hydrocarbons fall into two classes, which are defined by the operating procedure. The portion that condenses at 0 °C and remains as liquid in a room temperature trap at atmospheric pressure will be denoted as naphtha, and the remainder will be denoted as LPG, liquefied petroleum gas. The split between these fractions is somewhat arbitrary, but the total of these represents the liquid products of the reaction. Equations 3 to 5 are useful for design considerations, because they represent the proportion of feedstock converted to this product:

$$\text{Liquid yield} = \frac{\text{Mass of volatile hydrocarbons produced}}{\text{Mass of feedstock}} \tag{3}$$

$$\text{Naphtha yield} = \frac{\text{Mass of naphtha produced}}{\text{Mass of feedstock}} \tag{4}$$

$$\text{LPG yield} = \frac{\text{Mass of LPG produced}}{\text{Mass of feedstock}} \tag{5}$$

The yield of liquid can never be 100% because of the presence of the nonreactable materials in the feedstock. However, a useful measurement of the effectiveness of the process can be obtained by calculating the fraction of reactable material converted to the volatile hydrocarbon product as shown in equation 6:

$$\text{Liquid conversion} = \frac{\text{Mass of volatile hydrocarbons produced}}{\text{Mass of feedstock} \times \left(1 - \text{fraction of nonreactables}\right)} \tag{6}$$

Because there is insufficient hydrogen present to convert all rubber to saturated hydrocarbons, the reaction stoichiometry prevents 100% liquid conversion rates.

The depolymerization reaction also produces a solid residue product that includes both the nonvolatile hydrocarbons formed and the nonreactable material in the feedstock. At the end of the experiment, the reactor contains both the solid residue and catalyst, and the condensers contain some evaporated catalyst. All catalyst, solid residue, and liquid products must be accounted for to complete the material balance. The calculation of the liquid product mass is demonstrated in Appendix A. The calculation of the solid residue yield was done in two ways, one of which assumed that all catalyst was recovered (ideal residue yield, equation 7) and the other was based upon the solid residue remaining after washing with acid and drying (actual residue yield, equation 8).

$$\text{Ideal residue yield} = \frac{\text{Total solid mass} - \text{initial catalyst charge}}{\text{Mass of feedstock}} \tag{7}$$

$$\text{Actual residue yield} = \frac{\text{Mass of washed and dried residue}}{\text{Mass of feedstock}} \tag{8}$$

Differences between the two values have two principal sources: less than 100% recovery of the catalyst, which means that oxidation (or combustion) of the solid residue product during drying, or incomplete drying so that significant amounts of water remain in the residue.

2. Mass balance

The mass balances, product yields, and conversions of the reactable materials to liquid products obtained in these experiments are shown in Table 5.3. Because the total mass balances are based upon measurements made before any post-treatment of the solid residue, they provide an internal consistency test of the gas flow meter calibration. In general, the mass balances are satisfactory, although the last two runs support our suspicions from other observations that the gas flow meter performance had deteriorated over time. We since have replaced the flow meter for subsequent experiments, but the flow meter readings for experiments III-06 and III-07 may be too high.

3. Consistency test of solid residue treatment

Comparison of ideal residue yield with actual residue yield provides a consistency test for the solid residue treatment procedure. There are two primary effects in the residue treatment: 1) oxidation or combustion of sample during the drying procedure, and 2) incomplete removal of water during the drying procedure. Losses due to oxidation cause the actual residue yield to be lowered, whereas incomplete removal of water causes the opposite effect. In early runs, we had not expected significant oxidation to occur at temperatures as low as 100 to 120 °C, because these temperatures are below the ignition temperatures of most hydrocarbons. For experiments III-06 and

Table 5.3 Mass Balances and Conversions

run number		III-01D	III-02B	III-03	III-03A	III-04	III-06	III-07
run date		05/15/02	04/29/02	05/01/02	05/22/02	05/03/02	05/17/02	05/24/02
feedstock	rubber	SBR	natural	butyl	butyl	SBR	SBR	SBR
carbon black type		N234	N121	N650	N650	N234	N234	N234
carbon black content	(wt %)	35.8	30.0	33.5	33.5	35.8	35.8	35.8
blanket gas		argon	Argon	argon	argon	argon	argon	argon
nominal reactor temperature	(°C)	225	225	225	225	250	225	225
reflux condenser temperture	(°C)	70	70	70	70	70	100	70
pressure	(kPa)	270	270	270	270	270	270	270
time on line after last feed	(h)	2	2	2	2	2	2	6
rubber in	(g)	682.0	675.0	609.0	609.0	664.0	691.0	621.0
catalyst in	(g)	837.8	851.3	839.8	827.1	850.5	848.3	842.6
ratio (catalyst : rubber)		1.23	1.26	1.38	1.36	1.23	1.23	1.23
rubber feed rate	(g/min)	13.6	9.0	24.36	30.5	11.1	15.4	12.4
total mass balance	(%)	100.0	98.9	100.8	101.3	99.9	103.0	105.8
feedstock/products mass balance	(wt %)	70.6	86.1	80.3	92.9	82.3	103.9	114.2
nonreactables	(wt %)	37.0	32.9	36.3	36.3	37.0	37.0	37.0
ideal residue yield	(wt %)	78.6	74.6	65.6	62.1	77.6	80.4	76.7
actual residue yield	(wt %)	47.3	63.2	44.0	51.9	60.2	77.8	77.3
liquid yield	(wt %)	23.2	22.8	36.2	41.0	22.1	26.1	36.9
liquid conversion	(%)	36.9	34.0	56.9	64.4	35.1	41.5	58.5
naphtha yield	(wt %)	1.3	1.8	2.7	2.3	1.9	1.3	0.6
naphtha density	(g/cm^3)	---	---	---	0.79	0.74	0.72	---
LPG yield	(wt %)	21.9	21.1	33.5	38.8	20.2	24.8	36.2
LPG component yield		SBR	natural	butyl	butyl	SBR	SBR	SBR
C_1	(wt %)	0.02	0.00	0.00	0.00	0.00	0.00	0.03
C_2	(wt %)	0.00	0.02	0.00	0.00	0.05	0.02	0.04
C_3	(wt %)	6.30	3.25	1.68	1.94	7.89	8.81	11.91
i-C_4	(wt %)	10.49	12.56	29.13	33.72	7.08	9.18	11.06
n-C_4	(wt %)	2.58	3.81	0.37	0.43	2.62	3.88	6.75
i-C_5	(wt %)	1.91	1.16	2.16	2.50	1.80	1.98	3.62
n-C_5	(wt %)	0.38	0.20	0.00	0.00	0.30	0.43	1.32
un-C_5 [a]	(wt %)	0.00	0.00	0.00	0.00	0.08	0.05	0.21
i-C_6	(wt %)	0.20	0.05	0.13	0.15	0.23	0.21	0.63
n-C_6	(wt %)	0.00	0.00	0.00	0.00	0.09	0.07	0.23
un-C_6 [a]	(wt %)	0.00	0.00	0.00	0.00	0.00	0.07	0.22
i-C_7	(wt %)	0.00	0.00	0.02	0.02	0.11	0.10	0.21
n-C_7	(wt %)	0.00	0.00	0.00	0.00	0.00	0.00	0.00
un-C_7 [a]	(wt %)	0.00	0.00	0.00	0.00	0.00	0.00	0.00
C_8^+	(wt %)	0.00	0.00	0.00	0.00	0.00	0.00	0.00

[a] The prefix *un*- denotes unidentified isomers of C_n

III-07, the drying procedure was monitored very carefully in an attempt to avoid significant oxidation, and the ideal and actual residue yields are in much closer agreement. The recovery, treatment and characterization of the solid residue are discussed in detail by Liang (*20*).

4. Total liquid product yields

The data in Table 5.3 show that the liquid product yields are significantly higher for the butyl rubbers than for the SBR and natural rubber samples. The liquid yields for the butyl rubber samples ranged from 36 to 40% by weight of feedstock, whereas the SBR and natural rubber samples generally fell between 23 and 27%. (The liquid yield shown for experiment III-07 may be erroneously high due to deteriorating flow meter performance.) When considered in terms of the amount of potentially reactable material present, the conversions to liquid ranged from 35 to 40% for the SBR and natural rubber samples and from 57 to 64% for the butyl rubber samples. Experiment III-03 was replicated (experiment III-03A) to verify that the significantly different behavior of the butyl rubber was real. These experiments show that the depolymerization reaction of the rubber produces a significant amount of nonvolatile hydrocarbons. The nonvolatile hydrocarbons formed most likely remain on the surface of the carbon black after the reaction because removal of catalyst by acid washing produce a fine powder.

5. Naphtha yield

The *naphtha* yields are of the same order of magnitude as those obtained during Phase II. The yield was the highest for the butyl rubber at 2.3 to 2.7% and similar for the natural and SBR rubber at 1.3 to 1.9%. The *naphtha* products in Experiments III-03A, III-04 and III-06 had densities ranging from 720.0 kg/m^3 to 790.0 kg/m^3. As shown in Table 5.4, one sample analyzed by mass spectrometry indicates that the major constituents of the naphtha fraction are similar to those obtained during the Phase II work, consisting mainly of C_5, C_6, C_7 and C_8 isomers, benzene and some saturated cyclic hydrocarbons. The Phase II experiments and a Phase III startup experiment with normal decane, observed to depolymerize vigorously at 80 °C, suggest that the *naphtha* components are formed primarily from the extender oil in the rubber.

We believe that the longer chain hydrocarbon products are reduced to the observed propane, butane, and pentane products observed in the LPG fraction by reactions with $AlCl_3$ in both the liquid and vapor phases. This reaction is so effective that minimal naphtha products emerge from the reactor. The fact that little naphtha is observed may be as much a result of secondary depolymerization as of primary depolymerization. This hypothesis is consistent with the behavior observed when *n*-decane was observed to depolymerize vigorously at 80 °C during the start-up runs.

Table 5.4 Comparison of Principal Constituents for Naphtha Products Produced by Phase II and Phase III Experiments

component [a]	III-01A relative peak %	II-03 [b] volume %
iso-butane	6.7	0.46
pentane	13.13	7.19
not identified	5.33	
hexane	13.13	0.21
pentane, 2-methyl		4.26
pentane, 3-methyl	8.24	2.53
cyclo-pentane, methyl		6.511
cyclo-propane, 1-ethyl-1-methyl	6.90	
1-pentene, 4-methyl	11.10	
benzene	14.58	2.48
toluene		7.57
hexane, 2-ethyl		7.21
not identified	5.78	
cyclo-hexane, methyl-	13.95	8.64
not identified	0.43	
not identified	0.25	
unidentified $C_{22}H_{18}$ compound	0.42	-
heptane, 2-methyl		1.03
hexane, 3-ethyl		7.21
cyclo-pentane, 1c, 2t, 3-tri-metyl		2.67

[a] only those constituents that appear in significant quantity in one or the other sample are listed.
[b] Phase II study performed by Dawid J. Duvenhage during 1994-1995. [56]

No evidence of carbon-bonded sulfur or chloride compounds was found in the mass spectrometry analysis of the naphtha sample. However, the two scrubber units employed downstream before the tail gas is vented provide evidence of chloride transport through the reflux and liquid condensers to the liquid trap, probably as hydrogen chloride gas. The 25% NaOH solution typically changes in pH from >14 to as low as 2 during an experiment. The cadmium acetate solution normally showed a slight color change indicating the presence of some sulfur compounds, most likely H_2S. The sulfur and chloride levels were not quantified.

6. Production of LPG

The liquefied petroleum gas (LPG) fractions exhibit a pattern similar to that of the naphtha fractions, with similar yields from the SBR and natural rubber samples (22 to 26%), and significantly larger yields (36 to 41%) from the butyl rubber samples. It is clear that significantly more volatile hydrocarbons are produced from the butyl rubber than from SBR or natural rubber. The LPG fraction was similar in composition for the SBR and natural rubber samples, containing mostly propane and butane, with small amounts of heavier hydrocarbons present. Isobutane is the most abundant isomer in all cases. The butyl rubber experiments produced significantly larger fractions of isobutane and pentanes than the natural and SBR rubbers.

5.1.3 Process parameters

1. Reflux condenser temperature

The reflux condenser was included in the process design to accomplish two purposes: 1) to tailor the overhead products by recycling some heavier hydrocarbons into the reactor, and 2) to flush condensing solid catalyst back into the reactor to prevent plugging of the condenser. All of the experiments except one (III-06) were run with the condenser at 70 °C. (The temperature of 70 °C was chosen to be sufficiently low that reaction of *n*-decane with the catalyst would not occur.) There is no significant difference in results between the product spectrum for Run III-06 and the other experiments. Because the product distributions for these experiments are such that essentially none of the product condenses at 70 °C, increasing the reflux condenser temperature has no effect. In addition, because no condensation of hydrocarbons occurs, flushing of catalyst does not occur, resulting in accumulation of solid catalyst within the condenser and subsequent blockage of flow. The depolymerization reaction appears to reduce the molecular size so rapidly that the volatile hydrocarbons are reduced to the LPG constituents before they leave the reactor. Some condensation of hydrocarbons in the reflux condenser was observed in the early experiments in smaller reactors where the experimental conditions probably produced lower partial pressures of $AlCl_3$ in the vapor phase.

2. Duration of experiment

During most Phase II and Phase III experiments, the sample generally was fed over a period of approximately 1 h, and the reactor maintained at experimental conditions for approximately 2 h after the last rubber was fed. To test whether 2 h was sufficient to achieve complete conversion, experiment III-07 was maintained at reaction temperature for 6 h after the last sample was fed. The yields were essentially the same, except that the propane content of the LPG was elevated slightly. The overall mass balance is 105.8%, and we suspect that the discrepancy results from erroneously high gas flow meter readings. Because of this, the slightly higher yields shown in Table 5.3 for Experiment III-07 probably are not significant. Also, during this run the rubber feedstock was added over approximately 1 h, compared with 30 to 45 min for many of the experiments. The slower feed rate may have increased the residence time of products in the reactor, resulting in smaller product molecules. In addition, less liquid product was collected in the accumulator because the relatively volatile naphtha constituents evaporate into the LPG product as the sweep gas continues to pass through the liquid accumulator. Rubber feed rates and the effect thereof on the product spectrum also should be investigated in more detail.

3. Reactor temperature

For all experiments except one, the rubber was fed while the reactor temperature ranged from 210 to 225 °C. In Experiment III-04, the rubber was fed with the reactor temperatures between 225 °C and 250 °C, with approximately half of the rubber fed at the higher temperature. The differences do not appear to be significant, although the propane fraction in the LPG product is increased slightly and the naphtha fraction is slightly larger.

4. Reactor loading

For the experiments reported here, ratios of catalyst to rubber were slightly greater than unity, ranging from 1.1 to 1.4. These ratios were chosen to ensure that there was sufficient catalyst available to decompose the rubber. The rubber charges varied from 600 to 700 g, and the catalyst charges from 827 to 850 g. During the startup experiments, we found that catalyst charges in excess of 900 g introduced such severe problems with catalyst transport and downstream blockages that the experiments could not be completed.

5.2 Model tire rubber composites

5.2.1 Introduction

This section describes the results of thermocatalytic depolymerization experiments performed on three model tire composite samples. The samples were formulated to represent specific parts of typical tires. The model composites represented tires reinforced with silica (Silica), white side wall tires (WSW), and black side wall tires (BSW). The samples were fed as particles approximately 5 mm to 10 mm in diameter. The experiments were also performed at 225 °C, using pure aluminum chloride as the catalyst. The rubber generally was fed over a period of 40 to 50 min, and the reactor held at temperature for about 2 h after the last rubber was fed. As discussed before, there are two primary products of the reaction: volatile hydrocarbons that leave the reactor as vapors and nonvolatile hydrocarbons that remain in the reactor. The reactor residue was washed with water to remove the catalyst, yielding a fine black powder that contained both the carbon black and the nonvolatile products. The volatile hydrocarbons were divided into two fractions, those collected in an accumulator as a liquid at ambient conditions (naphtha) and those leaving the accumulator as vapor (LPG).

In general, the products from experimental tire rubber mixtures are consistent with those observed from thermocatalytic depolymerization on model compounds of SBR and natural rubber.

The WSW and BSW rubber samples yielded 18 and 21% by weight of the feedstock as liquid products (about 0.8% as naphtha and the remainder as LPG), respectively. The liquid yield from Silica was similar at 17% (about 1.8% naphtha) of the feed. The LPG products generally had a composition that would qualify them as isobutane in the market place.

The results of four runs performed on the model tire composite are described below.

5.2.2 Reactor operating procedure, and reaction

The laboratory depolymerization equipment, reaction, catalyst, and product work up are similar to the previous experiments before and will not be discussed in detail here. The equipment was modified to allow for capture of the entire vapor product over water in six 20 L water containers equipped with the necessary valve and manifolds. The procedure followed here is exactly the same as before, with an additional benefit, which allowed LPG fractions from three runs to be transferred into gas containers for further analysis at a later stage. Helium also replaced argon as the carrier gas.

5.2.3 Results and discussion

Four experiments were completed between September 23, 2002, and October 4, 2002. The resulst are discussed in detail below (III-9, III-9A, III-10, and III-11). In this notation, the numerals 1, 2, 3, … denote different experimental conditions and suffixes A, B, C, … denote replications of a particular set of conditions. An additional run, Run III-8, was performed on July 7, 2002 to obtain residue for a study to evaluate the removal of catalyst from the residue material. The results from Run III-9 are not considered for this discussion, as a leak in the downstream equipment resulted in a loss of large amount of LPG.

1. Process related issues

The reactor start-up and runs proceeded pretty much like the runs during Phase III Stage I. The condenser still blocked with catalyst during the run and had to be rammed clean. As discussed before, the catalyst progressively accumulated as the run proceeded, blocking the reflux condenser inlet section. As before, manual manipulation was required to prevent blockage of the reflux condenser by condensing solid catalyst.

2. Depolymerization results

The results of the depolymerization experiments on the model tire rubber composites are discussed below. The terminology, definitions and calculations are the same and covered in previous part.

These experiments investigated the thermo-catalytic depolymerization of three model tire rubber composites, Silica, WSW, and BSW, which represent typical automobile tires. Detailed compositions of the composite samples are not available. The experimental results are summarized in Table 5.5. The runs were performed at a nominal reactor temperature of 225 ^{o}C and a reflux condenser temperature of 70 ^{o}C. We did not observe any indication of unreacted rubber remaining in the reactor after these experiments.

Table 5.5 Experimental results (III-08 to III-13)

run number		III-08	III-09	III-09A	III-10	III-11	III-12	III-13
run date		09/07/02	09/23/02	09/26/02	09/30/02	10/04/02	10/23/02	10/29/02
Feedstock	(rubber)	SBR	silica	silica	WSW	BSW	SBR	SBR
feed gas		argon	helium	helium	helium	helium	helium	helium
nominal reactor temperature	(°C)	225	225	225	225	225	225	225
reflux condenser temperature	(°C)	70	70	70	70	70	70	120
pressure	(kPa)	270	270	270	270	270	270	135
time on line after last feed	(h)	2	2	2	2	2	2	1.5
rubber in	(g)	551	788	781	760	756	564	847
catalyst in	(g)	850	845	846.1	849.7	852	842.9	1016.4
ratio (catalyst : rubber)		1.54	1.07	1.08	1.12	1.13	1.49	1.2
rubber feed rate	(g/min)	5.2	15.76	17.35	13.82	15.12	11.28	18.82
residue in reactor	(g)	1223.5	1410	1399.4	1345.5	1367.9	1241.6	1552.6
evaporated catalyst	(g)	35.2	32.3	21.8	44.5	38.2	23.2	11.5
washed & dried residue	(g)	---	555.0	557.0	509.0	516.7	---	568.3
naphtha product (mass)	(g)	0.0	17.4	14.4	6.2	6.0	0.0	82.4
LPG rroducts (mass)	(gm)	85.67	29.07	120.02	130.90	153.76	159.32	83.85
flow meter reading (gas volume)	(L)	62.71	33.84	71.57	74.26	84.42	67.62	24.25
naphtha density	(g/cm^3)	---	0.70	0.69	0.69	0.75	---	0.90
LPG-average molecular weight	(g/mol)	49.99	56.26	57.67	59.70	58.82	---	82.26
LPG composition								
C_1	(vol %)	1.81	0.00	0.00	0.00	0.00	---	0.05
C_2	(vol %)	1.30	0.00	0.00	0.00	0.00	---	0.14
C_3	(vol %)	59.19	29.00	23.95	16.70	18.65	---	3.37
i-C_4	(vol %)	17.59	43.65	42.53	45.38	45.40	---	15.00
n-C_4	(vol %)	12.56	12.98	13.10	12.90	14.19	---	2.18
i-C_5	(vol %)	4.15	10.23	13.46	14.73	13.29	---	16.37

Table 5.5 (continued)

run number		III-08	III-09	III-09A	III-10	III-11	III-12	III-13
n-C_5		1.59	1.78	2.32	2.88	2.69	---	0.21
un-C_5 [a]	(vol %)	0.31	0.27	0.81	1.02	0.84	---	0.55
i-C_6	(vol %)	0.68	0.96	1.83	3.11	2.30	---	8.30
n-C_6	(vol %)	0.27	0.35	0.70	1.29	0.96	---	3.73
un-C_6 [a]	(vol %)	0.37	0.13	0.71	0.83	0.74	---	23.59
i-C_7	(vol %)	0.18	0.65	0.57	0.28	0.24	---	15.69
n-C_7	(vol %)	0.00	0.00	0.03	0.13	0.18	---	0.00
un-C_7 [a]	(vol %)	0.00	0.00	0.00	0.11	0.22	---	0.00
C_8^+	(vol %)	0.00	0.00	0.00	0.63	0.31	---	10.82
total	(vol %)	100.00	100.00	100.00	100.00	100.00	---	100.00

[a] The prefix *un*- denotes unidentified isomers of C_n

The experimental results are shown in Table 5.6. In general, the mass balances are satisfactory with an improvement from the poor observations that the gas flow meter gave during the previous experiments. Comparison of the ideal residue yield with the actual residue yield provides a consistency test for the solid residue treatment procedure. There are still two primary effects in the residue treatment: 1) oxidation (combustion) of the sample during the drying procedure, and 2) incomplete removal of water during the drying procedure. Losses due to oxidation (*20*) cause the actual residue yield to be lowered, while incomplete removal of water causes the opposite effect. In the early runs, we had not expected that significant oxidation could occur at temperatures as low as 100 to 120 °C, because these temperatures are well below the ignition temperatures of most hydrocarbons. In an attempt to avoid oxidation, the drying sequence was changed to 70 ^{o}C (±5 ^{o}C) over night (approximately 18 h), followed by 50 ^{o}C (±5 ^{o}C) for an additional 48 h. The resulting material was a soft dull black powder and the ideal and actual residue yields are in much closer agreement.

Table 5.6 Experimental Results: Mass Balances and Conversions (III-08 to III-13)

run number		III-08	III-09	III-09A	III-10	III-11	III-12	III-13
run date		09/07/02	09/23/02	09/26/02	09/30/02	10/04/02	10/23/02	10/29/02
feedstock	(rubber)	SBR	Silica	Silica	WSW	BSW	SBR	SBR
blanket gas		argon	helium	helium	helium	helium	helium	helium
nominal reactor temperature	(°C)	225	225	225	225	225	225	225
reflux condenser temperature	(°C)	70	70	70	70	70	70	120
pressure	(kPa)	270	270	270	270	270	270	135
time on line after last feed	(h)	2	2	2	2	2	2	1.5
rubber in	(g)	551	788	781	760	756	564	847
catalyst in	(g)	850	845	846.1	849.7	852	842.9	1016.4
ratio (catalyst : rubber)		1.54	1.07	1.08	1.12	1.13	1.49	1.2
rubber feed rate	(g/min)	5.2	15.76	17.35	13.82	15.12	11.28	18.82
total mass balance (pre-acid wash)	(%)	96.0	91.2	95.6	94.9	97.4	101.2	92.86
feedstock/products mass balance	(wt %)	n/a	76.3	88.5	85.0	89.5	n/a	86.72
nonreactables	(wt %)	37.0	37.0	37.0	37.0	37.0	37.0	37
ideal residue yield	(wt %)	74.2	75.8	73.6	71.1	73.3	74.8	64.66
actual residue yield	(wt %)	n/a	70.4	71.3	67.0	68.3	n/a	67.10
liquid yield	(wt %)	15.5	5.9	17.2	18.0	21.1	28.2	19.63
liquid conversion	(%)	24.7	9.4	27.3	28.6	33.5	44.8	31.16
naphtha yield	(wt %)	0.0	2.2	1.8	0.8	0.8	0.0	9.73
naphtha density	(g/cm^3)	n/a	0.70	0.69	0.69	0.75	0.75	0.9
LPG yield	(wt %)	15.5	3.7	15.4	17.2	20.3	28.2	9.90
LPG component yield								
C_1	(wt %)	0.09	0.00	0.00	0.00	0.00	n/a	0.00

Table 5.6 (continued)

run number		III-08	III-09	III-09A	III-10	III-11	III-12	III-13
C_2	(wt %)	0.12	0.00	0.00	0.00	0.00	n/a	0.00
C_3	(wt %)	8.12	0.84	2.78	2.10	2.81	n/a	0.18
i-C_4	(wt %)	3.18	1.66	6.52	7.51	9.03	n/a	1.04
n-C_4	(wt %)	2.27	0.49	2.01	2.14	2.82	n/a	0.15
i-C_5	(wt %)	0.93	0.48	2.56	3.03	3.28	n/a	1.41
n-C_5	(wt %)	0.36	0.08	0.44	0.59	0.66	n/a	0.02
un-C_5 [a]	(wt %)	0.07	0.01	0.15	0.21	0.21	n/a	0.05
i-C_6	(wt %)	0.18	0.05	0.41	0.76	0.68	n/a	0.86
n-C_6	(wt %)	0.07	0.02	0.16	0.32	0.28	n/a	0.39
un-C_6 [a]	(wt %)	0.10	0.01	0.16	0.20	0.22	n/a	2.44
i-C_7	(wt %)	0.06	0.04	0.15	0.08	0.08	n/a	1.88
n-C_7	(wt %)	0.00	0.00	0.01	0.04	0.06	n/a	0.00
un-C_7 [a]	(wt %)	0.00	0.00	0.00	0.03	0.08	n/a	0.00
C_8^+	(wt %)	0.00	0.00	0.00	0.20	0.12	n/a	1.48

[a] The prefix *un*- denotes unidentified isomers of C_n

The data in Table 5.6 show that the liquid product (LPG + naphtha) yields are relatively low. The liquid yields for the Silica rubber sample is approximately 17% by weight of feedstock, whereas the WSW and BSW rubber samples measured 18 and 21% respectively. When considered in terms of the amount of potentially reactable material present, the conversions to liquid ranged from 27 to 33% for the three rubber samples under discussion. These experiments again show that the depolymerization reaction of the rubber produces a significant amount of nonvolatile hydrocarbons. As previously indicated, the nonvolatile hydrocarbons formed most likely remain on the surface of the carbon black after the reaction.

The naphtha yields were low, but of the same order of magnitude as those obtained before. The highest yield was at 1.8% for Silica rubber and at 0.8% for the WSW and BSW rubber. The naphtha had densities ranging from 690.0 kg/m^3 to 750.0 kg/m^3.

The two scrubber units employed downstream after the liquid collector provide evidence of hydrogen chloride transport through the reflux and liquid condensers to the liquid trap. The 25% (wt) NaOH solution typically changed in pH from >14 to as low as 2 during an experiment. The cadmium acetate solution normally showed a slight color change indicating the presence of some sulfur compounds, most likely H_2S. The sulfur and hydrogen chloride levels were not quantified. Solid materials (1 to 2 g) were also present in the naphtha products recovered. (This is an estimation and as a result also influences the actual naphtha yield which should be lower by the amount of catalyst present.)

The liquid petroleum gas (LPG) fractions varied slightly with composite type according to BSW > WSW > Silica rubber. These results also resemble those for the SBR and natural rubbers evaluated before. The LPG fraction also was similar in composition, mainly containing propane, butane, and pentane. Small amounts of heavier hydrocarbons were present. Isobutane was the most abundant isomer in all cases. The BSW rubber produced slightly larger fractions of isobutane and pentane, whereas the WSW also appeared to produce more isobutane and pentane when compared to the Silica rubber.

5.3 Dual catalyst study

This section describes the results of thermocatalytic depolymerization on a SBR rubber/carbon black sample provided by Cooper Tire. The catalysts used were aluminum chloride as the primary catalyst and sodium chloride as the co-catalyst. The experiments were performed at 225 °C, 35 kPa (5 psig). The rubber was fed over a period of approximately 50 min, and the reactor held at temperature for about 2 h after the last rubber was fed. As in the single catalyst experiments, there are two primary products of the reaction: volatile hydrocarbons which leave the reactor as vapor and nonvolatile hydrocarbons that remain in the reactor. The reactor residue was washed with water to remove the catalyst, yielding a fine black powder that contained both the carbon black and the nonvolatile products. The volatile hydrocarbons were divided into two fractions: naphtha, the liquid collected in an accumulator at ambient conditions, and liquefied petroleum gas (LPG), the product leaving the accumulator as vapor. During this study, a significant shift in the product selectivity from light petroleum gas to liquid naphtha was observed. The total hydrocarbon selectivity however remained unchanged. Significant amounts of gaseous hydrochloric acid also were produced.

The SBR rubber sample depolymerized with the mixed catalyst system yielded approximately 20% by weight of the feedstock as liquid products (approximately 10% as naphtha and 10% as LPG, respectively). The naphtha fraction contained significant amounts of naphthene and aromatic components. The LPG products indicated a shift to a heavier hydrocarbon distribution when compared with earlier investigations and the composition indicated a significant amount of isobutene, isopentane, and isohexhane.

The solid residue samples were washed with acidic water followed by distilled water to remove the catalyst, and then dried in air in an oven at approximately 50 to 80 °C. The main sample, *i.e.,* from Run III-13, however indicated coarser material than that reported during earlier studies. The particle sizes of the dried powder were characterized by sieving and were similar to particles recovered from the depolymerization of butyl rubber studied earlier. For detailed information, please refer to the discussions by Liang (*20*).

5.3.1 Introduction

Recent studies suggest that a chemical complex forms between aluminum chloride and the carbon-like residue product resulting from the depolymerization reaction of tire rubber. The presence of this complex is consistent with reports of similar complexes that result from various reactions catalyzed by aluminum chloride (*53*). Although these complexes are stable, they are easily hydrolyzed in the presence of water, consequently destroying the complex structure.

Economic viability for the current process relies heavily on the successful recovery of the aluminum chloride catalyst. The catalyst is expensive because this process requires large quantities of aluminum chloride. It is therefore imperative that the catalyst be recovered in an active state for reuse. Another possible choice is to lower the expenses of catalyst by finding viable co-catalyst systems. The use of a dual catalyst system will lower significantly the working pressure and hence will improve the equipment operation condition. Another perceived benefit is that the use of dual catalyst will also dramatically reduce secondary decomposition in the vapor phase and then improve the product selectivity.

At least three mixed salt catalytic systems were found to operate within the current reaction regime. These systems are $AlCl_3/MgCl_2$, $AlCl_3/NaCl$, and $AlCl_3/KCl$. Using $MgCl_2$ as co-catalyst already had been investigated extensively during Phase II (1994/1995) and was operated at exactly the same reaction conditions as currently employed for the Phase III study. The use of $MgCl_2$ as co-catalyst to aluminum chloride at the time was ruled out once it was realized that it would be difficult to recover $MgCl_2$

from the residue product after depolymerization. The fact that $AlCl_3$ readily sublimes at temperatures below 190 °C opened the possibility to separate the catalyst *in-situ* by vaporization. However, the experiments showed that evaporation did not occur as expected, strongly suggesting the formation of the complex. Because the expected advantage of the single catalyst for separation was not realized, additional work was done with dual-catalyst systems. Two mixed salt systems with interesting properties were identified. Both mixtures form homogeneous molten salt liquids at temperatures significantly below the triple point temperature (~193 °C) of aluminum chloride.

This section presents the results of the dual salts studies.

5.3.2 Reactor operating procedure, and reaction

The process for the thermocatalytic decomposition of rubber using a molten salt catalyst (typically aluminum chloride) is an exothermic process if saturated hydrocarbons are formed from rubbers containing unsaturated bonds (*e.g.,* styrene rubber). The catalytic reaction between the rubber and the $AlCl_3$ produces short-chain hydrocarbon products (typically C_4 to C_{10}, but usually predominantly saturated C_3 to C_5 compounds) as well as a blackish, carbon-rich residue that contains the carbon black originally in the tire and some heavy products of the depolymerization reaction.

The laboratory depolymerization equipment, reaction, catalyst, and product work up are discussed in detail in Chapter IV and Section 5.2.2 and will not be repeated here.

5.3.3 Solid residue workup

After the depolymerization run was completed and the reactor cooled to 140 °C, a hydrochloric acid solution with a pH of approximately 3 was added to the reactor to remove the catalyst from the solid residue. The temperature of resulted slurry could be elevated up to 70 °C due to the exothermic reaction of the catalyst with water. The slurry suspension was stirred over night after it was transferred from the reactor to a plastic container. The residue then was washed with copious amounts of water to remove the acid solution and dried in an oven at 80 °C (± 5 °C) overnight and for an additional 48 h at 50 °C (± 5 °C). After drying, the residue was passed through a set of sieves, with the aid of a brush, to obtain the size distribution of the particles. More details of the residue treatment are provided by Liang (*20*).

5.3.4 Results and discussion

This study was divided into two sections. The first is a qualitative small-scale investigation evaluating the physical behavior of the mixed salts mentioned above and the second one large-scale depolymerization run that was completed on October 29, 2002. This run will be discussed in detail below (Run III-13). An additional run, Run III-12, was performed on October 23, 2002 to obtain residue for a study to test the removal of catalyst from the residue material employing solvent extraction procedures with xylene, benzene and THF, which was not successful.

1. Small scale bench investigation

As indicated above, two mixed-salt systems, $AlCl_3$/NaCl and $AlCl_3$/KCl were identified that form homogeneous molten salt liquids at temperature significantly below the sublimation temperature (180.2 °C) of aluminum chloride (see Figure 5.3).

The phase diagram information in Figure 5.3 is from Kendall *et al.* (*59*) who discuss the factors influencing "compound formation" and "solubility" in fused salt mixtures. It is clear from Figure 5.3 that both $AlCl_3$/NaCl and $AlCl_3$/KCl mixtures form eutectic points at temperatures significantly lower than that of $AlCl_3/MgCl_2$. The eutectic point is below 150 °C for the $AlCl_3$/NaCl system and just over 150 °C for the $AlCl_3$/KCl system. This is in comparison to a temperature near 190 °C for $AlCl_3/MgCl_2$ mixtures, which is very close to the triple point temperature of pure $AlCl_3$.

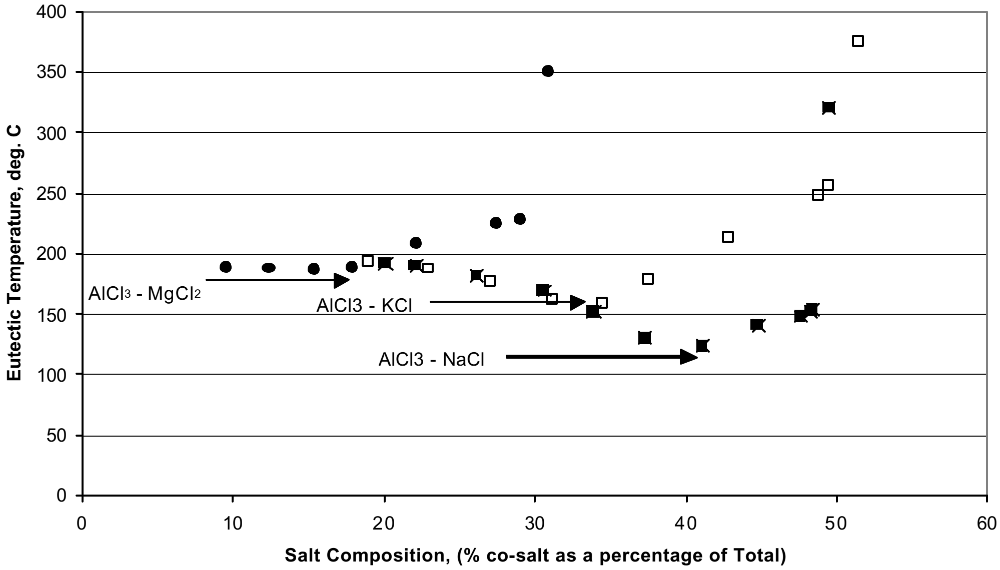

Figure 5.3 Phase diagrams for selected salt mixtures containing $AlCl_3$ as a constituent.

A series of small scale tests were performed to observe the physical behavior of the $AlCl_3/MgCl_2$, $AlCl_3/KCl$, and $AlCl_3/NaCl$ as they are heated to the reaction temperatures for depolymerization. The tests were carried out by placing approximately 100 g of salt in a round-bottom glass flask that was open to the atmosphere through a reflux condenser and then heating the flask gently. A thermocouple was used to measure the temperature. The mixtures containing NaCl and KCl formed homogeneous liquids at temperatures of 130 to 150 °C and 145 to 165 °C, respectively. The viscosity of these solutions appears to be only slightly greater than that of water. The mixtures containing $MgCl_2$ system formed a slurry at 195 °C and never formed a completely homogeneous liquid, even at a temperature as high as 250 °C.

When pure $AlCl_3$ and $AlCl_3/MgCl_2$ mixtures were heated, a vapor cloud began to appear at temperatures as low as 100 °C and the cloud became denser as the temperature increased. In addition, strong odors of chlorine and hydrogen chloride were present. These observations suggest than an appreciable partial pressure of $AlCl_3$ vapor was present over the mixture, which is not surprising because of the significant vapor pressure of pure $AlCl_3$ in this temperature range. In contrast, there is no evidence, either visual or olfactory, of significant partial pressures of $AlCl_3$ over the $AlCl_3$/NaCl or $AlCl_3$/KCl mixtures, even at temperatures as high as 300 °C.

After observing the attractive "qualitative" physical behavior with the $AlCl_3$/NaCl system, aluminum hexahydrate ($AlCl_3{\cdot}6H2O$) also was tested as a potential co-salt, because it is much less expensive and much more benign to handle than anhydrous $AlCl_3$. The first test observed behavior upon heating of the hexahydrate salt only, and the second test observed a mixture of the hexahydrate with sodium chloride (70 : 30 by weight).

All of the studies mentioned above are summarized below. The observations were obtained by heating approximately 100 g (total amount) of salt in a round-bottom flask equipped with a thermocouple and fitted with a cold reflux condenser. The main observations can be summarized as follows:

$AlCl_3$ only: This substance has a sublimation point at approximately 180.2 ^{o}C and that the vapor pressure increases dramatically (exponentially) above this temperature. These observations were confirmed during the small-scale heating of pure aluminum chloride.

$AlCl_3/MgCl_2$: At approximately 190 to 200 °C, the glass in contact with the salt mixture began to wet with molten salt; however, the molten salt mixture never formed a homogeneous liquid, even at temperatures between 200 and 250 °C. Three distinct phases were visible. First, a white vapor cloud with distinct chlorine smell started to appear at 100 °C and the denseness of this cloud kept on increasing until a quasi-liquid solid state was formed. Thereafter, the vapor cloud visibility decreases significantly, but it always was present. $AlCl_3$ was deposited as a white solid on the colder top sections of the glass flask and in the opening to the cold condenser. With no purge gas flow present, the driving force from the vapor was strong enough to have blocked the condenser opening after completing of the study. The material at the bottom of the flask was a solid-liquid slurry.

$AlCl_3/NaCl$: No or little vapor was present at 100 °C. No chlorine odor was prominent. When the reactor contents reached 150 °C, the solid salt mixture disappeared, exhibiting a homogeneous water-clear liquid. This liquid persisted, with no evidence of significant amounts of $AlCl_3$ in the gas phase, up to temperatures of 250 °C. The dramatic lowering in vapor pressure suggests that depolymerization of the tire rubber at pressures near atmospheric is a possibility. The lower eutectic temperature also increases the likelihood of further decreasing the reaction temperature.

$AlCl_3/KCl$: This system exhibited behavior similar to that of the $AlCl_3/NaCl$ system, with the difference that the homogeneous water-clear liquid appeared at a somewhat higher temperature, *i.e.,* 150 – 160 °C. During this evaluation, the system temperature was increased to approximately 350 °C and no evidence of $AlCl_3$ was observed in the vapor phase.

$AlCl_3 \cdot 6H_2O$: As expected from literature descriptions, this salt gave no evidence of transforming (melting) into the liquid phase and it started losing water vapor around 100 °C. A distinct chlorine odor was present, suggesting that the salt was also decomposing upon increasing temperature up to temperature of 250 °C.

$AlCl_3 \cdot 6H_2O$/NaCl: This mixture was tested with the hope that the presence of NaCl might mitigate the decomposition of the hexahydrate, but the results were similar to those for the pure aluminum hexahydrate.

2. Large scale depolymerization runs

The reactor start-up and run proceeded with significant differences when compared to previous runs. The run proceeded with ease at low pressure 30 to 35 kPa (4-5 psig). No blockage of condensers occurred during the run. In fact no catalyst deposition was observed in down-stream equipment.

The terminology, definitions, and calculations are covered in Section 5.1.2.1.

This section evaluates the thermo-catalytic depolymerization of a SBR rubber sample in the presence of a mixed $AlCl_3$-NaCl catalyst mixture. The rubber sample is a model rubber compound prepared by Cooper Tire. The composition of the sample is given in Table 5.1, both in terms of parts per hundred of rubber and as an overall weight fraction. The slats were added to the reactor as a 60% $AlCl_3$ and 40% NaCl mixture (by weight). The result was a liquid pool at the depolymerization temperature of 150 to 220 °C. The run was performed at 225 °C and a reflux condenser temperature of 120 °C. Due to a significant reduction in the partial pressure of the $AlCl_3$, the system pressure was maintained between 30 to 35 kPa (4 – 5 psig) through out the run. The down-stream flow was maintained at a high level throughout the run in an effort to remove any resulting hydrocarbon products before secondary cracking or depolymerization could occur. The experimental results are summarized in Table 5.5. We did not observe any indication of unreacted rubber remaining in the reactor after the experiment.

The experimental mass balances, product yields, and conversions of the potentially reactable materials to liquid products are shown in Table 5.6. The mass balance is satisfactory and an improvement from the poor observations that the gas flow meter gave during the latter experiments of Phase III Stage 1. The solid residue treatment procedures and results are presented elsewhere (*20*).

The data in Table 5.6 indicate that the total liquid product yield agrees well with that of Runs III-1D, III-04, and III-08 for SBR rubber. When considered in terms of the amount of potentially reactable material present, the conversion to liquid is slightly lower, but still consistent with the mentioned runs at 31%. These experiments again show that the depolymerization reaction of the rubber produces a significant amount of nonvolatile hydrocarbons. These products more than likely result from a hydrogen-deficient environment because the hydrogen-to-carbon ratio in the rubber is smaller than that in the liquid hydrocarbon products. Therefore it may be possible to increase the hydrocarbon product yield through the addition of hydrogen from a source, such as H_2 or CH_4.

The naphtha yield increased from 1 to 2% to 10% when compared with other Phase III runs. This yield increased at the expense of the LPG fraction, which decreased from 20 to 10%, indicating a selectivity shift from the lighter gas phase products to the heavier naphtha products. The naphtha density increased to about 900 kg/m^3 from the 690 to 750 kg/m^3 densities observed in earlier runs. An analysis of the naphtha breakdown by gas chromatography and simulated distillation indicated a shift towards C_8^+, naphthene, and aromatic products. Table 5.7 compares the naphtha fractions obtained in the various Phase III experiments. The paraffin and isoparaffin content decreased significantly from 18.0% to 3.0% and from 60.0% to 20.0% respectively, and the naphthene and aromatic content increased from 18.0 to 45.0% and 6.0 to 18.0% respectively. An organic micro-coulomb meter analysis performed by Core Lab, Houston, Texas indicated 178 ppm of organic chloride compounds in one particular sample. No inorganic chlorides were present in this naphtha sample.

Table 5.7 Comparison of Naphtha Product Fractions from Phase III Studies

run number	III-1D (wt %)	III-2B (wt %)	III-3A (wt %)	III-9 (wt %)	III-11 (wt %)	III-13 (wt %)
paraffin	17.57	18.12	3.70	13.01	11.46	3.20
iso-paraffin	56.93	60.27	95.13	49.49	58.98	21.56
olefin	0.00	0.00	0.00	0.00	0.00	0.00
naphthene	18.49	20.52	0.32	27.09	26.65	45.28
aromatic	6.41	0.73	0.00	9.78	2.42	18.58
oxygenates	0.00	0.00	0.00	0.00	0.00	0.00
unidentified	0.60	0.36	0.85	0.23	0.50	11.35
average MW	79.47	79.99	86.11	80.97	82.38	111.61

The number of unidentified products also increased from about 1.0% to 11.0% with the NaCl-$AlCl_3$ mixture. The average molecular weight for the hydrocarbon product also increased from 80.0 to 112.0 g/mol (as calculated by Core Lab from gas chromatography analysis). The shift in the properties and composition of the naphtha fraction strongly suggest that reactions in the vapor phase were suppressed significantly, and gives further indication that no or little catalyst was present in the vapor phase.

The fact that the total amount of liquid hydrocarbons did not change and only a shift from the LPG fraction to the naphtha fraction was observed suggests that there is still potential to improve the total liquid hydrocarbon yield by effecting a more complete depolymerization of the hydrogen-lean structures remaining in the residue material. The low depolymerization conversion of ~30% of reactable material observed to date suggest that hydrogen is the limiting species for the depolymerization reaction. All experiments to date have been performed with no hydrogen addition and an approximate catalyst-to-rubber ratio of 1.2. Hence the "reaction stoichiometry" was very similar for each of the deploymerization studies and therefore the results indicate comparable depolymerization conversions. This scenario probably can be improved by adding a hydrogen source such as hydrogen or methane.

An additional water scrubber unit was employed downstream before the tail gas reached sodium hydroxide and cadmium acetate scrubbers, which provided evidence of hydrogen chloride products. A titration of the trapped water contents with a NaOH solution indicated acidic products (presumed to be HCl) equal in weight to approximately 10.0% of the product feed. The literature indicates that HCl is produced in significant quantities during alkylation reactions, of the order of 1 mole per mole hydrocarbon reacted. Our results are consistent with that observation. No proof of chloride transport through the reflux and liquid condensers to the liquid trap could be found. The 25.0% (wt) sodium hydroxide solution typically changes in pH from >14 to as low as 2 during an experiment. The solution changes color from clear to dark brown during the run and a small layer of hydrocarbon product is visible on top of this solution. The cadmium acetate solution showed a color change from clear to light yellow, indicating the presence of some sulfur compounds, assumed to be H_2S. The sulfur levels were not quantified.

The liquid petroleum gas (LPG) fractions indicated a significant shift in composition towards heavier compounds. This result supports the higher naphtha yield observed and it is clear that this result is different from any other run evaluated during Phase III. Although some difficulties were experienced with the gas chromatograph during this experiment, the general trend is a significant shift towards the $C_6 - C_8$ fraction. The LPG fraction was also found to contain mainly *iso*-derivatives of C_4, C_5, C_6, and C_7 and to contain small percentages of propane, *n*-butane, and *n*-pentane. Larger amounts of heavier hydrocarbons ($>C_8$) were present than in the earlier Phase III runs.

The solid residues obtained from the depolymerization runs were recovered and stored until they could be characterized. The solid residue characterization is discussed elsewhere (*20*).

5.4 Naphtha product analysis

Six naphtha fraction samples were submitted to Core Lab – Petroleum Services, Houston, Texas for detailed composition analysis. The six samples represented one each for SBR, natural rubber, butyl rubber, silica rubber, and black side wall rubber, as well as SBR rubber decomposed with NaCl/$AlCl_3$. The detailed analysis results are listed in Appendix B. A comparison of the significant constituents appear in Table 5.8.

It is clear from Table 5.8 that *iso*-pentane is by far the most abundant species present in the first five samples. The next more abundant species are 2-methylpentane and *n*-pentane for SBR and natural rubber, and 3-methylpentane for butyl rubber. SBR rubber produced by far the most benzene and toluene. SBR and natural rubber produced similar product distributions that differed from butyl rubber in that 95.0% of the total product spectrum is isoparaffins for butyl rubber whereas SBR and natural rubber produced 57.0% and 60.0% respectively. SBR and natural rubber also formed large quantities of naphthene (18.5% and 20.5% respectively) and paraffin (17.6% and 18.1% respectively). SBR rubber forms the only significant quantities of aromatic products at approximately 6.4%. The NaCl/$AlCl_3$ catalyst mixtures gave significantly different results than pure $AlCl_3$ for SBR rubber in that more aromatics and naphthene were produced.

The results are consistent with our knowledge of the base rubber materials. For instance, SBR rubber contains butyl and styrene groups in a ratio of 3:1 in mole, hence the explanation for the presence of aromatic products, whereas butyl rubber, which consists mainly of butyl monomers linked together, primarily breaks down to isobutane (see Table 5.9). Some cyclic-constituents are also present in some cases. Under no circumstances were any olefin products formed. The lack of olefins and the presence of only a small percentage of ring compounds may be indicate the aggressiveness of the catalytic scission of the hydrocarbon chains.

The density of the three samples, as determined from gas chromatography analysis, is similar but decreasing in the order SBR (722 kg/m^3) > natural rubber (704 kg/m^3) > butyl rubber (686 kg/m^3) and is in line with that determined and reported at 720 kg/m^3 for SBR. However, our estimation for the butyl rubber naphtha density is unexplainably high at 790 kg/m^3. The result for the dual catalyst system gives a denser product (~900 kg/m^3).

Simulated distillation curves were obtained for the three naphtha samples using a constant heating profile gas chromatography technique. The initial boiling points were −13.8 °C, −13.8 °C, and −15.6 °C and the final boiling points were 192.8 °C, 201.1 °C, and 200.5 °C respectively for SBR, natural, and butyl rubbers. The distillation curves of the samples are very similar. Even the profiles of the heating curves, *i.e.,* percentage of product removed as a function of temperature (see Figure 5.4) are identical. However, the distillation curve for the SBR depolymerized by the dual catalyst system indicates a much heavier product spectrum.

Qualitative mass spectroscopy scans for molecular weights are in agreement with the previously mentioned results and only for a depolymerization run with SBR rubber we have a compound with molecular weight in the order of 281 g/mol. For a butyl sample two molecular weights above 100 g/mol were noted. The intensity is however reasonably low indicating low concentrations. The spectrum for a natural rubber, like the other two samples, mainly indicates molecular weights lower than 100 g/mol. If one therefore considers the carbon weight in a C_6 straight or ring structure to have a mass of 72, hydrogen = 1, and a methyl group = 15, one can get a clear indication that the largest components present are that in the C_6 range. A detailed GC-MS analysis, to identify the products associated with the molecular weights, was performed on the SBR sample only. The results agree with the Core Lab GC analysis.

Table 5.8 A Comparison of Major Constituents in Naphtha Fraction (mol %)

run number	1D	2B	3A	9	11	13 [a]
rubber type	SBR	natural	butyl	silica	BSW	SBR
propane	0.16	0.20	0.18	0.40	0.15	0.28
iso-butane	5.50	5.64	7.07	4.83	3.61	2.42
n-Butane	5.92	6.14	1.81	4.40	2.55	0.52
isopentane	24.82	25.31	31.21	21.11	26.40	5.48
n-Pentane	8.04	8.34	1.77	6.17	6.27	0.06
2,2-dimethylbutane	2.61	2.65	0.60	1.83	1.96	0.00
cyclopentane	2.40	1.65	0.00	2.55	1.36	0.21
2,3-dimethylbutane	3.33	3.84	9.75	3.46	4.20	0.84
2-methylpentane	11.40	13.26	11.56	11.99	14.01	3.65
3-methylpentane	6.81	7.66	6.03	7.21	8.40	2.23
n-hexane	3.88	4.23	0.51	3.72	3.58	0.05
methylcyclopentane	4.49	4.77	0.03	6.16	5.89	6.14
benzene	5.54	0.23	0.00	6.98	1.29	3.81
cyclohexane	1.96	2.34	0.03	2.66	2.39	0.17
2-methylhexane	0.23	0.34	3.19	0.38	0.79	1.67
2,3-dimethylpentane	0.07	0.10	3.34	0.11	0.25	0.50
1,1-dimethylcyclopentane	0.36	0.38	0.01	0.45	0.39	0.01
3-methylhexane	0.21	0.29	2.54	0.34	0.71	1.39
cis-1,3-dimethylcyclopentane	0.53	0.51	0.01	0.73	0.82	1.49
2,2,4-trimethylpentane	0.00	0.00	2.80	0.00	0.00	0.00
methylcyclohexane	4.79	6.09	0.11	6.21	6.78	7.22
2,5-dimethylhexane	0.01	0.02	1.59	0.02	0.06	0.36
2,4-dimethylhexane	0.01	0.02	1.34	0.02	0.06	0.36
cis-1,3 dimethylcyclohexane	0.84	1.21	0.00	1.02	1.10	4.30
toluene	2.12	0.57	0.00	2.28	0.80	1.39
2,2,5-trimethylhexane	0.00	0.00	1.36	0.00	0.00	0.00

Table 5.8 (continued)

run number	1D	2B	3A	9	11	13 [a]
molar mass of sample	79.47	79.99	86.11	80.97	82.38	111.61
molar mass of C_6 plus	88.28	89.73	98.46	88.36	90.41	115.93
density of sample	0.6762	0.6659	0.6594	0.6877	0.6768	0.7714
density C_6 plus	0.7219	0.7044	0.6856	0.7280	0.7103	0.7834
paraffins	17.57	18.12	3.70	14.28	12.24	3.60
iso-paraffins	56.93	60.27	95.13	53.56	61.96	24.67
olefins	0.00	0.00	0.00	0.00	0.00	0.00
naphthene	18.49	20.52	0.32	24.35	23.53	45.08
aromatic	6.41	0.73	0.00	7.64	1.86	16.26

[a] $NaCl/AlCl_3$ catalytic system. The composition distribution differs significantly from others. The constituent list given here is only for comparison with the components of the foregoing runs listed in the table.

Table 5.9 A Comparison of Major Constituents in LPG Product Fraction (vol %)

run number		III-01D	III-02B	III-03A	III-09A	III-10	III-11	III-13
run date		05/15/02	04/29/02	05/22/02	09/26/02	09/30/02	10/04/02	10/29/02
feedstock	(rubber)	SBR	natural	butyl	silica	WSW	BSW	SBR
carbon black	(type/wt %)	N234/35.8	N121/30.0	N650/33.5				
feed gas		argon	argon	argon	helium	helium	helium	helium
nominal reactor temperature	(°C)	225	225	225	225	225	225	225
reflux condenser temperature	(°C)	70	70	70	70	70	70	120
pressure	(kPa)	270	270	270	270	270	270	135
time on line after last feed	(h)	2	2	2	2	2	2	2
rubber in	(g)	682.0	675.0	609.0	781	760	756	847
catalyst in	(g)	837.8	851.3	827.1	846.1	849.7	852	1016.4
ratio (catalyst : rubber)		1.23	1.26	1.36	1.08	1.12	1.13	1.2
rubber feed rate	(g/min)	13.6	9.0	30.5	17.35	13.82	15.12	18.82
residue in reactor	(g)	1345.4	1289	1165.5	1399.4	1345.5	1367.9	1552.6
evaporated catalyst	(g)	28.4	66.0	39.6	21.8	44.5	38.2	11.5
washed & dried residue	(g)	322.9	426.8	315.9	557.0	509.0	516.7	568.3
naptha product (mass)	(g)	9.0	12.0	13.9	14.4	6.2	6.0	82.4
LPG products (mass)	(g)	149.3	142.1	236.0	120.02	130.90	153.76	83.9
flow meter reading (gas Volume)	(L)	87.73	82.5	119.5	71.57	74.26	84.42	24.25
naphtha density	(g/cm^3)	---	---	0.79	0.69	0.69	0.75	0.90
LPG-average molecular weight	(g/mol)	54.28	56.08	58.02	57.67	59.70	58.82	82.26
actual LPG composition								
C_1	(vol %)	0.34	0.00	0.00	0.00	0.00	0.00	0.05
C_2	(vol %)	0.00	0.15	0.00	0.00	0.00	0.00	0.14
C_3	(vol %)	35.44	19.64	6.59	23.95	16.70	18.65	3.37
i-C_4	(vol %)	44.75	57.55	86.82	42.53	45.38	45.40	15.00
n-C_4	(vol %)	11.01	17.44	1.10	13.10	12.90	14.19	2.18

Table 5.9 (continued)

run number		III-01D	III-02B	III-03A	III-09A	III-10	III-11	III-13
i-C_5	(vol %)	6.57	4.30	5.19	13.46	14.73	13.29	16.37
n-C_5	(vol %)	1.31	0.75	0.00	2.32	2.88	2.69	0.21
un-C_5 [a]	(vol %)	0.00	0.00	0.00	0.81	1.02	0.84	0.55
i-C_6	(vol %)	0.59	0.17	0.26	1.83	3.11	2.30	8.30
n-C_6	(vol %)	0.00	0.00	0.00	0.70	1.29	0.96	3.73
un-C_6 [a]	(vol %)	0.00	0.00	0.00	0.71	0.83	0.74	23.59
i-C_7	(vol %)	0.00	0.00	0.03	0.57	0.28	0.24	15.69
n-C_7	(vol %)	0.00	0.00	0.00	0.03	0.13	0.18	0.00
un-C_7 [a]	(vol %)	0.00	0.00	0.00	0.00	0.11	0.22	0.00
C_8^+	(vol %)	0.00	0.00	0.00	0.00	0.63	0.31	10.82
total	(vol %)	100.00	100.00	100.00	100.00	100.00	100.00	100.00

[a] The prefix *un*- denotes unidentified isomers of C_n

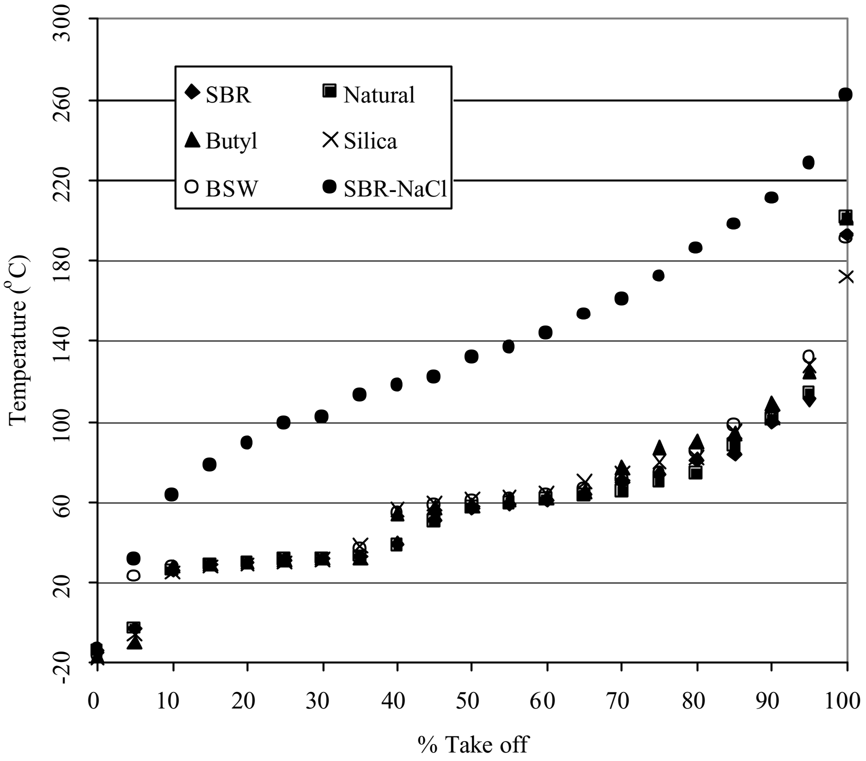

Figure 5.4 Simulated distillation curves for naphtha fractions from various rubbers. (SBR-NaCl denotes the sample from the NaCl/$AlCl_3$ mixture.)

5.5 Result comparison

The results of the Phase III experiments are consistent with those of Phase II, especially Experiments II-21 through II-28. There appears to be no significant differences between the results obtained in Phase II using catalyst mixtures ($AlCl_3$/$MgCl_2$) and in Phase III using pure $AlCl_3$ and its salt mixtures as the catalyst. The most relevant work reported in the literature is that of Ivanova, *et al.* (*43*), who studied the decomposition of butyl rubbers at 300 °C using several molten salt catalysts, including pure $AlCl_3$ and mixtures of $AlCl_3$ with other salts. Figure 5.5 shows the results reported for $AlCl_3/MgCl_2$ mixtures. For pure $AlCl_3$, our conversions of approximately 60% of the butyl rubber in the feedstock are larger than the 40% obtained by Ivanova *et al.* (shown in Figure 5.5). The volatile hydrocarbon compositions differ slightly, in that our experiments produced more isobutane and less C_5^+ components.

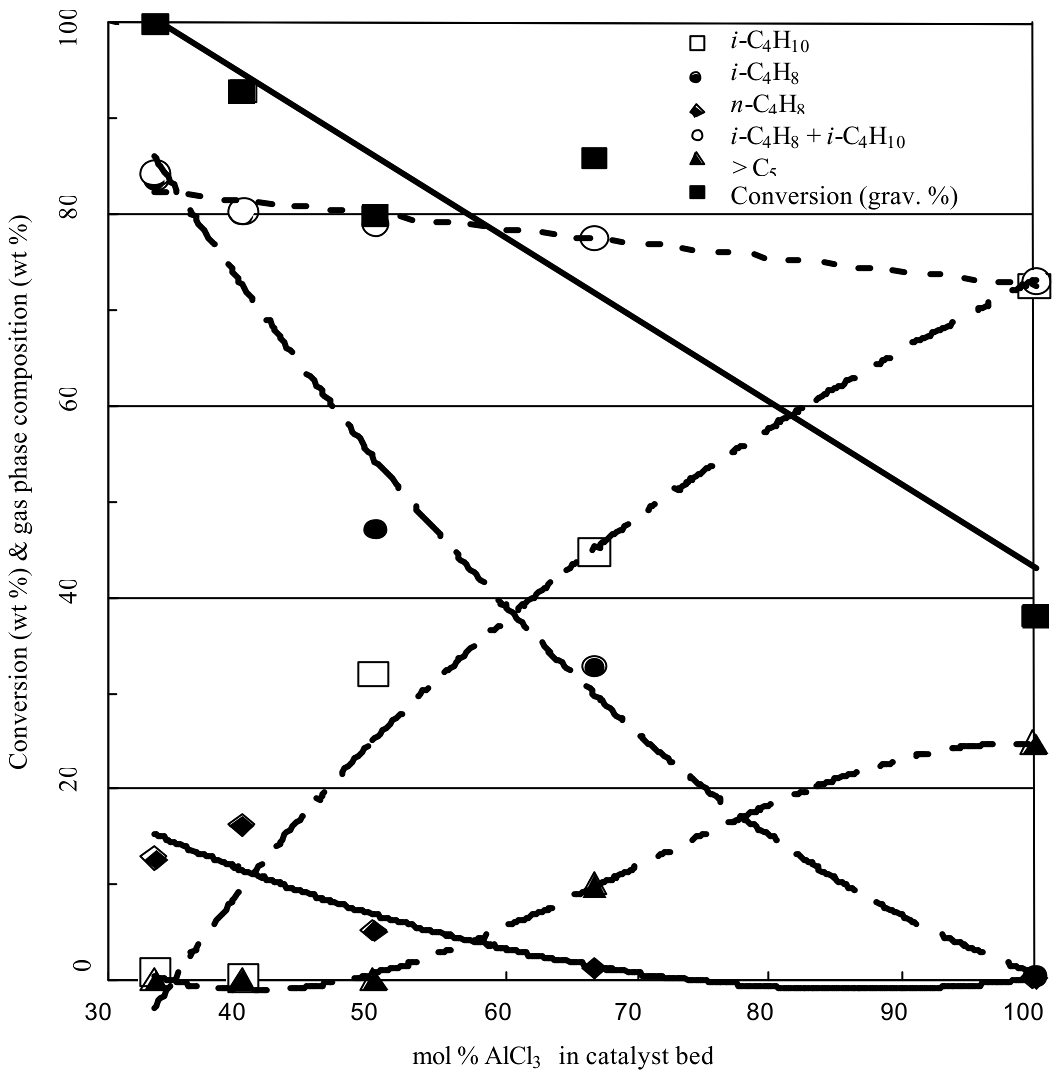

Figure 5.5 Results for butyl rubber and $AlCl_3/MgCl_2$ catalysts at 300 °C. (*43*)

The study of Ivanova, *et al.* is limited because the work was performed on neat butyl rubber on very small scale (utilizing 20 cm^3 glass reactors) and focused on the degree of conversion to volatile hydrocarbons. No information was provided on the residue remaining in the reactor or catalyst recovery. Our results indicate that the butyl rubber responds differently than the natural and the synthetic rubbers that also are present in automobile tires. Furthermore, our samples also contain extender oil, carbon black, and other materials. The most significant information contained in the paper of Ivanova, *et al.* is that higher conversion rates are obtained using mixtures containing both $AlCl_3$ and $MgCl_2$. Mixtures of $AlCl_3$ and NaCl proved to be equally effective.

5.6 Catalytic depolymerization mechanism

Few discussions of possible catalytic mechanisms for rubber depolymerization have been published. However, the model organic synthesis mechanisms of aluminum chloride and classical organic chemistry knowledge can be used to formulate a possible reaction mechanism. The resulting mechanism is discussed in the following sections.

5.6.1 Aluminum chloride chemistry

Aluminum chloride, $AlCl_3$, is a strong Lewis acid that can accept an electron pair (the electron pair being the acid, and the donor of the electron pair the Lewis base) during a reaction. A covalent bond is formed when the electron pair is accepted. This happens because the central aluminum ion has only a sextet of electrons and are, therefore, electron deficient. By accepting the electron pair, aluminum chloride is, in the Lewis definition, acting as an acid. Thus any electron-deficient atom can act as a Lewis acid (typically Group IIIA elements). Other compounds that have atoms with vacant orbits also may act as Lewis acids.

The active "species" of aluminum chloride is viewed to be the tetrahedral coordinated $AlCl_4^-$, which is typically produced in the following reactions 9 to 11 (*51*):

$$AlCl_3 + Cl_2 \rightarrow AlCl_4^- + Cl^+ \qquad (9)$$

$$AlCl_3 + HCl \rightarrow AlCl_4^- + H^+ \qquad (10)$$

$$RX + Mg \rightarrow RMgX + AlCl_3 \rightarrow AlX^- \quad + RMg^+ \qquad (11)$$

where X = Cl, Br, or I, and R = ethyl, methyl, phenyl, *etc.*

The formation of $AlCl_4^-$ is essential to the functioning of Al_2Cl_6 as a Friedel-Crafts catalyst. This way, the necessary carbonium ions (when a positive charge is carried on a carbon atom ready for reaction) are formed simultaneously. Sykes (*51*) illustrates in Figure 5.6 how aluminum bromide interacts with propane. A cyclo-propane intermediate is formed that rearranges back to form propane again, *i.e.*, shifting the position of a carbon 13 labeled species (1-propyl cation rearrange to the 2-propyl cation through the migration of a hydrogen atom):

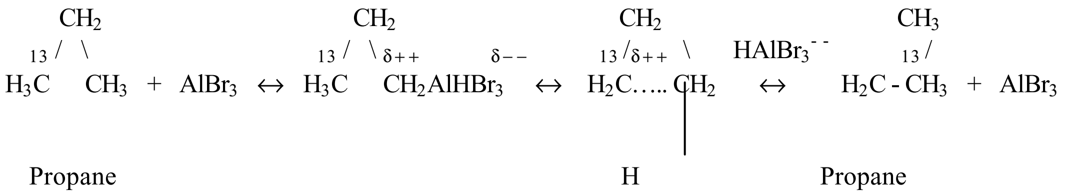

Figure 5.6 The behavior of $^{13}CH_3CH_2CH_3$ with $AlBr_3$.

One of the most important aspects of the chemistry of the Group III elements is that they form 1:1 adducts within a great variety of Lewis acids. They also, as shown below, react with themselves to form dimers of distorted tetrahedral coordination. $AlCl_3$ also forms a 1:1 adduct with THF which is molecular, but the 1:2 adduct is ionic, $[AlCl_2(THF)_4]^+AlCl_4^-$.

According to Cotton and Wilkinson (*58*) $AlCl_3/NaCl$ gives rise to the following equilibria 12 to 14:

$$2AlCl_3\ (l) \leftrightarrow Al_2Cl_6 \quad K = 2.86 \times 10^7 \tag{12}$$

$$AlCl_4^- + AlCl_3 \leftrightarrow Al_2Cl_7^- \quad K = 2.40 \times 10^4 \tag{13}$$

$$Al_2Cl_7^- + Cl^- \leftrightarrow 2AlCl_4^- \quad K = 9.43 \times 10^6 \tag{14}$$

Also, $AlCl_3$ is planar, and the only Group III metal to react directly with nitrogen (*58*). On reaction with nitrogen it is postulated to form a pyramidal species, $N_2/AlCl_3$ complex. It forms 1:1 compounds with Group V elements, and this is frequently referred to as the III-V compounds. In the vapor phase aluminum chloride is also dimeric, Al_2Cl_6 (Figure 5.7), so there is a radical change of coordination number. These are covalent structures (there is a dative bond from the two chlorines to the two aluminum atoms) that persist in the vapor phase and are the result of the tendency of the metal atom to complete its octet.

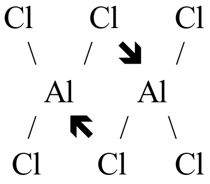

Figure 5.7 Al_2Cl_6 dimer.

Most reactions (remember these would be polymerization or addition reactions) with aluminum chloride require 0.1 – 0.5 mole of catalyst per mole of reactant. The general mechanism in these cases involves the formation of carbonium ions, which are used to attach a benzene nucleus. The result, amongst others, is the addition of an acyl group ($R-C^*=O$), activation of condensation of olefins and importantly the cracking of naphthenic compounds (*52*). The exception is found with acylation reactions, where higher quantities of catalyst are needed. Acid chlorides (R-(C=O)-Cl) [1.1 mol/mol] and acid anhydrides [2.2 mol/mol] form stable oxonium salts (R_2-O^+-H) with aluminum chloride.

5.6.2 Basic catalytic behavior of $AlCl_3$

The use of $AlCl_3$ as an organic synthesis catalyst is well known and proven, as described for $AlBr_3$ above. One can typically explain the mechanism of reactions employing $AlCl_3$ as the catalyst, through the acylation reaction of benzene, where an acyl group is coupled to a benzene ring. In this case, an organic chloride is necessary to initiate the $AlCl_4^-$ species and at the same time the reactive carbonium ion is created to which the reactant, in this case an acyl group, can connect. HCl is a typical by product to such reactions. See the reaction scheme shown in Figure 5.8 (*51*).

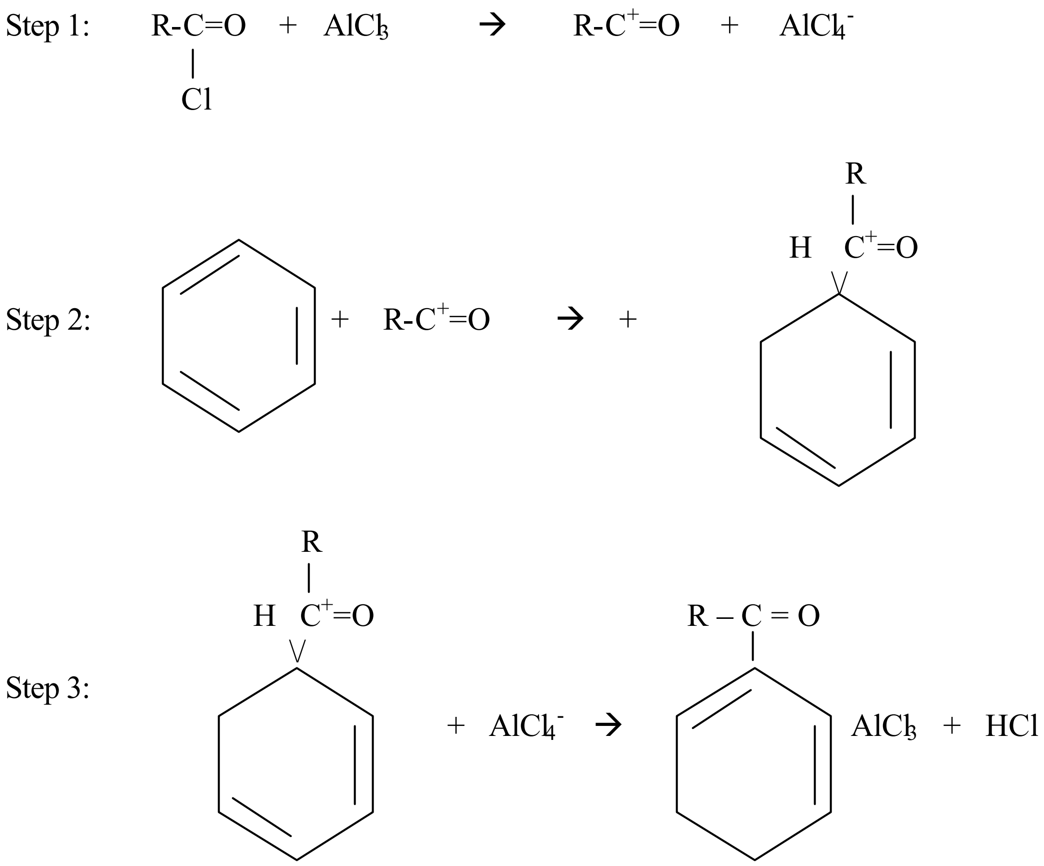

Figure 5.8 Acylation reaction of benzene.

5.6.3 Related industrial processes

Thermal cracking, or pyrolysis reactions (*60*) of alkanes occur between 400 and 900 °C and yield short-chain alkanes, alkenes, and some hydrogen. A modification of this process is steam cracking where the hydrocarbon is diluted in a stream of steam and cracked at approximately 700 – 900 °C to ethylene, propylene, butadiene, isoprene, and cyclopentadiene. Hydro-cracking is yet another process where the feed is cracked in the presence of hydrogen and a catalyst at high pressure, but at much lower temperatures, 250 to 450 °C. Hydro-cracking combines the effect of cracking and hydrogenation to yield low-molecular-weight products to be used as feedstock in large-scale synthesis operations. Another development in this field is that of catalytic cracking and reforming.

Catalytic cracking (CC) and catalytic reforming (CR) reactions are well-known and used industrially to produce high-octane fuels (*n*-heptane octane rating = zero, *iso*-octane rating = 100) processes. Both processes employ catalysts at high temperature (450 °C – 550 °C) and slight pressure, but the CR process produces a product with a high octane number. The mechanisms proposed for cracking reactions may be similar to the current thermocatalytic decomposition process in that acid catalysis breaks down the hydrocarbon chains through the formation of either free radical mechanisms or carbonium ion chemistry, as discussed below. The mechanism to these processes is well documented (*60*).

For catalytic cracking, the mechanism can be explained using the scheme depicted below, First, small amounts of alkenes are formed by dehydrogenation shown in reaction 15:

$$R_1CH_2\text{-}CH_2R_2 \rightarrow R_1CH{=}CHR_2 + H_2 \qquad (15)$$

Second, reaction 16 shows the alkenes react with the protons (in the presence of an acidic catalyst) to give carbonium ions:

$$R_1CH{=}CHR_2 + H^+ \rightarrow R_1CH_2\text{-}C^+HR_2 \qquad (16)$$

The sequence of stability for these ions is: primary < secondary < tertiary. Reaction 17 shows the movement of a hydride ion (H^-) changes a primary to a secondary ion,

$$R_1CH_2\text{-}C^+HR_2 + R_3C^+H_2(CH_3)\text{-}CH_2R_4 \rightarrow R_1CH_2\text{-}CH_2R_2 + R_3C^+(CH_3)\text{-}CH_2R_4 \qquad (17)$$

whereas reaction 18 shows the migration of a methyl group ($-CH_3$) forms the tertiary ion.

$$CH_3\text{-}CH_2\text{-}C^+HR_6 \rightarrow C^+H_2\text{-}CH(CH_3)R_6 \rightarrow CH_3\text{-}C^+(CH_3)R_6 \qquad (18)$$

Third, long-chain carbonium ions are unstable (with respect to shorter ones) and the carbon-carbon bonds are broken by β-scission (at carbons next to the α-carbon in the chain structure) to give an alkene and a primary carbonium ion as reaction 19 indicates.

$$R_3C^+(CH_3)\text{-}CH_2\text{-}CH_2R_5 \rightarrow R_3C(CH_3){=}CH_2 + C^+H_2R_5 \qquad (19)$$

Xiao *et al.* (*61*) also describe the mechanism of breaking down poly-propylene by an acid catalyst via β-scission. The resulting species can go through addition or rearrangements to more stable organic species. See the scheme below, Figure 5.9.

5.6.4 Hypothesis to current process mechanism

The depolymerization reaction is perceived to initialize via classical chemistry as reaction 20 indicates. First aluminum chloride [I] forms a Lewis acid [III] by acquiring a chlorine atom from a suitable chlorine donor or co-catalyst [II] ($FeCl_3$, $AlCl_3$, Cl_2, HCl, or NaCl).

$$\underset{[I]}{AlCl_3} + \underset{[II]}{HCl} \rightarrow \underset{[III]}{AlCl_4^-} + H^+ \qquad (20)$$

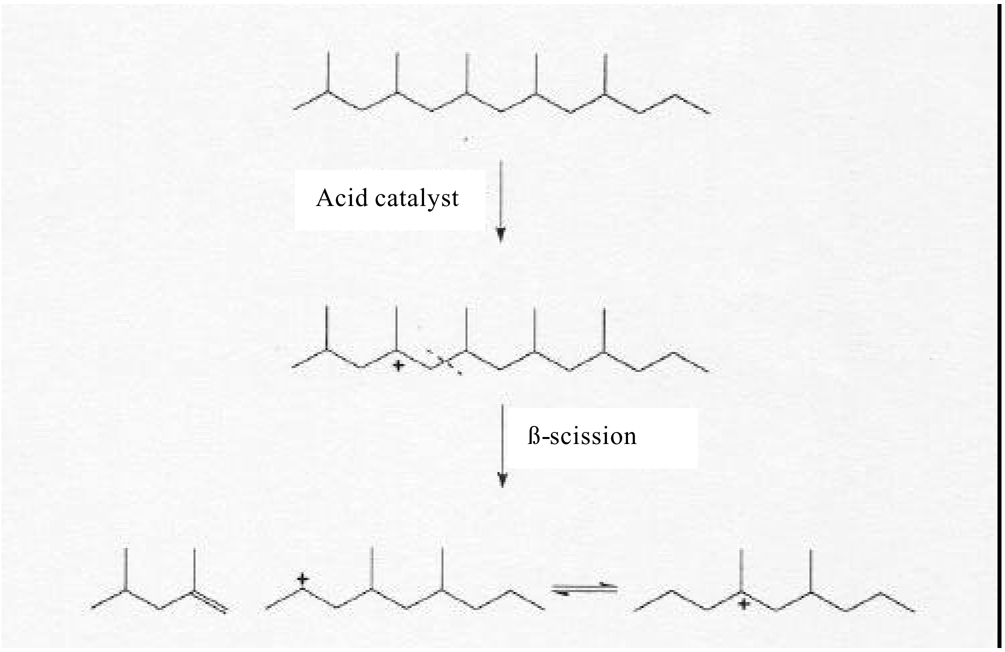

Figure 5.9 Mechanism proposed by Xiao *et al.* (*61*)

Once the Lewis acid [III] has been formed the catalyst can attack the polymer [V] at a saturated position (or the double bond) and creates two intermediate species [VI] and [IX] as reaction 21 indicates.

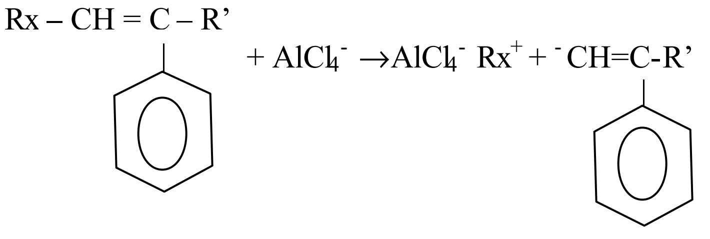

$$\mathrm{Rx - CH = \underset{\substack{|\\ C_6H_5}}{C} - R'} + \mathrm{AlCl_4^-} \rightarrow \mathrm{AlCl_4^-\ Rx^+} + {}^{-}\mathrm{CH{=}\underset{\substack{|\\ C_6H_5}}{C}\text{-}R'} \qquad (21)$$

[V] [III] [VI] [IX]

The mechanism to form these two species is not clear. The creation of such unstable long-chain carbonium ions gives rise to bond breakage. If the mentioned intermediate species form, the resulting organic metallic intermediate [VI] then would form a primary product Rx-Cl and hence releases the catalyst [I] through reaction 22 to take part in subsequent cycles of depolymerization. The alkyl halide is necessary to form the ionized complex of aluminum chloride to make this reaction continue.

$$\underset{[VI]}{AlCl_4^- \, Rx^+} \rightarrow AlCl_3 + RxCl \qquad (22)$$

Parallel to the described regeneration of catalyst, the species [VI] can react with hydrogen-rich resources to yield a polymeric product Rx-H shorter than the original species. In such a case, the chlorine ion is released to either satisfy the production of the ionized complex of aluminum chloride or to attach to a hydrogen ion to form HCl.

The species [IX] can undergo hydrogenation (reaction 23) to yield another polymeric product [IIX] shorter than when the cycle commenced.

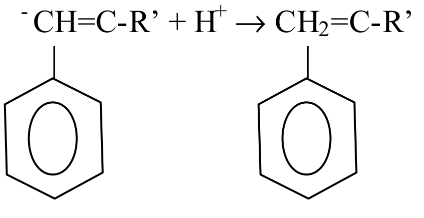

$$^-CH{=}C\text{-}R' + H^+ \rightarrow CH_2{=}C\text{-}R' \qquad (23)$$

[IX] [IIX]

The intermediate products, Rx-H or [IIX] will go into the reaction cycle again under suitable conditions.

The cycle described above repeats until no reactable material is present, and only carbon black remains in the reactor. However, if the reaction system should become hydrogen deficient, the catalyst renewal cycle will break down and will not continue. Consequently, the catalyst cannot be refreshed or released from the organometallic complex [VI]. Hence, any further depolymerization is terminated.

The presence of the strong Lewis acid also may produce undesirable low-molecular-weight hydrocarbon products, like propane and butane, and the hydrogen deficiency will result in the carbon-rich residues. The catalyst can be removed from the residue species only through hydrolysis, a process that destroys the initial activity of the catalyst. However, if adequate amounts of hydrogen are available, the catalyst renewal cycle may be able to continue. To obtain long-chain hydrocarbon products in the carbon range C_6 to C_{12}, it is imperative that the formed products be removed as soon as they come into existence. If not, the aggressive Lewis acid will attack these products and produce short-chain hydrocarbon products in the range C_3 to C_6. It is believed that some degree of secondary depolymerization will always be present and one must therefore aim at minimizing the occurrence thereof. Hence, vapor phase catalysis reactions must be inhibited in so far as possible and the products also must be removed from the reactor as quickly as possible.

The foregoing schemes suggest the mechanisms through which the Lewis acid forms and the depolymerization reactions occur. Our own experimental observations are consistent with these mechanisms.

5.6.5 Organo metallic complex formation

The experimental results and the chemistry described in the previous section suggest that hydrolyzable organo-metallic complexes form when tire rubber is decomposed using $AlCl_3$ in a hydrogen-deficient environment. Aluminum chloride can form 1:1 adducts and complexes with compounds such as the depolymerization residue, and $AlCl_4^-$ acts as the reactive catalytic species. The current studies and the literature (*53*) suggest that $AlCl_3$ forms metal-carbon complexes in the residue that make it nearly impossible to separate the catalyst from the residue without destroying the catalyst. The existence of such complexes and the extreme difficult recovery of $AlCl_3$ in its original (or any active form) from the complex are well documented in patents (and other literature). This metal-carbon complex easily hydrolyses, but the catalyst is destroyed by the reaction. The observations from the patent literature are summarized by a position paper (*62*), which states,

(1) "Strictly speaking the Lewis acids (typically $AlCl_3$, $TiCl_4$) used are not true catalysts as they are used in more than stoichiometric amounts. This is because they form more strongly bonded complexes with the product compounds than with the reagents. A destructive method (aqueous hydrolysis) is necessary to retrieve the product, and so the Lewis acids are non-recoverable."

(2) It is mentioned that any new solution for acylation catalysis should be cost competitive and it asks for a reaction that is "truly" catalytic, and that the catalyst should not be forming strong complexes with the product, must be recyclable, *etc*.

It may however still be possible to recover the catalyst from the complex. A procedure for the recovery of $AlCl_3$ from such residues is described in a recent patent (*63*), by which 100 % $AlCl_3$ recovery is possible from a metal-carbon complex which appears to be similar to that obtained form the S-P process. This is the only patent found for a process that recovers the catalyst as an active entity and not destroy it. One of the future areas of research will be focused on the recovery of the active catalyst.

CHAPTER VI

CONCLUSIONS AND RECOMMENDATIONS

The results described above lead to the following conclusions.

1. The rubber depolymerization reaction occurs rapidly for all catalysts tested, and the hydrocarbon product distribution is significantly different from other reported rubber decomposition methods, such as pyrolysis and catalytic degradation. The products appear to be of better commercial values, in that there are no fuel gas or fuel oil products.

2. Separation of the $AlCl_3$ by evaporation from the residue does not appear to be feasible because of the formation of an organometallic complex, therefore an alternate separation method must be developed.

3. $NaCl/AlCl_3$ catalyst mixtures eliminate many operational difficulties resulting from the high vapor pressure of $AlCl_3$. Methods for recovering the dual catalyst from the solid residue remain to be developed.

4. Stoichiometric hydrogen deficiency seems to promote the formation of carbon-rich residues. The addition of a hydrogen-rich source may inhibit this reaction.

Finally, the depolymerization process appears to be commercial viable if a few important issues can be addressed and solved. The critical issues follow:

- Separation of the catalyst from the solid residue without destroying the activity of the catalyst.

- The preservation of catalyst activity by preventing the formation of the organometallic complexes.
- Compensating for the stoichiometric deficiency of hydrogen
- Suppression of hydrogen chloride formation.

Additional research is required to obtain a definitive conclusion about the economic feasibility of this process. The additional research should address the following:

- Use of $NaCl$-$AlCl_3$ and $AlCl_3$-KCl mixtures as catalysts.
- Separation of catalyst from residue, most likely by filtration.
- Compensation for the hydrogen deficiency by introducing H_2, CH_4, C_3H_8, and C_4H_{10} into the reactor vessel. Elevated pressures most likely will be required to accomplish the hydrogen addition.

LITERATURE CITED

(1) Baumen, B. D. *Rubber World* **1995**, *212*, 30.

(2) *Scrap Tire News* **2000**, *14*, 4.

(3) Strong, D. L. *Recyling in America*; Second ed.; ABC-CLIO, Inc.: Santa Barbara, CA, 1997.

(4) Allred, R.E.; Coons, N.C.; Finley, D.J.; Shoemaker, J.M.; Wilder, R.L.; Wilder, J.D. In *32nd International SAMPE Technical Conference*; Adams, P. J., Ed.; Society for the Advancement of Material and Process Engineering: Boston, MA, 2000; pp 398-408.

(5) *Rubber World* **2001**, *224*, 20.

(6) Truini, J. *Waste News* **2002**, *8*, 4.

(7) EPA; Clark, C.; Meardon, K.; Russell, D. *Scrap Tire Technology and Markets*; Noyes Data Corp.: Park Ridge, NJ, 1993.

(8) Holste, J. C. "Thermocatalytic Conversion of Tires, Plastics and other Organic Materials to Chemical Feedstocks," private communication, 1999.

(9) Cyr, D. R. S. In *Encyclopedia of Polymer Science and Engineering*; Second ed.; Mark, H. F., Bikales, N. M., Overberger, C. G., Menges, G., Kroschwitz, J. I., Eds.; John Wiley & Sons: New York, NY, 1985; Vol. 14, pp 708-710.

(10) Furuta, I.; Kimura, S.-I.; Iwama, M. In *Polymer Handbook*; Fourth ed.; Brandrup, J., Immergut, E. H., Grulke, E. A., Eds.; Wiley: New York, NY, 1999; pp V5-V6.

(11) Barlow, F. W. *Rubber Compounding: Principles, Materials, and Techniques*; Second ed.; Marcel Dekker, Inc.: New York, NY, 1993.

(12) Subramaniam, A. In *Rubber Technology*; Third ed.; Morton, M., Ed.; Van Nostrand Reinhold Co.: New York, NY, 1987; p 180.

(13) Franta, I.; Duchacek, V. In *Elastomers and Rubber Compounding Materials*; Franta, I., Ed.; Elsevier: New York, NY, 1989; p 60.

(14) Degering, F., Ed. *Organic Chemistry*; Sixth ed.; Barnesl & Noble, Inc.: New York, NY, 1951.

(15) Allen, P. W. *Natural Rubber and the Synthetics*; John Wiley & Sons: New York, NY, 1972.

(16) Morrison, R. T.; Boyed, R. N., Eds. *Organic Chemistry*; Fourth ed.; Allyn and Bacon, Inc.: Boston, MA, 1983.

(17) Copley, C. B. *Rubber Chemistry and Technology* **1982**, *55*, 416-427.

(18) Ismail, M. N.; El-Sabbagh, S. H.; Yehia, A. A. *Journal of Elastomers and Plastics* **1999**, *31*, 255-270.

(19) Amari, T.; Themelis, N. J.; Wernick, I. K. *Resources Policy* **1999**, *25*, 179-188.

(20) Liang, L. "Treatment and Evaluation of Solide Residue from Thermocatalyitc Decomposition of Tire Rubber Compounds," dissertation, Texas A&M University, 2004.

(21) Shemenski, R. M. *Wire Journal International* **1994**, 70.

(22) Wake, W. C., Tidd, B.K., and Loadman, M.J.R., Ed. *Analysis of Rubber and Rubber-like Polymers*; Third ed.; Applied Science Publishers Ltd: Barking,

Essex, England, 1983.

(23) Alliger, G., Sjothun, I.J. *Vulcanization of Elastomers*; Van Nostrand Reinhold: New York, NY, 1964.

(24) Roberts, A. D., Ed. *Natural Rubber Science and Technology*; Oxford University Press: Oxford, England, 1988.

(25) Krebs, H. *Rubber Chem. Technol.* **1957**, *30*, 962.

(26) Coran, A. Y. *Rubber Chem. Technol.* **1995**, *68*, 351.

(27) Saville, B., Watson, A.A. *Rubber Chem. Technol.* **1967**, *40*, 100.

(28) Wiles, L. L. *Fire Engineering* **2003**, *156*, 55-60.

(29) Blumenthal, M. *BioCycle* **2002**, *43*, 58-62.

(30) E.I.A. "Annual Energy Outlook 2003 with Projections to 2025," Office of Integrated Analysis and Forecasting, US Department of Energy, Washington, DC, 2003.

(31) Farrell, M. *BioCycle* **1999**, *40*, 50-52.

(32) Shulman, B.L.; White, P.A. In *ACS Symposium Series 76*; Jones, J. L., Radding, S.B., Ed.; Americal Chemical Society: Washington DC, 1978; p 274.

(33) Maruhnic, P.; Wolk, R.H.; Battista, C.A. Recovering Carbon Black from Waste Rubber. U.S. Patent 3,978,199, 1976.

(34) Pakdel, H.; Roy, C.; Aubin, H.; Jean, G.; Coulombe, S. *Environ Sci Technol* **1991**, *25*, 1646-1649.

(35) Williams, P. T.; Besler, S.; Taylor, D. T. *P I Mech Eng a-J Pow* **1993**, *207*, 55-63.

(36) Benallal, B.; Roy, C.; Pakdel, H.; Chabot, S.; Poirier, M. A. *Fuel* **1995**, *74*, 1589-1594.

(37) Williams, P. T.; Besler, S.; Taylor, D. T.; Bottrill, R. P. *J I Energy* **1995**, *68*, 11-21.

(38) Aguado, J.; Serrano, D. P. *Feedstock Recycling of Plastic Wastes*; Royal Society of Chemistry: Cambridge, 1999.

(39) Teng, H.; Serio, M. A.; Wojtowicz, M. A.; Bassilakis, R.; Solomon, P. R. *Industrial & Engineering Chemistry Research* **1995**, *34*, 3102.

(40) Merchant, A. A.; Petrich, M. A. *Aiche J* **1993**, *39*, 1370.

(41) Larsen, J.W. Conversion of Waste Rubber to Fuel and other Useful Products. U.S. Patent 3,996,022, 1976.

(42) Larsen, J.W.; Chang, B. In *A Meeting of the Rubber Division*; American Chemical Society: Minneapolis, 1976.

(43) Ivanova, S.R.; Romanko, T.V.; Shaekhova, V.G.; Sangalov, Y.A.; Berlin, A.A.; Minsker, K.S. *Polymer Science, USSR* **1985**, *27*, 265.

(44) Wingfield Jr., R.C.; Braslaw, J.; Gealer, R.L. Use of Zinc and Copper (I) Salts to Reduce Sulfur and Nitrogen Impurities during the Pyrolysis of Plastic and Rubber Waste to Hydrocarbons. U.S. Patent 4,458,095, 1984.

(45) Wingfield Jr., R.C.; Braslaw, J.; Gealer, R.L. Pyrolytic Conversion of Plastic and Rubber Waste to Hydrocarbons with Basic Salt Catalysts. U.S. Patent 4,515,659, 1985.

(46) Butcher Jr., J.A. Method of Cracking Polymeric Materials Catalyzed by Copper.

U.S. Patent 5,315,055, 1994.

(47) Chen, N.Y.; Yan,T. Method for Treatment of Rubber and Plastic Wastes. U.S. Patent 4,108,730, 1978.

(48) Platz, G.M. Depolymerization Method for Resource Recovery from Polymeric Wastes. U.S. Patent 5,264,640, 1993.

(49) Platz, G.M. Depolymerization Method for Resource Recovery from Polymeric Wastes. U.S. Patent 5,369,215, 1994.

(50) Platz, G.M. Resource Recovery by Catalytic Conversion of Polymers. U.S. Patent 5,504,267, 1996.

(51) Sykes, P. A. *A Guidebook to Mechanism in Organic Chemistry*; Fifth ed.; Longman: New York, NY, 1981.

(52) Grams, G. W. In *Kirk-Othmer Encyclopedia of Chemical Technology*; Fourth ed.; Howe-Grant, M., Ed.; A Wiley-Interscience Publication: New York, NY, 1991; Vol. 2, pp 281-290.

(53) Thomas, C. A. *Anhydrous Aluminum Chloride in Organic Chemistry*; Reinhold Publishing Corp.: New York, NY, 1941.

(54) Smits, A., Meyering, J. L., and Kamermans, M. A. *Proc. Acad. Sci. Amsterdam* **1932**, *35*, 193-196.

(55) Olah, G. A. *Friedel-Crafts Chemistry*; John Wiley & Sons, Inc.: New York, NY, 1973.

(56) Duvenhage, D. J.; Holste, J. C. "Polymer Recycling Studies - Phase II," private communication, 1995.

(57) Ullmann, F. In *Encyclopedia of Industrial Chemistry*; Fifth ed.; VCH: Weinheim, Germany; Deerfield Beach, FL, 1985; Vol. A1, pp 536-541.

(58) Cotton, F. A. a. W., G. *Advanced Inogranic Chemistry, a Comprehensive Text*; Fourth ed.; A Wiley-Interscience Publication: New York, NY, 1980.

(59) Kendall, J., Crittnden, E.D., and Miller, H.K. *J. Amer. Chem. Soc.* **1923**, *45*, 963-996.

(60) Bond, G. C. *Heterogeneous Catalysis - Principles and Applications*; Second ed.; Oxford University Press: New York, NY, 1990.

(61) Xiao, X.; Zmierczak, W.; Shabtai, J. In *209th ACS National Meeting*; Am Chem Soc (Div of Fuel Chemistry): Anaheim, CA, 1995.

(62) The Institute of Applied Catalysis, New Catalytic Process Technology for Acylation. The Institute of Applied Catalysis, London, England, 2000.

(63) Doane, E.P.; Low, J.Y.; Sherman, L.G.; Yuill, W.A. Aluminum Promoted Hydrogen of Alkylation Sludge for Aluminum Chloride Recovery. U.S. Patent 6,004,519, 1999.

APPENDIX A

MASS BALANCE CALCULATIONS

Run III-06 is used as the example for mass balance calculations.

Input Weights:	Rubber:	691.0 g
	Catalyst:	848.3 g
Output Weights:	Reactor Residue:	1338.9 g
	Evaporated Catalyst:	65.2 g
	Naphtha products:	9.3 g
	LPG products:	171.3g
Solid Residue Recovered (washed & dried):		537.4 g

Total Mass Balance (pre-acid wash):

$$\text{Mass in} = \text{rubber} + \text{catalyst} = 691.0 + 848.3 = 1539.3\,\text{g}$$

$$\begin{aligned}\text{Mass out} &= (\text{reactor residue} + \text{evaporated catalyst}) + \text{naphtha} + \text{LPG} \\ &= 1338.9 + 65.2 + 9.30 + 171.3 = 1584.7\,\text{g}\end{aligned}$$

$$\text{Total Mass Balance (\%)} = 100\left(\frac{\text{mass out}}{\text{mass in}}\right) = 100\left(\frac{1584.7}{1539.3}\right) = 102.9\%$$

Feedstock/Products Mass Balance:

$$\begin{aligned}\text{Product mass} &= \text{acid washed solid residue} + \text{naphtha} + \text{LPG} \\ &= 537.4 + 9.30 + 171.3 = 718.0\,\text{g}\end{aligned}$$

$$\text{Feedstock/product mass balance} = \frac{\text{product mass}}{\text{mass of feedstock}} = \frac{718.0}{691.0} = 103.9\%$$

Reactor Residue:

This material contains both catalyst and solid residue product. The amount of reactor residue is determined by weighing.

Evaporated Catalyst:

The amount of evaporated catalyst is determined by weighing the two condensers and the liquid accumulator vessel after the naphtha product has been removed. The net increase in weight is caused by catalyst vapor flow and condensation.

Naphtha Product:

The amount of naphtha product is determined by weighing the liquid in the accumulator at the end of the experiment.

LPG Products:

This product is evolved as gas. The volume of gas evolved from the reactor is measured at atmospheric pressure and ambient temperature using an electronic flow meter operating in the totalizer mode. However, the flow meter reading is not the volume of LPG product formed because sweep gas is added during the experiment and the final conditions in the reactor differ from the initial conditions. (The pressure in the system changes from the starting pressure of 140 kPa (20 psig) at the beginning of the experiment to 0 kPa (0 psig) at the end of the experiment, and the temperature changes from the reactor operating temperature to approximately 77 °C.)

The unsteady state molar material balance for the apparatus is

$$n_2 - n_1 = n_{sg} - n_{fm} + n_{LPG} \quad \Rightarrow \quad n_{LPG} = n_{fm} - n_{sg} + n_2 - n_1$$

where, n_1 and n_2 are the number of moles of gas in the apparatus at the beginning and the end of the experiment respectively, n_{sg} is the number of moles of sweep gas added during the experiment, n_{fm} is the number of moles passing through the flow meter, and n_{LPG} is the number of moles of LPG product formed during the experiment.

The *flow meter* contribution is calculated using the ideal gas law:

$$n_{fm} = \frac{P_0 V_{fm}}{RT_0}$$

where, P_0 is the atmospheric pressure 0.1 MPa (approximately 14.7 psia) and T_0 is ambient temperature at approximately 294 K (21 °C), and V_{fm} is the totalized flow meter reading.

The *sweep gas* contribution is calculated as follows, using the volumetric flow rate of the sweep gas, Q, the elapsed time of the experiment, t, and the ideal gas law:

$$n_{sg} = \frac{QtP_0}{RT_0}$$

The flow rate is approximately 0.02 L/min, and the elapsed time is approximately 1 h longer than the time after the last rubber is fed.

For the *unsteady state* contribution, there are three general regions of the apparatus that must be considered separately: the feeder assembly, the reactor vessel, and downstream components (condensers and liquid accumulator). The number of moles of gas in the apparatus is given by

$$n = n_f + n_r + n_{ds} = \frac{PV_f}{RT_f} + \frac{PV_r}{RT_r} + \frac{PV_{ds}}{RT_{ds}}$$

where the subscripts *f, r,* and *ds* denote the feeder assembly, the reactor vessel, and the downstream components respectively. The feeder assembly and the downstream components are at ambient temperature, so that the previous expression becomes

$$n = \frac{P}{RT_0}\left(V_f + V_{ds} + V_r \frac{T_0}{T_r}\right)$$

and the unsteady state contribution is

$$n_2 - n_1 = \frac{(P_2 - P_1)(V_f + V_{ds})}{RT_0} + \frac{V_r}{R}\left(\frac{P_2}{T_{r2}} - \frac{P_1}{T_{r1}}\right)$$

where the initial reactor temperature, T_{r1}, is the reactor operating pressure, and the final reactor temperature, T_{r2}, is approximately 77 °C.

The expression for the number of moles of LPG product then is:

$$n_{LPG} = \frac{P_0\left(V_{fm} - Qt\right)}{RT_0} + \frac{\left(P_2 - P_1\right)\left(V_f + V_{ds}\right)}{RT_0} + \frac{V_r}{R}\left(\frac{P_2}{T_{r2}} - \frac{P_1}{T_{r1}}\right)$$

The *mass of LPG product* is calculated from the number of moles and the average molecular weight

$$m_{LPG} = n_{LPG} M_{ave}$$

$$M_{ave} = \sum x_i M_i$$

where x_i is the mole fraction and M_i is the molecular weight of substance i in the LPG product. The volume fractions given in Table 5.2 are used as the mole fractions in this calculation.

Physical parameters used for calculations:

The values used for the calculations are shown in Table A.1:

Table A.1 Physical Parameters Used for Calculations

variable	value	physical significance
T_0	21 °C (294 K)	standard temperature
P_0	0.10 mPa (14.7 psia)	standard pressure
Q	20 cm^3/min	sweep gas flow rate
t	variable	time after last rubber fed + 1 h
V_{fm}	variable	totalized flow meter reading
P_1	0.24 mPa (34.7 psia)	initial reactor pressure
P_2	0.10 mPa (14.7 psia)	ending pressure
V_f	7 L	feeder assembly volume
V_r	10 L	reactor vessel volume
V_{ds}	2 L	downstream components volumes
T_{r1}	variable	reactor operating temperature
T_{r2}	77 °C (350 K)	final reactor temperature
R	1.2058 l-psia/(mol·K)	universal gas constant

APPENDIX B

CORE LAB NAPHTHA ANALYSIS

Six naphtha fraction samples were submitted to Core Lab – Petroleum Services, Houston, Texas for detailed composition analysis. The six samples represented one each for SBR, natural rubber, butyl rubber, silica rubber, and black side wall rubber, as well as SBR rubber decomposed with NaCl-$AlCl_3$. The detailed analysis results are listed below.

Table B.1 SBR Rubber – Gas Chromatography Analysis

component name	wt %	lv %	mole %
propane	0.09	0.12	0.16
iso-butane	4.02	4.83	5.50
n-butane	4.33	5.01	5.92
iso-pentane	22.52	24.36	24.82
n-pentane	7.30	7.82	8.04
2,2-dimethylbutane	2.83	2.93	2.61
cyclopentane	2.12	1.91	2.40
2,3-dimethylbutane	3.61	3.66	3.33
2-methylpentane	12.36	12.68	11.40
3-methylpentane	7.38	7.45	6.81
n-hexane	4.21	4.29	3.88
2,2-dimethylpentane	0.05	0.05	0.04
methylcyclopentane	4.75	4.26	4.49
2,4-dimethylpentane	0.10	0.10	0.08
2,2,3-trimethylbutane	0.03	0.03	0.02
benzene	5.45	4.16	5.54
3,3-dimethylpentane	0.04	0.04	0.03
cyclohexane	2.08	1.79	1.96
2-methylhexane	0.29	0.29	0.23
2,3-dimethylpentane	0.09	0.09	0.07
1,1-dimethylcyclopentane	0.45	0.40	0.36
3-methylhexane	0.26	0.25	0.21
cis-1,3-dimethylcyclopentane	0.66	0.59	0.53
trans-1,3-dimethylcyclopentane	0.57	0.51	0.46
trans-1,2-dimethylcyclopentane	0.90	0.80	0.73
n-heptane	0.12	0.12	0.10
methylcyclohexane	5.92	5.17	4.79
1,1,3-trimethylcyclopentane	0.17	0.15	0.12
ethylcyclopentane	0.07	0.06	0.06
2,5-dimethylhexane	0.02	0.02	0.01

Table B.1 SBR Rubber – Gas Chromatography Analysis (continued)

component name	wt %	lv %	mole %
2,4-dimethylhexane	0.02	0.02	0.01
trans,cis-1,2,4-trimethylcyclopentane	0.13	0.12	0.09
trans,cis-1,2,3-trimethylcyclopentane	0.11	0.10	0.08
toluene	2.46	1.91	2.12
2,3-dimethylhexane	0.04	0.04	0.03
2-methylheptane	0.03	0.03	0.02
4-methylheptane	0.01	0.01	0.01
cis-1,3 dimethylcyclohexane	1.19	1.04	0.84
3-methylheptane	0.02	0.02	0.01
trans-1,4-dimethylcyclohexane	0.58	0.51	0.41
1,1-dimethylcyclohexane	0.15	0.13	0.11
trans-1-ethyl-3-methylcyclopentane	0.01	0.01	0.01
trans-1-ethyl-2-methylcyclopentane	0.02	0.02	0.01
1-ethyl-1-methylcyclopentane	0.02	0.02	0.01
trans-1,2,dimethylcyclohexane	0.30	0.26	0.21
n-octane	0.22	0.21	0.15
cis-1,2-dimethylcyclohexane	0.03	0.03	0.02
ethylcyclohexane	0.21	0.18	0.15
1,1,3-trimethylcyclohexane	0.11	0.09	0.07
C_9 naphthenes	0.08	0.07	0.05
ethylbenzene	0.25	0.19	0.19
trans,trans-,1,2,4-trimethylcyclohexane	0.17	0.15	0.11
*cis,trans-,*1,3,5-trimethylcyclohexane	0.02	0.02	0.01
meta-xylene	0.09	0.07	0.07
para-xylene	0.02	0.02	0.01
3-ethylheptane	0.01	0.01	0.01
3-methyloctane	0.02	0.02	0.01
ortho-xylene	0.01	0.01	0.01
trans-1-ethyl-4-methylcyclohexane	0.05	0.04	0.03
isobutylcyclopentane	0.03	0.03	0.02
trans,trans,1,2,3,trimethylcyclohexane	0.01	0.01	0.01
trans-1-ethyl-3-methylcyclohexane	0.02	0.02	0.01
n-propylbenzene	0.01	0.01	0.01
1-methyl-3-ethylbenzene	0.04	0.03	0.03
1-methyl-4-ethylbenzene	0.01	0.01	0.01
unidentified C_{10} compound	0.35	0.30	0.20
C_{11} unidentified	0.01	0.01	0.00
dodecanes	0.19	0.15	0.09
tetradecanes	0.08	0.07	0.03
hexadecanes	0.05	0.04	0.02
heptadecanes	0.02	0.02	0.01
octadecanes	0.01	0.01	0.00
total	100.00	100.00	100.00

Table B.1 SBR Rubber – Gas Chromatography Analysis (continued)

composite by carbon

$C_\#$	olefin	naphthene	aromatic
C_2			
C_3			
C_4	0.00		
C_5	0.00	1.91	
C_6	0.00	6.05	4.16
C_7	0.00	7.53	1.91
C_8	0.00	2.57	0.29
C_9	0.00	0.43	0.05
C_{10}	0.00	0.00	0.00
C_{11}			0.00
C_{12}			
C_{13}			
C_{14}			
total lv %	0.00	18.49	6.41
unidentified=			

Table B.2 Natural Rubber – Gas Chromatography Analysis

component name	wt %	lv %	mol %
propane	0.11	0.14	0.20
isobutane	4.10	4.85	5.64
n-butane	4.46	5.08	6.14
2,2-dimethylpropane	0.01	0.01	0.01
isopentane	22.84	24.33	25.31
n-pentane	7.52	7.93	8.34
2,2-dimethylbutane	2.85	2.90	2.65
cyclopentane	1.45	1.29	1.65
2,3-dimethylbutane	4.14	4.14	3.84
2-methylpentane	14.29	14.45	13.26
3-methylpentane	8.25	8.21	7.66
n-hexane	4.56	4.57	4.23
2,2-dimethylpentane	0.05	0.05	0.04
methylcyclopentane	5.02	4.43	4.77
2,4-dimethylpentane	0.16	0.16	0.13
2,2,3-trimethylbutane	0.04	0.04	0.03
benzene	0.22	0.17	0.23
3,3-dimethylpentane	0.05	0.05	0.04
cyclohexane	2.46	2.09	2.34
2-methylhexane	0.42	0.41	0.34
2,3-dimethylpentane	0.12	0.11	0.10
1,1-dimethylcyclopentane	0.47	0.41	0.38
3-methylhexane	0.36	0.35	0.29
cis-1,3-dimethylcyclopentane	0.63	0.56	0.51
trans-1,3-dimethylcyclopentane	0.55	0.49	0.45
trans-1,2-dimethylcyclopentane	0.88	0.77	0.72
n-heptane	0.13	0.13	0.10
methylcyclohexane	7.47	6.42	6.09
1,1,3-trimethylcyclopentane	0.17	0.15	0.12
ethylcyclopentane	0.05	0.04	0.04
2,5-dimethylhexane	0.03	0.03	0.02
2,4-dimethylhexane	0.03	0.03	0.02
trans,cis-1,2,4-trimethylcyclopentane	0.13	0.12	0.09
trans,cis-1,2,3-trimethylcyclopentane	0.11	0.10	0.08
toluene	0.66	0.50	0.57
2,3-dimethylhexane	0.04	0.04	0.03
2-methylheptane	0.04	0.04	0.03
4-methylheptane	0.01	0.01	0.01
cis-1,3 dimethylcyclohexane	1.70	1.47	1.21
3-methylheptane	0.03	0.03	0.02

Table B.2 Natural Rubber – Gas Chromatography Analysis (continued)

component name	wt %	lv %	mol %
trans-1,4-dimethylcyclohexane	0.83	0.72	0.59
1,1-dimethylcyclohexane	0.21	0.18	0.15
trans-1-ethyl-3-methylcyclopentane	0.01	0.01	0.01
trans-1-ethyl-2-methylcyclopentane	0.01	0.01	0.01
1-ethyl-1-methylcyclopentane	0.02	0.02	0.01
trans-1,2,dimethylcyclohexane	0.39	0.33	0.28
n-octane	0.29	0.27	0.20
cis-1,2-dimethylcyclohexane	0.04	0.03	0.03
ethylcyclohexane	0.30	0.25	0.21
1,1,3-trimethylcyclohexane	0.17	0.14	0.11
C_9 naphthenes	0.11	0.09	0.07
ethylbenzene	0.03	0.02	0.02
*trans,trans,*1,2,4-trimethylcyclohexane	0.26	0.22	0.16
*cis,trans,*1,3,5-trimethylcyclohexane	0.03	0.03	0.02
meta-xylene	0.03	0.02	0.02
para-xylene	0.01	0.01	0.01
3-ethylheptane	0.01	0.01	0.01
3-methyloctane	0.02	0.02	0.01
ortho-xylene	0.01	0.01	0.01
cis-1-ethyl-3-methylcyclohexane	0.01	0.01	0.01
trans-1-ethyl-4-methylcyclohexane	0.08	0.07	0.05
isobutylcyclopentane	0.04	0.03	0.03
trans,trans,1,2,3,trimethylcyclohexane	0.01	0.01	0.01
trans-1-ethyl-3-methylcyclohexane	0.02	0.02	0.01
trans-1-ethyl-2-methylcyclohexane	0.01	0.01	0.01
unidentified C_{10} compound	0.14	0.12	0.08
C_{11} unidentified	0.01	0.01	0.00
dodecanes	0.20	0.15	0.10
tridecanes	0.02	0.02	0.01
tetradecanes	0.04	0.03	0.02
hexadecanes	0.02	0.02	0.01
heptadecanes	0.01	0.01	0.00
total	100.00	100.00	100.00

Table B.2 Natural Rubber – Gas Chromatography Analysis (continued)

composite by carbon

$C_{\#}$	olefin	naphthene	aromatic
C_2			
C_3			
C_4	0.00		
C_5	0.00	1.29	
C_6	0.00	6.52	0.17
C_7	0.00	8.69	0.50
C_8	0.00	3.39	0.06
C_9	0.00	0.63	0.00
C_{10}	0.00	0.00	0.00
C_{11}		0.00	0.00
C_{12}			
C_{13}			
C_{14}			
total lv %	0.00	20.52	0.73
unidentified=			

Table B.3 Butyl Rubber – Gas Chromatography Analysis

component name	wt %	lv %	mol %
propane	0.09	0.12	0.18
isobutane	4.77	5.59	7.07
n-butane	1.22	1.38	1.81
isopentane	26.16	27.59	31.21
n-pentane	1.48	1.55	1.77
2,2-dimethylbutane	0.60	0.60	0.60
2,3-dimethylbutane	9.76	9.66	9.75
2-methylpentane	11.57	11.58	11.56
3-methylpentane	6.03	5.94	6.03
n-hexane	0.51	0.51	0.51
2,2-dimethylpentane	0.07	0.07	0.06
methylcyclopentane	0.03	0.03	0.03
2,4-dimethylpentane	6.05	5.89	5.20
2,2,3-trimethylbutane	1.56	1.48	1.34
3,3-dimethylpentane	0.08	0.08	0.07
cyclohexane	0.03	0.03	0.03
2-methylhexane	3.71	3.58	3.19
2,3-dimethylpentane	3.89	3.67	3.34
1,1-dimethylcyclopentane	0.01	0.01	0.01
3-methylhexane	2.96	2.82	2.54
cis-1,3-dimethylcyclopentane	0.01	0.01	0.01
3-ethylpentane	0.13	0.12	0.11
2,2,4-trimethylpentane	3.72	3.52	2.80
n-heptane	0.11	0.11	0.09
methylcyclohexane	0.12	0.10	0.11
1,1,3-trimethylcyclopentane	0.05	0.04	0.04
2,5-dimethylhexane	2.11	1.99	1.59
2,4-dimethylhexane	1.78	1.66	1.34
3,3-dimethylhexane	0.02	0.02	0.02
2,3,4-trimethylpentane	0.74	0.67	0.56
2,3,3-trimethylpentane	0.70	0.64	0.53
2,3-dimethylhexane	0.65	0.60	0.49
2-methyl-3-ethylpentane	0.04	0.04	0.03
2-methylheptane	0.68	0.64	0.51
4-methylheptane	0.31	0.29	0.23
3,4-dimethylhexane	0.12	0.11	0.09
3-methylheptane	0.71	0.66	0.54
trans-1,4-dimethylcyclohexane	0.03	0.03	0.02
2,2,5-trimethylhexane	2.03	1.88	1.36
trans-1,2,dimethylcyclohexane	0.02	0.02	0.02
2,2,4-trimethylhexane	0.13	0.12	0.09

Table B.3 Butyl Rubber – Gas Chromatography Analysis (continued)

component name	wt %	lv %	mol %
n-octane	0.03	0.03	0.02
2,4,4-trimethylhexane	0.22	0.20	0.15
2,3,5-trimethylhexane	0.38	0.34	0.26
2,4-dimethylheptane	0.18	0.16	0.12
ethylcyclohexane	0.03	0.02	0.02
2,6-dimethylheptane	0.20	0.18	0.13
1,1,3-trimethylcyclohexane	0.03	0.03	0.02
2,5-dimethylheptane	0.41	0.37	0.28
3,5-dimethylheptane	0.04	0.04	0.03
2,3,3,trimethylhexane	0.04	0.04	0.03
2,3,4,trimethylhexane	0.07	0.06	0.05
2,3-dimethylheptane	0.08	0.07	0.05
3,4-dimethylheptane d/l	0.02	0.02	0.01
3,4-dimethylheptane l/d	0.02	0.02	0.01
4-ethylheptane	0.01	0.01	0.01
4-methyloctane	0.06	0.05	0.04
2-methyloctane	0.08	0.07	0.05
3-ethylheptane	0.01	0.01	0.01
3-methyloctane	0.08	0.07	0.05
2,2,6-trimethylheptane	0.27	0.23	0.16
2,4-dimethyloctane	0.06	0.05	0.04
2,6-dimethyloctane	0.05	0.05	0.03
2,5-dimethyloctane	0.02	0.02	0.01
2,7-dimethyloctane	0.01	0.01	0.01
4-methylnonane	0.22	0.20	0.13
2-methylnonane	0.01	0.01	0.01
3-methylnonane	0.02	0.02	0.01
C_{10} paraffin	1.50	1.32	0.83
unidentified C_{10} compound	0.03	0.03	0.02
C_{11} unidentified	0.56	0.46	0.30
dodecanes	0.34	0.26	0.18
tridecanes	0.09	0.07	0.04
tetradecanes	0.02	0.02	0.01
pentadecanes	0.01	0.01	0.00
unidentified	0.00	0.00	0.00
total	100.00	100.00	100.00

Table B.3 Butyl Rubber – Gas Chromatography Analysis (continued)

composite by carbon

$C_\#$	olefin	naphthene	aromatic
C_2			
C_3			
C_4	0.00		
C_5	0.00	0.00	
C_6	0.00	0.06	0.00
C_7	0.00	0.12	0.00
C_8	0.00	0.11	0.00
C_9	0.00	0.03	0.00
C_{10}	0.00	0.00	0.00
C_{11}		0.00	0.00
C_{12}			
C_{13}			
C_{14}			
total lv %	0.00	0.32	0.00
unidentified=			

Table B.4 Silica Rubber – Gas Chromatography Analysis

component name	wt %	lv %	mol %
propane	0.22	0.30	0.40
isobutane	3.47	4.24	4.83
n-butane	3.16	3.72	4.40
isopentane	18.81	20.71	21.11
n-pentane	5.50	5.99	6.17
2,2-dimethylbutane	1.95	2.05	1.83
cyclopentane	2.21	2.03	2.55
2,3-dimethylbutane	3.68	3.80	3.46
2-methylpentane	12.76	13.33	11.99
3-methylpentane	7.67	7.88	7.21
n-hexane	3.96	4.10	3.72
2,2-dimethylpentane	0.04	0.04	0.03
methylcyclopentane	6.40	5.84	6.16
2,4-dimethylpentane	0.17	0.17	0.14
2,2,3-trimethylbutane	0.05	0.05	0.04
benzene	6.73	5.23	6.98
3,3-dimethylpentane	0.05	0.05	0.04
cyclohexane	2.76	2.42	2.66
2-methylhexane	0.47	0.47	0.38
2,3-dimethylpentane	0.14	0.14	0.11
1,1-dimethylcyclopentane	0.54	0.49	0.45
3-methylhexane	0.42	0.42	0.34
cis-1,3-dimethylcyclopentane	0.88	0.81	0.73
trans-1,3-dimethylcyclopentane	0.76	0.69	0.63
trans-1,2-dimethylcyclopentane	1.20	1.09	0.99
n-heptane	0.15	0.15	0.12
methylcyclohexane	7.53	6.69	6.21
1,1,3-trimethylcyclopentane	0.22	0.20	0.16
ethylcyclopentane	0.08	0.07	0.07
2,5-dimethylhexane	0.03	0.03	0.02
2,4-dimethylhexane	0.03	0.03	0.02
trans,cis-1,2,4-trimethylcyclopentane	0.17	0.16	0.12
trans,cis-1,2,3-trimethylcyclopentane	0.13	0.12	0.09
toluene	2.59	2.04	2.28
1,1,2-trimethylcyclopentane	0.06	0.05	0.04
2-methylheptane	0.04	0.04	0.03
4-methylheptane	0.02	0.02	0.01
cis-1,3 dimethylcyclohexane	1.42	1.27	1.02
3-methylheptane	0.06	0.06	0.04
trans-1,4-dimethylcyclohexane	0.71	0.64	0.51
1,1-dimethylcyclohexane	0.19	0.17	0.14

Table B.4 Silica Rubber – Gas Chromatography Analysis (continued)

component name	wt %	lv %	mol %
trans-1-ethyl-3-methylcyclopentane	0.01	0.01	0.01
trans-1-ethyl-2-methylcyclopentane	0.01	0.01	0.01
1-ethyl-1-methylcyclopentane	0.02	0.02	0.01
trans-1,2,dimethylcyclohexane	0.66	0.58	0.48
cis-1,4-dimethylcyclohexane	0.24	0.21	0.17
n-octane	0.02	0.02	0.01
cis-1,2-dimethylcyclohexane	0.04	0.03	0.03
ethylcyclohexane	0.25	0.22	0.18
1,1,3-trimethylcyclohexane	0.14	0.12	0.09
C_9 naphthenes	0.11	0.10	0.07
ethylbenzene	0.25	0.20	0.19
trans,trans,1,2,4-trimethylcyclohexane	0.20	0.17	0.13
*cis,trans,*1,3,5-trimethylcyclohexane	0.02	0.02	0.01
meta-xylene	0.10	0.08	0.08
para-xylene	0.01	0.01	0.01
3-ethylheptane	0.01	0.01	0.01
3-methyloctane	0.02	0.02	0.01
trans-1-ethyl-4-methylcyclohexane	0.06	0.05	0.04
isobutylcyclopentane	0.04	0.04	0.03
trans-1-ethyl-3-methylcyclohexane	0.01	0.01	0.01
1-methyl-3-ethylbenzene	0.05	0.04	0.03
1-methyl-4-ethylbenzene	0.01	0.01	0.01
1,2,3,4 tet-methylcyclohexane	0.02	0.02	0.01
1,3-dimethyl-2-ethylbenzene	0.01	0.01	0.01
1,2,3,4-tetramethylbenzene	0.01	0.01	0.01
4-methylundecane	0.01	0.01	0.00
C_{11} aromatic	0.02	0.01	0.01
unidentified	0.22	0.16	0.11
total	100.00	100.00	100.00

Table B.4 Silica Rubber – Gas Chromatography Analysis (continued)

summary by group

group	%wt	% vol
paraffin	13.01	14.28
isoparafin	49.89	53.56
olefin	0.00	0.00
naphthene	27.09	24.35
aromatic	9.78	7.64
unidentified	0.23	0.17

summary by carbon

group	%wt	% vol
C_2	0.00	0.00
C_3	0.22	0.30
C_4	6.63	7.96
C_5	26.52	28.73
C_6	45.91	44.65
C_7	15.07	13.37
C_8	4.69	4.18
C_9	0.67	0.59
C_{10}	0.04	0.04
C_{11}	0.02	0.01

composite by carbon

group	$C_\#$	%wt	% vol
paraffin	C_2	0.00	0.00
	C_3	0.22	0.30
	C_4	3.16	3.72
	C_5	5.50	5.99
	C_6	3.96	4.10
	C_7	0.15	0.15
	C_8	0.02	0.02
	C_9	0.00	0.00
	C_{10}	0.00	0.00
	C_{11}	0.00	0.00

Table B.4 Silica Rubber – Gas Chromatography Analysis (continued)

composite by carbon

group	C#	%wt	% vol
isoparaffin	C_4	3.47	4.24
	C_5	18.81	20.71
	C_6	26.06	27.06
	C_7	1.34	1.34
	C_8	0.18	0.18
	C_9	0.03	0.03
	C_{10}	0.00	0.00
	C_{11}	0.00	0.00
olefin	C_4	0.00	0.00
	C_5	0.00	0.00
	C_6	0.00	0.00
	C_7	0.00	0.00
	C_8	0.00	0.00
	C_9	0.00	0.00
	C_{10}	0.00	0.00
naphthene	C_5	2.21	2.03
	C_6	9.16	8.26
	C_7	10.99	9.84
	C_8	4.13	3.69
	C_9	0.58	0.51
	C_{10}	0.02	0.02
	C_{11}	0.00	0.00
aromatic	C_6	6.73	5.23
	C_7	2.59	2.04
	C_8	0.36	0.29
	C_9	0.06	0.05
	C_{10}	0.02	0.02
	C_{11}	0.02	0.01

Table B.5 Black Side Wall Rubber – Gas Chromatography Analysis

component name	wt %	lv %	mol %
propane	0.08	0.11	0.15
isobutane	2.55	3.07	3.61
n-butane	1.80	2.09	2.55
isopentane	23.13	25.03	26.40
n-pentane	5.49	5.89	6.27
2,2-dimethylbutane	2.05	2.12	1.96
cyclopentane	1.16	1.05	1.36
2,3-dimethylbutane	4.39	4.46	4.20
2-methylpentane	14.65	15.02	14.01
3-methylpentane	8.79	8.89	8.40
n-hexane	3.75	3.82	3.58
2,2-dimethylpentane	0.06	0.06	0.05
methylcyclopentane	6.02	5.40	5.89
2,4-dimethylpentane	0.36	0.36	0.30
2,2,3-trimethylbutane	0.10	0.10	0.08
benzene	1.22	0.93	1.29
3,3-dimethylpentane	0.07	0.07	0.06
cyclohexane	2.44	2.11	2.39
2-methylhexane	0.96	0.95	0.79
2,3-dimethylpentane	0.31	0.30	0.25
1,1-dimethylcyclopentane	0.46	0.41	0.39
3-methylhexane	0.86	0.84	0.71
cis-1,3-dimethylcyclopentane	0.98	0.88	0.82
trans-1,3-dimethylcyclopentane	0.86	0.77	0.72
3-ethylpentane	0.04	0.04	0.03
trans-1,2-dimethylcyclopentane	1.33	1.19	1.12
2,2,4-trimethylpentane	0.02	0.02	0.01
n-heptane	0.22	0.22	0.18
methylcyclohexane	8.08	7.06	6.78
1,1,3-trimethylcyclopentane	0.26	0.23	0.19
ethylcyclopentane	0.13	0.11	0.11
2,5-dimethylhexane	0.08	0.08	0.06
2,4-dimethylhexane	0.09	0.09	0.06
trans,cis-1,2,4-trimethylcyclopentane	0.20	0.18	0.15
3,3-dimethylhexane	0.01	0.01	0.01
trans,cis-1,2,3-trimethylcyclopentane	0.16	0.14	0.12
toluene	0.90	0.70	0.80
1,1,2-trimethylcyclopentane	0.08	0.07	0.06
2-methylheptane	0.12	0.12	0.09
4-methylheptane	0.04	0.04	0.03
*cis,trans,*1,2,4-trimethylcyclopentane	0.02	0.02	0.01

Table B.5 Black Side Wall Rubber – Gas Chromatography Analysis (continued)

component name	wt %	lv %	mol %
cis-1,3 dimethylcyclohexane	1.50	1.32	1.10
3-methylheptane	0.17	0.16	0.12
trans-1,4-dimethylcyclohexane	0.75	0.66	0.55
1,1-dimethylcyclohexane	0.19	0.16	0.14
trans-1-ethyl-3-methylcyclopentane	0.02	0.02	0.01
cis-1-ethyl-3-methylcyclopentane	0.02	0.02	0.01
trans-1-ethyl-2-methylcyclopentane	0.02	0.02	0.01
1-ethyl-1-methylcyclopentane	0.02	0.02	0.01
trans-1,2,dimethylcyclohexane	0.41	0.36	0.30
cis-1,4-dimethylcyclohexane	0.21	0.18	0.15
n-octane	0.11	0.10	0.08
cis-1,2-dimethylcyclohexane	0.05	0.04	0.04
ethylcyclohexane	0.32	0.27	0.23
1,1,3-trimethylcyclohexane	0.19	0.16	0.12
C_9 naphthenes	0.15	0.13	0.10
ethylbenzene	0.08	0.06	0.06
*trans,trans,*1,2,4-trimethylcyclohexane	0.30	0.26	0.20
*cis,trans,*1,3,5-trimethylcyclohexane	0.03	0.03	0.02
meta-xylene	0.07	0.05	0.05
para-xylene	0.02	0.02	0.02
3,4-dimethylheptane l/d	0.01	0.01	0.01
4-methyloctane	0.01	0.01	0.01
2-methyloctane	0.02	0.02	0.01
3-ethylheptane	0.02	0.02	0.01
3-methyloctane	0.04	0.04	0.03
cis,cis,1,2,4,trimethylcyclohexane	0.02	0.02	0.01
ortho-xylene	0.03	0.02	0.02
cis-1-ethyl-3-methylcyclohexane	0.02	0.02	0.01
trans-1-ethyl-4-methylcyclohexane	0.10	0.08	0.07
isobutylcyclopentane	0.06	0.05	0.04
trans,trans,1,2,3,trimethylcyclohexane	0.02	0.02	0.01
n-nonane	0.01	0.01	0.01
trans-1-ethyl-3-methylcyclohexane	0.03	0.03	0.02
trans-1-ethyl-2-methylcyclohexane	0.01	0.01	0.01
sec-butylcyclopentane	0.01	0.01	0.01
2,4-dimethyloctane	0.01	0.01	0.01
n-propylcyclohexane	0.01	0.01	0.01
1-methyl-3-ethylbenzene	0.01	0.01	0.01
1-methyl-4-ethylbenzene	0.01	0.01	0.01
1,2,3,4 tet-methylcyclohexane	0.01	0.01	0.01
C_{11} paraffins	0.02	0.02	0.01

Table B.5 Black Side Wall Rubber – Gas Chromatography Analysis (continued)

component name	wt %	lv %	mol %
C_{11} unidentified	0.02	0.02	0.01
1,2,3,4-tetramethylbenzene	0.06	0.04	0.04
2-methylundecane	0.01	0.01	0.00
C_{11} aromatic	0.02	0.02	0.01
n-dodecane	0.01	0.01	0.00
dodecanes	0.35	0.27	0.18
tridecanes	0.04	0.03	0.02
tetradecanes	0.02	0.02	0.01
hexadecanes	0.02	0.02	0.01
heptadecanes	0.02	0.02	0.01
unidentified	0.01	0.01	0.01
total	100.00	100.00	100.00

<u>summary by group</u>

group	%wt	% vol
paraffin	11.46	12.24
isoparaffin	58.98	61.96
olefin	0.00	0.00
naphthene	26.65	23.53
aromatic	2.42	1.86
unidentified	0.50	0.41

<u>summary by carbon</u>

group	%wt	% vol
C_2	0.00	0.00
C_3	0.08	0.11
C_4	4.35	5.16
C_5	29.78	31.97
C_6	43.31	42.75
C_7	15.72	14.06
C_8	5.06	4.48
C_9	1.08	0.96
C_{10}	0.08	0.06
C_{11}	0.04	0.04

Table B.5 Black Side Wall Rubber – Gas Chromatography Analysis (continued)

composite by carbon

group	$C_\#$	%wt	% vol
paraffin	C_2	0.00	0.00
	C_3	0.08	0.11
	C_4	1.80	2.09
	C_5	5.49	5.89
	C_6	3.75	3.82
	C_7	0.22	0.22
	C_8	0.11	0.10
	C_9	0.01	0.01
	C_{10}	0.00	0.00
	C_{11}	0.00	0.00
isoparaffin	C_4	2.55	3.07
	C_5	23.13	25.03
	C_6	29.88	30.49
	C_7	2.76	2.72
	C_8	0.53	0.52
	C_9	0.10	0.10
	C_{10}	0.01	0.01
	C_{11}	0.02	0.02
olefin	C_4	0.00	0.00
	C_5	0.00	0.00
	C_6	0.00	0.00
	C_7	0.00	0.00
	C_8	0.00	0.00
	C_9	0.00	0.00
	C_{10}	0.00	0.00
naphthene	C_5	1.16	1.05
	C_6	8.46	7.51
	C_7	11.84	10.42
	C_8	4.23	3.71
	C_9	0.95	0.83
	C_{10}	0.01	0.01
	C_{11}	0.00	0.00

Table B.5 Black Side Wall Rubber – Gas Chromatography Analysis (continued)

composite by carbon

group	$C_\#$	%wt	% vol
aromatic	C_6	1.22	0.93
	C_7	0.90	0.70
	C_8	0.20	0.15
	C_9	0.02	0.02
	C_{10}	0.06	0.04
	C_{11}	0.02	0.02

additional group information

molecular weight of sample	82.38
molecular weight of C_6 plus	90.41
density of sample	0.6768
density C_6 plus	0.7103

Table B.6 SBR Rubber (NaCl: $AlCl_3$) – Gas Chromatography Analysis

component name	wt %	lv %	mol %
propane	0.11	0.17	0.28
isobutane	1.26	1.73	2.42
n-butane	0.27	0.36	0.52
isopentane	3.54	4.37	5.48
n-pentane	0.04	0.05	0.06
cyclopentane	0.13	0.13	0.21
2,3-dimethylbutane	0.65	0.75	0.84
2-methylpentane	2.82	3.30	3.65
3-methylpentane	1.72	1.98	2.23
n-hexane	0.04	0.05	0.05
methylcyclopentane	4.63	4.74	6.14
2,4-dimethylpentane	0.32	0.36	0.36
2,2,3-trimethylbutane	0.02	0.02	0.02
benzene	2.67	2.33	3.81
cyclohexane	0.13	0.13	0.17
2-methylhexane	1.50	1.69	1.67
2,3-dimethylpentane	0.45	0.50	0.50
1,1-dimethylcyclopentane	0.01	0.01	0.01
3-methylhexane	1.25	1.39	1.39
cis-1,3-dimethylcyclopentane	1.31	1.35	1.49
trans-1,3-dimethylcyclopentane	1.19	1.22	1.35
3-ethylpentane	0.06	0.07	0.07
trans-1,2-dimethylcyclopentane	1.11	1.13	1.26
n-heptane	0.02	0.02	0.02
methylcyclohexane	6.35	6.33	7.22
1,1,3-trimethylcyclopentane	0.70	0.72	0.70
ethylcyclopentane	0.48	0.48	0.55
2,5-dimethylhexane	0.37	0.41	0.36
2,4-dimethylhexane	0.31	0.34	0.30
trans,cis-1,2,4-trimethylcyclopentane	1.03	1.06	1.02
trans,cis-1,2,3-trimethylcyclopentane	0.55	0.56	0.55
toluene	1.15	1.02	1.39
2,3-dimethylhexane	0.36	0.39	0.35
2-methyl-3-ethylpentane	0.02	0.02	0.02
2-methylheptane	0.73	0.80	0.71
4-methylheptane	0.26	0.28	0.25
3,4-dimethylhexane	0.03	0.03	0.03
cis,trans,1,2,4-trimethylcyclopentane	0.23	0.23	0.23
cis-1,3 dimethylcyclohexane	4.32	4.32	4.30
3-methylheptane	0.58	0.63	0.57
trans-1,4-dimethylcyclohexane	2.08	2.09	2.07

Table B.6 SBR Rubber (NaCl: $AlCl_3$) – Gas Chromatography Analysis (continued)

component name	wt %	lv %	mol %
1,1-dimethylcyclohexane	0.03	0.03	0.03
trans-1-ethyl-3-methylcyclopentane	0.48	0.48	0.48
cis-1-ethyl-3-methylcyclopentane	0.41	0.41	0.41
trans-1-ethyl-2-methylcyclopentane	0.23	0.23	0.23
trans-1,2,dimethylcyclohexane	0.98	0.97	0.97
trans-1,3,dimethylcyclohexane	0.03	0.03	0.03
n-octane	2.45	2.67	2.39
2,3,5-trimethylhexane	0.01	0.01	0.01
cis-1-ethyl-2-methylcyclopentane	0.08	0.08	0.08
cis-1,2-dimethylcyclohexane	0.51	0.49	0.51
2,4-dimethylheptane	0.22	0.24	0.19
4,4-dimethylheptane	0.06	0.06	0.05
ethylcyclohexane	1.70	1.65	1.69
*cis,cis,*1-3-5,trimethylcyclohexane	0.14	0.14	0.12
2,6-dimethylheptane	0.16	0.17	0.14
1,1,3-trimethylcyclohexane	0.80	0.79	0.71
C_9 naphthenes	2.56	2.51	2.26
2,5-dimethylheptane	0.31	0.33	0.27
3,5-dimethylheptane	0.03	0.03	0.03
ethylbenzene	0.61	0.54	0.64
*trans,trans,*1,2,4-trimethylcyclohexane	1.93	1.88	1.71
*cis,trans,*1,3,5-trimethylcyclohexane	0.53	0.52	0.47
meta-xylene	0.88	0.78	0.93
para-xylene	0.29	0.26	0.30
2,3-dimethylheptane	0.09	0.10	0.08
3,4-dimethylheptane d/l	0.02	0.02	0.02
3,4-dimethylheptane l/d	0.07	0.07	0.06
4-ethylheptane	0.07	0.07	0.06
4-methyloctane	0.22	0.23	0.19
2-methyloctane	0.33	0.35	0.29
*cis,cis,*1,2,3,trimethylcyclohexane	0.10	0.10	0.09
3-ethylheptane	0.24	0.26	0.21
3-methyloctane	0.85	0.90	0.74
*cis,trans,*1,2,4,trimethylcyclohexane	0.05	0.05	0.04
*cis,cis,*1,2,4,trimethylcyclohexane	0.44	0.43	0.39
ortho-xylene	0.60	0.52	0.63
cis-1-ethyl-3-methylcyclohexane	0.24	0.23	0.21
trans-1-ethyl-4-methylcyclohexane	1.16	1.11	1.03
isobutylcyclopentane	0.63	0.62	0.56
1-ethyl-1-methylcyclohexane	0.13	0.13	0.11
*cis,trans,*1,2,3,trimethylcyclohexane	0.07	0.07	0.06

Table B.6 SBR Rubber (NaCl/AlCl$_3$) – Gas Chromatography Analysis (continued)

component name	wt %	lv %	mol %
*trans,trans,*1,2,3,trimethylcyclohexane	0.03	0.03	0.03
n-nonane	0.18	0.19	0.16
trans-1-ethyl-3-methylcyclohexane	0.67	0.66	0.59
trans-1-ethyl-2-methylcyclohexane	0.23	0.23	0.20
cis-1-ethyl-4-methylcyclohexane	0.01	0.01	0.01
isopropylbenzene	0.28	0.25	0.26
2,2-dimethyloctane	0.30	0.32	0.24
isopropylcyclohexane	0.11	0.11	0.10
cis-1-ethyl-2-methylcyclohexane	0.05	0.05	0.04
2,4-dimethyloctane	0.19	0.20	0.15
2,6-dimethyloctane	0.23	0.24	0.18
n-propylcyclohexane	0.29	0.28	0.26
n-butylcyclopentane	0.10	0.10	0.09
n-propylbenzene	0.45	0.40	0.42
3,6-dimethyloctane	0.04	0.04	0.03
1-methyl-3-ethylbenzene	0.61	0.54	0.57
1-methyl-4-ethylbenzene	0.56	0.50	0.52
1,3,5-trimethylbenzene	0.39	0.35	0.36
4-methylnonane	0.11	0.12	0.09
1-methyl-2-ethylbenzene	0.42	0.37	0.39
3-ethyloctane	0.14	0.15	0.11
1,2,3,5 tet-methylcyclohexane	0.16	0.16	0.13
3-methylnonane	0.41	0.43	0.32
1-methyl-trans-4-isopropylcyclohexane	0.14	0.14	0.11
1,2,3,4 tet-methylcyclohexane	0.17	0.17	0.14
1,4 dimethyl-2-ethylcyclohexane	0.06	0.06	0.05
C_{10} naphthenes	2.65	2.59	2.11
C_{10} paraffin	0.63	0.65	0.45
1,2,4-trimethylbenzene	0.73	0.64	0.68
cis-1-methyl-3-propylcyclohexane	0.38	0.37	0.30
trans 1,4 diethylcyclohexane	0.29	0.28	0.23
trans-1-methyl-3-propylcyclohexane	0.17	0.17	0.14
1-ethyl-2,3-dimethylcyclohexane	0.11	0.11	0.09
isobutylbenzene	0.12	0.11	0.10
cis-1-methyl-4-propylcyclohexane	0.11	0.11	0.09
1,2,3,4 tet-methylcyclohexane	0.24	0.23	0.19
trans 1,3 diethylcyclohexane	0.15	0.15	0.12
1,2,3-trimethylbenzene	0.12	0.10	0.11
1-methyl-3-isopropylbenzene	0.17	0.15	0.14
indan (2,3-dihydroindene)	0.27	0.22	0.25
sec-butylcyclohexane	0.20	0.20	0.16

Table B.6 SBR Rubber (NaCl/$AlCl_3$) – Gas Chromatography Analysis (continued)

component name	wt %	lv %	mol %
butylcyclohexane	0.13	0.12	0.10
1,3-diethylbenzene	0.28	0.25	0.23
C_{11} naphthenes	0.78	0.75	0.56
1-methyl-3-*n*-propylbenzene	0.32	0.29	0.27
1-methyl-4-*n*-propylbenzene	0.12	0.11	0.10
1,4-diethylbenzene	0.25	0.22	0.21
1,3-dimethyl-5-ethylbenzene	0.31	0.27	0.26
1,2-diethylbenzene	0.10	0.09	0.08
1-methyl-2-*n*-propylbenzene	0.10	0.09	0.08
cis 1-methyl 4-ter-butylcyclohexane	0.13	0.12	0.09
5-methyldecane	0.11	0.11	0.08
4-methyldecane	0.09	0.09	0.06
C_{11} paraffins	0.21	0.22	0.15
1,4-dimethyl-2-ethylbenzene	0.40	0.35	0.33
1,3-dimethyl-4-ethylbenzene	0.21	0.18	0.17
3-methyldecane	0.09	0.09	0.06
1,2-dimethyl-4-ethylbenzene	0.44	0.39	0.37
1,3-dimethyl-2-ethylbenzene	0.12	0.10	0.10
tricyclodecane	0.18	0.17	0.15
1-methylindan	0.10	0.08	0.08
1,2-dimethyl-3-ethylbenzene	0.25	0.22	0.21
n-undecane	0.09	0.09	0.06
1,2,4,5-tetramethylbenzene	0.11	0.10	0.09
1,2,3,5-tetramethylbenzene	0.10	0.09	0.08
C_{11} unidentified	0.55	0.53	0.38
4-methylindan	0.23	0.19	0.19
5-methylindan	0.38	0.31	0.32
1,2,3,4-tetramethylbenzene	0.21	0.18	0.17
6-methylundecane	0.11	0.11	0.07
5-methylundecane	0.12	0.12	0.08
4-methylundecane	0.04	0.04	0.03
naphthalene	0.22	0.17	0.19
C_{11} aromatic	3.35	2.97	2.52
dodecanes	4.27	3.78	2.94
pentamethylbenzene	0.13	0.11	0.10
2-methylnaphthalene	0.36	0.29	0.28
1-methylnaphthalene	0.17	0.13	0.13
tridecanes	2.18	2.06	1.40
n-tridecane	0.12	0.12	0.07
tetradecanes	1.41	1.31	0.83
pentadecanes	0.91	0.83	0.49
hexadecanes	0.70	0.64	0.35

Table B.6 SBR Rubber (NaCl/AlCl$_3$) – Gas Chromatography Analysis (continued)

component name	wt %	lv %	mol %
heptadecanes	0.57	0.52	0.27
octadecanes	0.29	0.26	0.13
nonadecanes	0.06	0.05	0.03
eicosanes	0.03	0.03	0.01
heneicosanes	0.03	0.03	0.01
docosanes	0.02	0.02	0.01
tricosanes	0.02	0.02	0.01
tetracosanes	0.02	0.02	0.01
pentacosanes	0.01	0.01	0.00
total	100.00	100.00	100.00

summary by group

group	%wt	% vol
paraffin	3.20	3.60
isoparaf.	21.59	24.67
olefin	0.00	0.00
naphthene	45.28	45.08
aromatic	18.58	16.26
unidentified	11.35	10.39

summary by carbon

group	%wt	% vol
C_2	0.00	0.00
C_3	0.11	0.17
C_4	1.53	2.09
C_5	3.71	4.55
C_6	12.66	13.28
C_7	15.22	15.59
C_8	21.11	21.28
C_9	16.96	16.45
C_{10}	11.73	11.12
C_{11}	5.62	5.08

Table B.6 SBR Rubber (NaCl/AlCl$_3$) – Gas Chromatography Analysis (continued)

composite by carbon

group	$C_\#$	%wt	% vol
paraffin	C_2	0.00	0.00
	C_3	0.11	0.17
	C_4	0.27	0.36
	C_5	0.04	0.05
	C_6	0.04	0.05
	C_7	0.02	0.02
	C_8	2.45	2.67
	C_9	0.18	0.19
	C_{10}	0.00	0.00
	C_{11}	0.09	0.09
isoparaffin	C_4	1.26	1.73
	C_5	3.54	4.37
	C_6	5.19	6.03
	C_7	3.60	4.03
	C_8	2.66	2.90
	C_9	2.68	2.84
	C_{10}	2.05	2.15
	C_{11}	0.61	0.62
olefin	C_4	0.00	0.00
	C_5	0.00	0.00
	C_6	0.00	0.00
	C_7	0.00	0.00
	C_8	0.00	0.00
	C_9	0.00	0.00
	C_{10}	0.00	0.00
naphthene	C_5	0.13	0.13
	C_6	4.76	4.87
	C_7	10.45	10.52
	C_8	13.62	13.61
	C_9	10.27	10.05
	C_{10}	5.14	5.03
	C_{11}	0.91	0.87

Table B.6 SBR Rubber (NaCl/$AlCl_3$) – Gas Chromatography Analysis (continued)

composite by carbon

group	$C_\#$	%wt	% vol
aromatic	C_6	2.67	2.33
	C_7	1.15	1.02
	C_8	2.38	2.10
	C_9	3.83	3.37
	C_{10}	4.54	3.94
	C_{11}	4.01	3.50

additional group information

molecular weight of sample	111.61
molecular weight of C_6 plus	115.93
density of sample	0.7714
density C_6 plus	0.7834

VITA

Feng Qin was born on February 20, 1970, in Jilin, China. In 1993, he received a Bachelor's degree in chemical engineering from Tsinghua University, Beijing, China. In 1996, he received a master's degree in chemical engineering from the same school. Subsequently, he worked for Beijing Petrochemical Engineering Company for approximately three years. In the fall of 1999, he enrolled in Texas A&M University, College Station, TX to work on his PhD degree. He received his PhD degree in May 2004.

His permanent address is:

25 Chengshousi Road, #A2004
Fentai, Beijing, China 100078